

March 2010

Mini PCB Input Sensor and Display Circuits

Ian Samuel Schwartz
Worcester Polytechnic Institute

Follow this and additional works at: <https://digitalcommons.wpi.edu/mqp-all>

Repository Citation

Schwartz, I. S. (2010). *Mini PCB Input Sensor and Display Circuits*. Retrieved from <https://digitalcommons.wpi.edu/mqp-all/2599>

This Unrestricted is brought to you for free and open access by the Major Qualifying Projects at Digital WPI. It has been accepted for inclusion in Major Qualifying Projects (All Years) by an authorized administrator of Digital WPI. For more information, please contact digitalwpi@wpi.edu.



Mini PCB Input Sensor and Display Circuits

A Major Qualifying Project Report submitted to the Faculty of the

Worcester Polytechnic Institute

in partial fulfillment of the requirements for the Degree of Bachelor of Science

By

Ian Schwartz

Lena Dagher

Chris Thomson

Renee Walker

Submitted to:

Dr. John McNeill, Advisor

Abstract

The objective of this MQP was to use analog and other design techniques to build a circuit using one of Analog Device's new IC's. After much thought, research, and collaboration, the project chosen was the "Mini PCB Input Sensor and Display Circuits". This project has two parts: the first being a small, inexpensive, and portable circuit designed to be distributed to high school seniors who attend WPI's ECE undergraduate recruitment open houses. The second phase is a more complex version of the portable circuit, and would allow the user to connect to a PC via USB and display the output of the various sensors on a computer monitor. This paper guides the reader through the design process as seen through the eyes of the designers, detailing the unique processes considered to reach the final outcome.

Table of Contents

Abstract.....	1
Executive Summary.....	10
Acknowledgments.....	10
Introduction	10
1 Background	10
-(Defining Project Goals)	10
2 Brainstorming Applications.....	10
2.1 Potential Applications	10
2.1.1 Home Appliance Power Monitor and Controller System.....	11
2.1.2 Control Feedback Application	15
2.1.3 Motion-Controlled TV Remote	19
2.1.4 Magnetically-Controlled Axis Meter.....	21
2.1.5 Laser Microphone Application	26
2.1.6 LED Travel Game Set.....	30
2.1.7 Mini PCB Input Sensor and Display Circuit	33
2.2 Choice of Application	34
2.2.1 Discussion of Potential Circuit Options	34
2.2.2 Plan of Attack.....	35
3 Design Details.....	38
3.1 Overall Design	38
3.1.1 Block Diagram.....	38
3.1.2 Power Supply	38
3.1.3 Automatic Power Switch	41
3.2 Skin Resistance	42
3.2.1 Background Research	42
3.2.2 Experimentation and Design	43
3.2.3 Reason for Rejection.....	46

3.3 Temperature.....	47
3.3.1 Background Research	47
3.3.2 Progression of Design: Measurements and Results	47
3.3.3 Final Circuit Design	47
3.3.4 Component Selection	47
3.4 Pulse Circuit.....	48
3.4.1 Background Research	48
3.4.2 Circuit Design	58
3.4.3 Difficulties.....	74
3.4.4 Component Selection	79
3.4.5 Measurement and Results.....	79
3.5 Electrocardiogram (ECG)	80
3.5.1 Background Research	80
3.5.2 Progression of Design: Measurement and Results	82
3.5.3 Final Circuit Design	123
3.5.4 Component Selection	128
3.6 PC Interface	130
3.6.1 Selection of Components	130
3.6.2 Progression of Design: Measurement and Results	132
3.6.3 Final Design.....	132
4 Final Board Design	133
4.1 Simple Board	133
4.1.1 Circuits Chosen for Simple Board	133
4.1.2 MOSFET integration switch	133
4.1.3 Final Simple Board	133
4.2 Complex Board	134
4.2.1 Circuits Chosen for Complex Board	134
4.2.2 Final Complex Board	134
5. Conclusion.....	135

Appendix A – Derivation of Cut-off Frequency for Sallen-Key Filter 136

Figures

Figure 1 Individual appliance monitor (left) and central control hub (right)	12
Figure 2 Block diagram for Home Appliance Power Monitor	13
Figure 3 Gain vs. Temperature (left) and Small signal frequency response vs Gain (right)	16
Figure 4 Functional block diagram of application.....	17
Figure 5 Logitech MX Air aerial mouse	19
Figure 6 Magnetic axis sensor.....	21
Figure 7 Measuring circuit (left) and corresponding capacitance voltage ratios (right)	22
Figure 8 Measuring circuit (left) and corresponding capacitance voltage ratios (right)	23
Figure 9 Block diagram.....	24
Figure 10 Laser Interferometer Designs	26
Figure 11 Laser gun example	28
Figure 12 Block diagram.....	28
Figure 13 Artist Render of Travel Game (top view)	30
Figure 14 Artist's Rendition of testing PCB	36
Figure 15 Layout of prototyping PCB using Eagle.....	37
Figure 16 Using the DMM to find skin resistance.....	43
Figure 17 Circuit used for simulation (left) and Measured voltage values (right).....	44
Figure 18 Electrode with large surface area	45
Figure 19 Electrode with multiple contact points	45
Figure 20 Light Absorption by Blood.....	51
Figure 21 Transmittance probe diagram	55
Figure 22 Reflectance probe diagram.....	55
Figure 23 Pulse Circuit Block Diagram	59
Figure 24 Infrared LED drive circuit	61
Figure 25 Front end of signal path.....	62
Figure 26 Pulse signal centered between rails schematic	63
Figure 27 Non-inverting gain of 100V/V	64
Figure 28 Amplifier stage schematic for final board	65
Figure 29 New pulse signal with capacitor (gain of 43.4V/V).....	66
Figure 30 Low pass filter	67
Figure 31 Filtered pulse signal	68
Figure 32 Determining threshold values	69
Figure 33 Comparator with threshold network.....	70
Figure 34 Comparator inputs and output.....	71
Figure 35 Schematic of output stage	72

Figure 36 Oscillating system	75
Figure 37 Oscillating circuit.....	77
Figure 38 Effects of oscillating input.....	78
Figure 39 Side by side (left) and end to end (right)	78
Figure 40 Side by side (left) and end to end (right)	79
Figure 41 Typical human pulse	81
Figure 42 Initial ECG block diagram	83
Figure 43 Sallen-Key circuit topology.....	84
Figure 44 High-pass Sallen-Key second order filter	85
Figure 45 High-pass filter used in design	86
Figure 46 Low-pass Sallen-Key second order filter	87
Figure 47 Low-pass filter used in design.....	88
Figure 48 Complete Sallen-Key second order bandpass Butterworth filter.....	89
Figure 49 Linear frequency response of bandpass filter	89
Figure 50 Bode plot of bandpass filter (dB)	89
Figure 51 Phase versus frequency of bandpass filter	90
Figure 52 First ECG circuit, using the AD624	91
Figure 53 ECG output signal across heart.....	92
Figure 54 ECG output signal on back of hands	93
Figure 55 ECG output signal on thumbs	93
Figure 56 ECG output signal on thumbs zoomed in	94
Figure 57 Second ECG circuit using the AD8236.....	94
Figure 58 ECG output signal across heart.....	96
Figure 59 AD8236 output signal across heart.....	96
Figure 60 AD8236 output signal across heart (zoomed in)	97
Figure 61 AD8236 output signal across heart (greatly zoomed in)	97
Figure 62 AD8236 output signal on thumbs	98
Figure 63 AD8236 output signal on thumbs (zoomed in).....	98
Figure 64 Passive Twin T configuration	99
Figure 65 60 Hz Twin T notch filter used in design	100
Figure 66 Frequency and phase plot for 60 Hz notch filter	101
Figure 67 Complete filter for second prototype circuit	102
Figure 70 Frequency and phase response of filter	103
Figure 71 Comparison of first filter (blue) to the second filter (red).....	104
Figure 72 Transient response for simulated bandpass filter circuit	105
Figure 73 Transient response for simulated bandpass and 60 Hz notch filter circuit.....	105
Figure 74 Second ECG circuit, using the AD624.....	106
Figure 75 Frequency response of filter, 1 to 1 kHz.....	106

Figure 76 Output pulse before (ch1) and after (ch2) notch filter.....	107
Figure 77 Output pulse across heart, ch1 = amplified output, ch2 = threshold, ch3 = unamplified pulse, ch4 = LED	108
Figure 78 Output pulse on thumbs (ch1).....	108
Figure 79 Output pulse on thumbs zoomed in (ch1).....	109
Figure 80 AC coupled AD8236 configuration from datasheet.....	110
Figure 81 AC coupled AD8236 configuration used in the design	111
Figure 82 Pulse output across heart using AC coupling.....	112
Figure 83 Pulse output on thumbs using AC coupling.....	112
Figure 84 Second ECG circuit, with AC coupled AD8236	113
Figure 85 Frequency response of AC coupled circuit	114
Figure 86 Amplified pulse output on thumbs (ch4).....	115
Figure 87 AC Coupled in amp with one electrode grounded	116
Figure 88 Amplified pulse output one electrode grounded (ch4)	116
Figure 89 Complete ECG filter circuit.....	118
Figure 90 Frequency response of full filter.....	119
Figure 91 Bode Plot comparison of the first filter (green), second filter (blue), and final filter (red).....	120
Figure 92 Completed ECG prototype	121
Figure 93 Pulse output across heart before second filter (ch2) and after second filter (ch4) ...	122
Figure 94 Pulse output on thumbs before second filter (ch2) and after second filter (ch4)	122
Figure 95 Pulse output on thumbs after full filtering	123
Figure 96 ECG - Full Circuit.....	124
Figure 97 Twin T filter topology	127
Figure 98 Bode Plot of full filter	128
Figure 99 Pulse output of ECG	128
Figure 100 Generalized Sallen-Key filter topology	136

Tables

Table 1 Battery choice comparison	39
Table 2 Lithium coin data.....	40
Table 3 Skin resistance values.....	43
Table 4 ECG circuit components	129

Equations

Equation 1 Position of magnet	23
Equation 2 Received light intensity	52
Equation 3 Transmittance of light	52
Equation 4 Light absorption.....	52
Equation 5 Non-inverting gain	64
Equation 6 New gain equation with C	65
Equation 7 Filter cutoff frequency.....	67
Equation 8 Voltage divider for threshold	70
Equation 9 Duty cycle (left) and frequency (right)	76
Equation 10 Quality Factor, f_r = resonant frequency, BW = bandwidth.....	83
Equation 11 Sallen-Key filter cutoff frequency.....	85
Equation 12 Sallen-Key high-pass filter Q Factor.....	85
Equation 13 Sallen-Key low-pass filter Q Factor.....	87
Equation 14 Gain equation for the AD8236	95
Equation 15 Center frequency for notch filter	100
Equation 16 (above).....	136
Equation 17 Transfer function for Sallen-Key topology (above)	137
Equation 18 Transfer function for Sallen-Key high-pass filter	137
Equation 19 Transfer function for Sallen-Key low-pass filter	138

Executive Summary

Acknowledgments

Introduction

1 Background

-(Defining Project Goals)

2 Brainstorming Applications

2.1 Potential Applications

There were many choices for a potential project. This section will briefly discuss the top candidates, including an introduction to the project, and pros and cons for each choice.

2.1.1 Home Appliance Power Monitor and Controller System

In today's society, many homeowners are trying to find efficient ways to lower the cost of their bills. Electric bills are typically high, due to the high demand and cost of power. Many people are trying to lower the cost of their electric bill. One solution to this problem is a device that can wirelessly monitor and control any home appliance.

Basic Concept

This would be done by intercepting the power transmission line in an appliance by using step-down and step-up converters. The power status (on/off, and watts used) would be wirelessly transmitted to a central hub that displays the power status of the device and allows the user to change the status, if needed. The device would also include a USB flash memory drive which, when plugged into a PC, displays the power usage of all appliances being monitored.

Analog Devices Chips

To send and receive wireless signals, the ADF7020 RF transceiver would be used. To monitor the current of the appliance, the AD8202 difference amplifier would be used with a current sensing shunt resistor.

Artist's Rendition

An artist's rendition and a block diagram of the system are seen in Figure 1 below:



<http://www.microsoft.com/windowsxp/using/networking/setup/xbox.msp#>



http://ep.yimg.com/ca/I/yhst-95622685483394_2067_547064072

Figure 1 Individual appliance monitor (left)¹ and central control hub (right)²

Block Diagram

A block diagram of the system is seen in Figure 2 below.

¹ <http://www.microsoft.com/windowsxp/using/networking/setup/xbox.msp#>

² http://ep.yimg.com/ca/I/yhst-95622685483394_2067_547064072

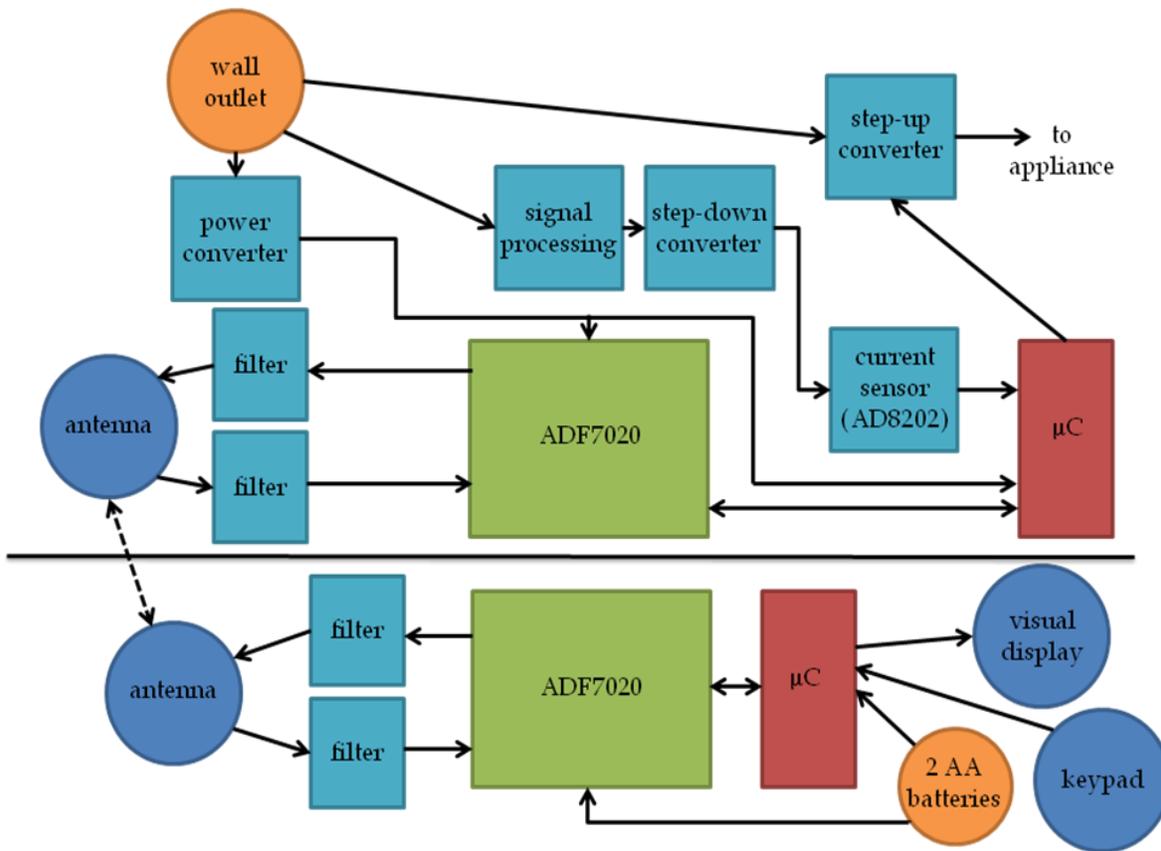


Figure 2 Block diagram for Home Appliance Power Monitor

Advantages

This project has several key advantages. First, it is a unique idea with potential for a patent. It could utilize the up-and-coming io-homecontrol[®] project: a company that works with engineers on wirelessly controlling everything in a home. This project also uses two ADI chips, one of which, the AD8202, is new on the market. Such a device would help “show off” the capabilities of the AD8202. Another advantage to this project is that, once completed, a demo version would be fun and easy for others to use.

Disadvantages

One of the major disadvantages for this project is that none of the participating team members have taken the high-level communications and signals courses required to understand and use RF transceivers properly.

2.1.2 Control Feedback Application

Using the variable gain and ADC interfacing features of the AD8264, an environmental control system can be implemented using environment sensors and controllers in a feedback configuration. This device may be used as an environmental control system in snake tanks, due to the sensitivity that snakes have with their environment. The following factors will be controlled in this application:

Light: Light is converted to signal using a photodiode.

Humidity: The ratio of the density of the liquid to the density of water in the air.

Pressure: The pressure sensor will produce an electrical signal proportional to pressure or changes in pressure.

Temperature: Thermistors measure temperature and output an according voltage.

Basic Concept

This application would use the variable gain and ADC interfacing features of the AD8264. There are four environmental sensors that produce signals that are proportional to their respective environmental factors. These signals are amplified by the four channels of the AD8264 and sent as differential output voltages into an ADC and then into a microcontroller. The microcontroller sends signals to peripherals that adjust the level of the environmental factors based on the amplitudes of the output signals of the AD8264. The sensors' output signals are scaled to $\pm 0.625V$ (the input range of the gain controller), inputted into the gain control stage of the AD8264, and referenced to the respective reference voltages, which are

proportional (by the same above mentioned scale factor) to the desired levels of the respective environmental factors. The microcontroller responds to changes in output amplitude (caused by changes in the gain from the changes in the sensor signal) by proportionally adjusting the environmental factors via the environment peripherals (pressure controller, humidifier, etc.).

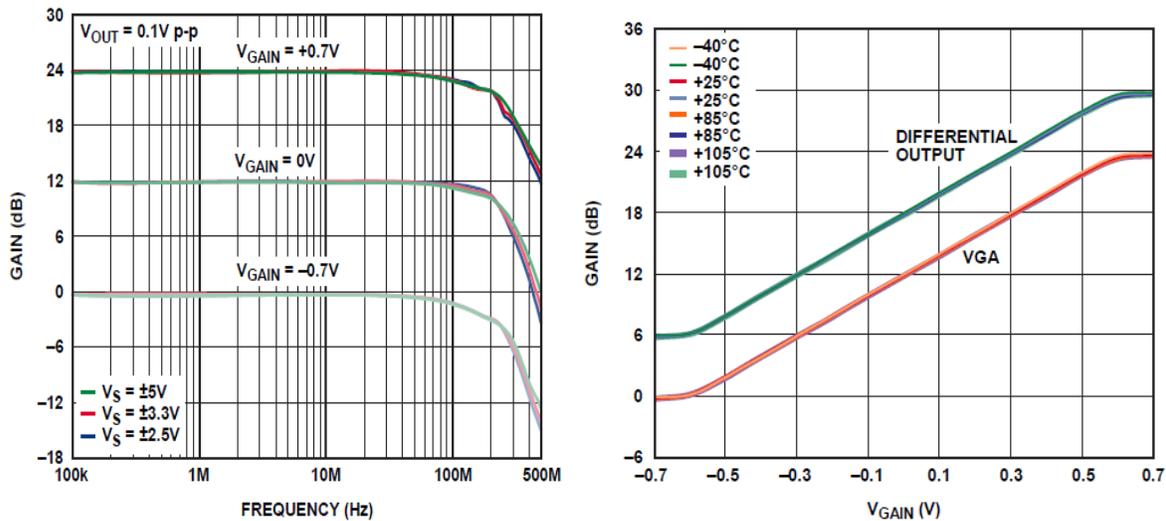


Figure 3 Gain vs. Temperature (left) and Small signal frequency response vs Gain (right)

As shown above the accuracy of the chip is very consistent over different ranges of supply voltages and temperature.

The AD8264 Chip

The AD8264 is a 4-channel, linear-in-dB, general-purpose variable gain amplifier (VGA) with a preamplifier (preamp), and a flexible differential output buffer. This chip will function properly in a temperature range of $-40^\circ C$ to $+105^\circ C$ and supply voltage of $\pm 2.5 V$ to $\pm 5 V$. The AD8264 would be a good choice to use in this application because the chip can take in four unrelated inputs and output them independently.

Block Diagram

Seen in Figure 4 is a block diagram of the circuit.

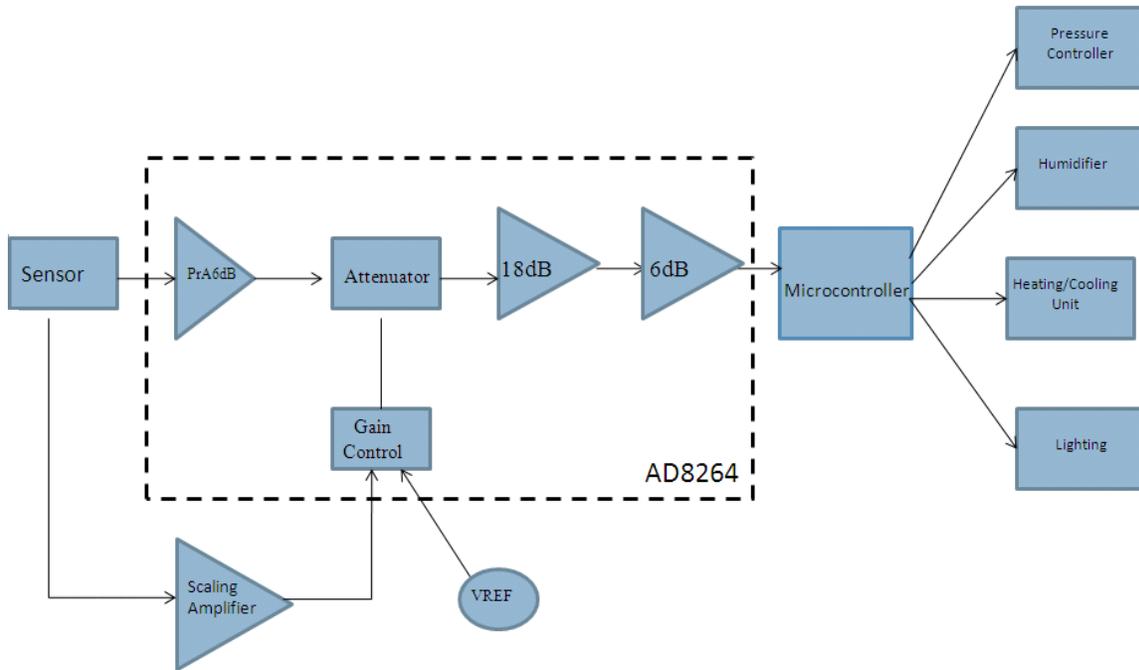


Figure 4 Functional block diagram of application

Advantages

This application would take use of the four inputs and four differential amplifier outputs. The control feedback application could replace up to four different control devices. Lastly, this application could be demonstrated in a trade show.

Disadvantages

The AD8264 is particularly well suited for use in the analog front end of medical PET imaging systems instead of control feedback applications. In order to use this device as a control feedback application, users would also have to purchase the four peripherals to maintain the environment. Thus after purchasing the device and four peripherals, the

application could be costly. Although this application could be demonstrated at a trade show it would have no user interactions.

2.1.3 Motion-Controlled TV Remote

This idea is a straight forward porting of all functions of a TV remote control into various hand movements. Such movements can include moving the remote to the right to change the channel up, and move it left to change the channel down. Using a three dimensional accelerometer, the ADXL335, this application can also allow the user to "draw" the channel number in the air in order to switch to a specific channel. The accelerometer will send signals from each axis to a processor, which in turn will send out the corresponding signal through the common communication method of an infrared LED.

Artist's Rendition

Seen below in Figure 5 is an artist's rendition of the item.



Figure 5 Logitech MX Air aerial mouse³

Background Research

Similar applications already exist, but none are quite the same. There exists a computer mouse that can be waved around in the air and the cursor moves accordingly on the display. A

³ <http://www.hardwarezone.com/news/view.php?cid=2&id=8006>

more similar application is the Nintendo Wii remote, which is able to track aerial movements of the controller.

Advantages

There is room in the market to explore the idea of "drawing" the channel numbers to select a channel as well as a TV specific application. This idea makes for a very entertaining demo at any sort of trade show as a way to show off the accelerometer. It also has a practical side in that users may wish to have such a remote in their own homes, which could spark other ideas for more home theater equipment.

Disadvantages

While having only the drawing capability different from most other devices on the market, this idea may prove to be a waste in resources as the end user will not care to add this small functionality. In addition, the use of a processor with flash memory to "remember" the user drawings may be too complex for such a simple device, which in turn may lead to more broken parts due to the inevitable dropping of such devices on a regular basis.

2.1.4 Magnetically-Controlled Axis Meter

One potential project idea is a magnetically-controlled axis meter. The device will be able to sense the presence of a magnet, and detect the location of this magnet. The location of the magnet will be monitored using one sensor for each the x, y, and z-axes. Each sensor will output a voltage corresponding to the strength of the magnet present. By this, a precise 3-dimensional location of the magnet can be determined.

Applications for the circuit can be a magnetically-controlled computer mouse or a joystick. Consider implementing this method as a joystick for a video game. Its movement would be controlled via the x and y-axes of the magnet, and a “click” would be a certain motion in the z-axis.

Basic Concepts

The first thing to consider is how to turn the magnetic strength into a voltage. Consider first the x-axis only. A simple device using three pieces of metal can be constructed and set up parallel to each other, then mounted to a board, as portrayed in Figure 6.

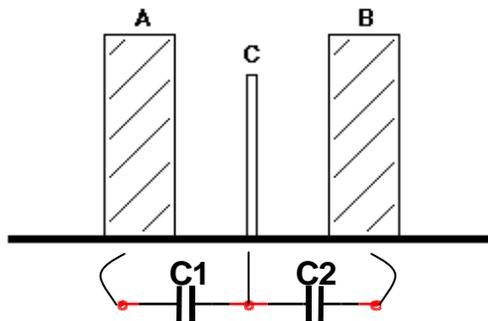


Figure 6 Magnetic axis sensor

Above, metal pieces A and B are fixed into the horizontal plate. Piece C is also mounted to the surface but is flexible and magnetic. Therefore, as a magnet approaches the contraption,

plate C will flex towards the magnet, changing the capacitance of the device. If a magnet approaches plate B, C will flex towards it, increasing the capacitance C2. If a magnet approaches plate A, capacitor C1 will increase.

Therefore, a voltage can be applied across these two capacitors and the ratio of their voltages can be measured; in effect determining the location of the magnet relative to plate C. Seen in Figure 7 is a simple circuit under such conditions with no apparent magnetic force applied ($C1 = C2$) and the resulting voltage ratio ($\frac{V_{C1}}{V_{C2}}$).

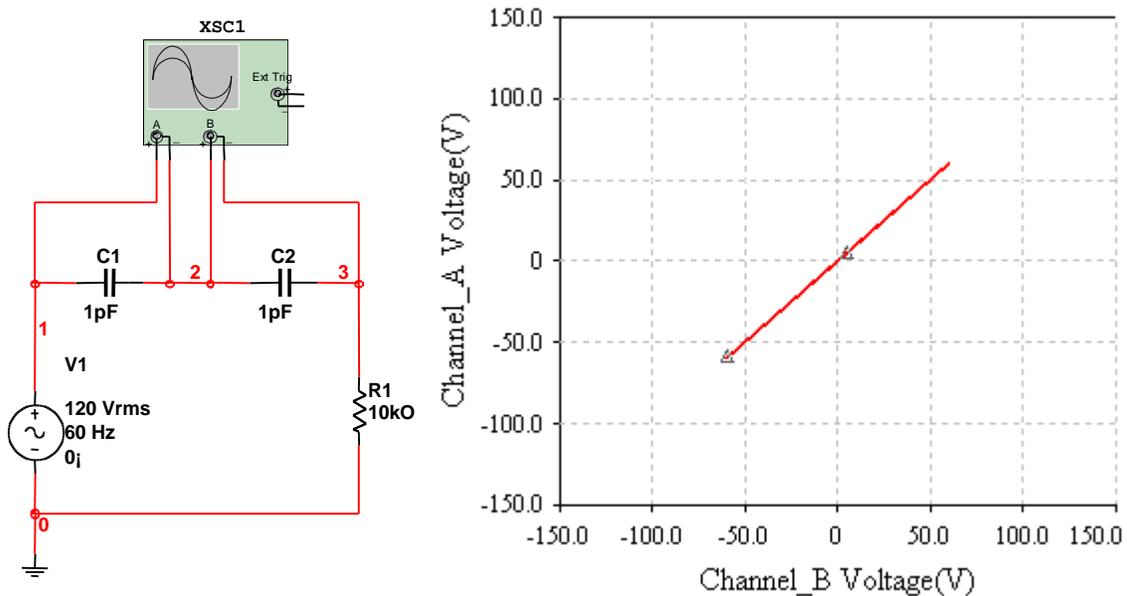


Figure 7 Measuring circuit (left) and corresponding capacitance voltage ratios (right)

Seen in Figure 7 above, the slope is $m = 1$. Now suppose a magnet approaches plate B. In this experiment, it will be assumed that the plates are set up in x-axis orientation. Therefore, when a magnet approaches plate B, the corresponding voltage should be positive. The results of such an experiment are seen in Figure 8 (note: capacitance values are estimated for proof of concept).

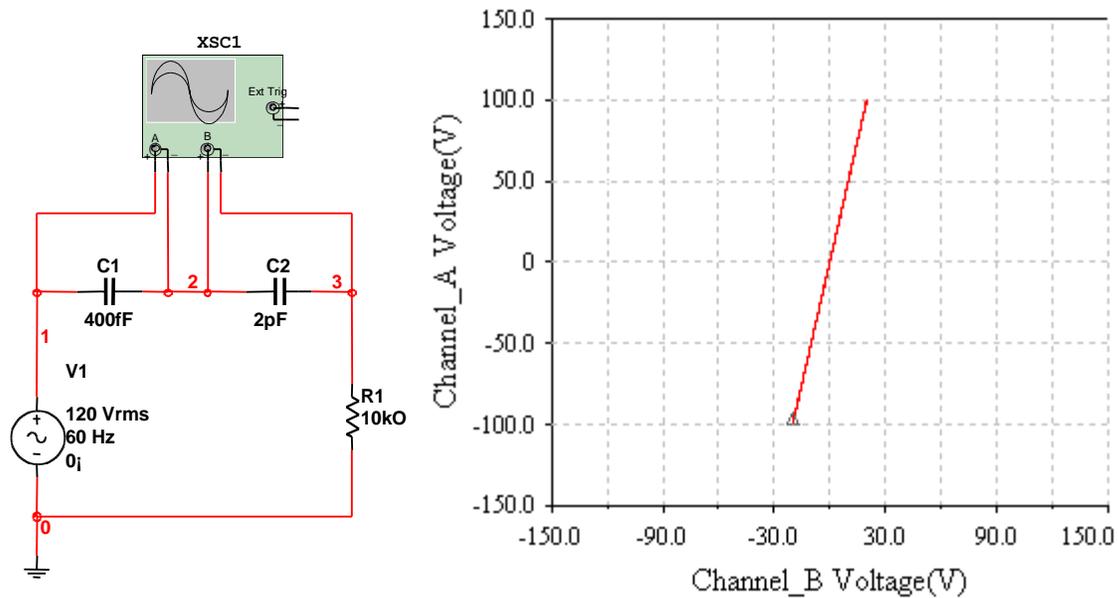


Figure 8 Measuring circuit (left) and corresponding capacitance voltage ratios (right)

Therefore, the position of the magnet is represented by:

$$x = \frac{\delta \left(\frac{VC1}{VC2} \right)}{\delta t}$$

Equation 1 Position of magnet

Analog Devices Chips

In the previous example, the capacitor values were very different from each other. Therefore, the differential signals can be easily ascertained. In reality, however, the capacitor values will only slightly differ from each other. Therefore, the differential signal will need to be amplified in order to make proper use of it. If two axes are being used, two differential signals need to be found.

The AD8222 is a very versatile chip with two built in instrumentation amplifiers. It can run using either single or dual supply ranging between $\pm 2.3V$ to $\pm 18V$. The gain can be set

anywhere from 1 to 10,000 $\frac{V}{V}$. With a CMRR of between 80 and 140dB (depending on the gain), this chip is very efficient.

Block Diagram

Seen in Figure 9 is the top-level block diagram for the circuit.

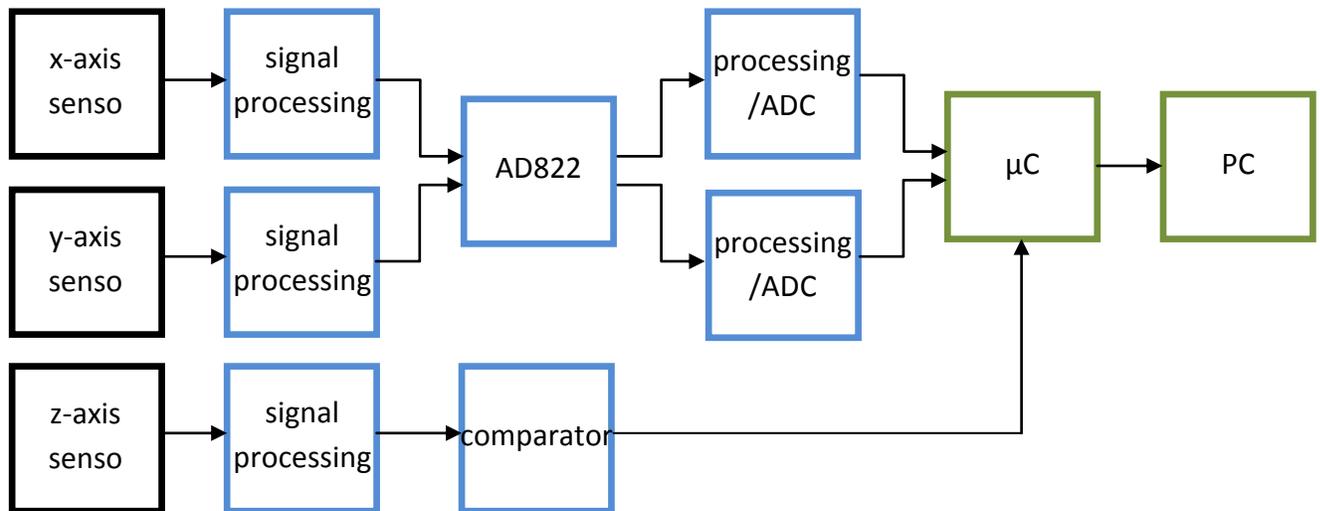


Figure 9 Block diagram

To successfully build this device, there are several different skills needed: signals processing, analog design, and computer interface engineering. Building the sensors would take a good deal of trial and error until accurate results are seen. Then, some signals processing and design skills would be needed in order to manipulate the signal to the size needed. This would include using a comparator and two instrumentation amplifiers (AD822), and then sending the resulting x-axis and y-axis signals into an ADC and into a microcontroller. The rest will mostly be coding the microcontroller and the PC interface, as well as sending the signal from the microcontroller to the PC.

Advantages

This project involves a good deal of circuit design, which is a positive attribute. Also, building the sensors involves creating something new and unique. Lastly, the interface could potentially be interactive.

Disadvantages

One worry is that the sensors will not work efficiently enough. Another con is that, although the idea itself is unique, many projects have gone through a similar process to build a circuit, so the design process may not be entirely unique.

2.1.5 Laser Microphone Application

A laser microphone is a surveillance device that uses a laser beam to detect sound vibrations in a distant object (window). The beam could be bounce off the window itself. The minute differences in the distance traveled by the light as it reflects from the vibrating object are detected interferometrically. The interferometer converts the variations to intensity variations, and electronics are used to convert these variations to signals that can be converted back to sound.

Basic Concept

This application would begin by pointing a laser beam at an angle to the plane of the glass (45-deg), with the photo detector at a complementary angle, and located at a near distance on the other side of the window, shown in Figure 10.

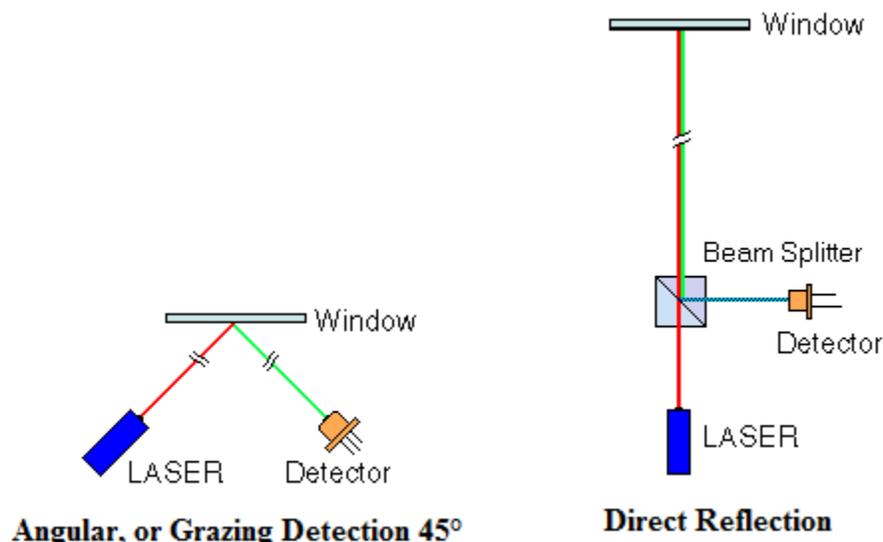


Figure 10 Laser Interferometer Designs⁴

A laser diode is a laser where the active medium is a semiconductor similar to that found in a light-emitting diode. The most common and practical type of laser diode is formed

⁴ <http://www.williamson-labs.com/laser-mic.htm>

from a p-n junction and powered by injected electric current. Preferably we would choose a laser that beamed infrared light because windows are opaque to this light range therefore no detection could be seen from the receiving side. The sound vibrations will cause the window glass to move sufficient enough to deflect the laser beam across the receiving photo-detector. The photo-detector would then send this signal to at least one or possible two low noise amplifiers. The purpose of sending this signal through low noise amplifiers is to minimize undesired noise while amplifying the desired signal. This amplified signal will need to go through a final amplification stage. This signal could then be sent to a speaker or headphones.

AD8264 Chip

The design of this project would focus around the AD8264 chip. Its specifications are listed below:

Voltage noise: $2.3 \text{ nV}/\sqrt{\text{Hz}}$

Current noise: $2 \text{ pA}/\sqrt{\text{Hz}}$

Artist's Rendition

An artist's rendition of the item is seen below in Figure 11.



Figure 11 Laser gun example⁵

Block Diagram

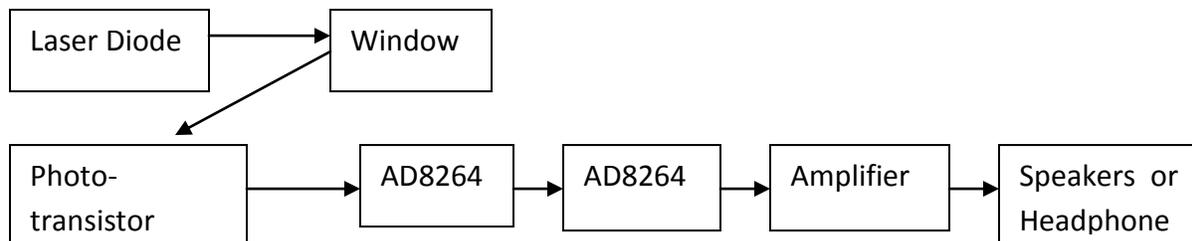


Figure 12 Block diagram

Advantages

The primary advantage to this application is the ability to hear long distance. This technology can be used to eavesdrop with minimal chance of exposure. Therefore, this device could be used in spy operations. Another advantage of the laser microcontroller is that it could be completed primarily through analog means, which is a positive attribute. The laser microcontroller would take advantage of the low noise amplifier AD8264. Lastly, this application could be shown in a tradeshow and interact with users via headphones.

Disadvantages

One disadvantage to this application could be that the signal is distorted due to temperature or undesired noise. This device could have socially unacceptable applications.

⁵ <http://www.alexismorin.com/ss/images/laser-gun.jpg>

Countermeasures exist in the form of specialized light sensors that can detect the light from the beam; therefore this device may not work on every window. Rippled glass can be used as a defense, as it provides a poor surface for a laser microphone.

2.1.6 LED Travel Game Set

The main idea of this application is to allow the user to play either checkers or tic-tac-toe using only LEDs. The lights will negate the need for any sort of markers or checker pieces to play the game. Instead, the user will press the board, thus activating a switch and turning on the LEDs for tic-tac-toe and as a way to move the markers in checkers. This idea also aims to be in a rather small package to promote its portability and ability to travel without worrying about the loose pieces.

Artist's Rendition

An artist's rendition of the item is seen below in Figure 13.

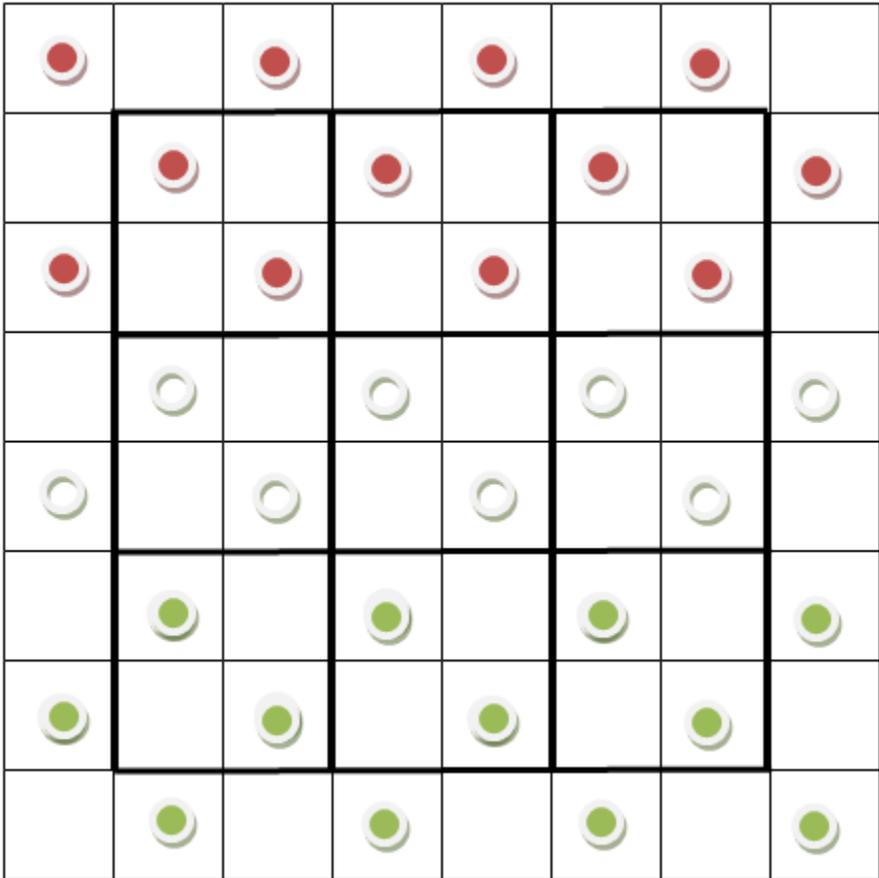


Figure 13 Artist Render of Travel Game (top view)

Theory

The basic theory of operation is quite simple. The switches will be in a normally open position and connected to an LED drive circuit. The LEDs will be of the multi color variety, which allows the one position to be occupied by either color. In the game of tic-tac-toe a processing chip will be needed to detect when three circuits are all on at the same time, signifying a win, as well as a way to keep count of games one. At the same time, in the game of checkers, a processor will be needed to detect when a player jumps over another "checker" and decide whether to open the circuit (if it is an opposing checker) or keep it closed (if it was the same side).

Analog Devices Chip

This idea will make use of a micro controller from the family ADuC7xx. This family integrates 12-, 16- and 24-bit A/D converters, 12-bit DACs with flash, SRAM, and a host of digital peripherals designed for industrial, instrumentation, medical, communications and automotive applications. Most also include various ways to connect with a computer such as UART, SPI, and JTAG interfaces. The use of this chip will be only to monitor the games and increment the counters, and send a signal to the 7-segment display. At this time, the exact chip to use is unknown because what will be needed in terms of peripherals and internal functions to get this application working is not known.

Steps to Completion

Step 1 involves looking at an overview of the problem. Most of the actual circuitry will be easy. However, connecting the two games together in such a way as to change the "rules" of the board to accommodate either tic-tac-toe or checkers with only the flick of a switch may

prove challenging. There also requires a little coding in order for the game to know what is going on and keep score for each side.

Step 2 will be to start designing the game in a way where it will work once. This stage includes being able to play a full game of either tic-tac-toe or checkers with no hitches, individually, with no great focus on getting to game two or switching from one to the other.

Step 3 is when the two games must be integrated together so the user can choose one or the other and play more than one round with the score being kept and displayed. This step also includes all the debugging of the code and troubleshooting and circuit problems.

Advantages

This idea can almost be completed entirely with analog components. It also will be easy to show off, since the application is a game meant to be played. It also provides a solution for making the ordinary classic games of checkers and tic-tac-toe more interesting. It also has the ability to be connected to a computer and the game be transferred to the hard drive, where a simulation program could render the game in a more aesthetically pleasing way.

Disadvantages

At first glance the circuits seem quite trivial. The end product may not actually have a need for the specific features of the AD8235 or the particular processor. The software application may be too complex given the time constraints of this project.

2.1.7 Mini PCB Input Sensor and Display Circuit

This project requires the construction of a very small circuit with several inputs and LED outputs. The ultimate goal for this board shall be a handout at an ECE college recruiting presentation. It will take any or all of the following inputs: skin resistance, skin temperature, heart rate, and pulse oximetry. There would then be some signals processing, including the use of the AD8235 instrumentation amplifier. The output would then be displayed via LEDs for the user to see. The final product should portray a good example of “what ECE is” to the unfamiliar person. It also should cost as cheap as possible.

The second part of this project would be to design a similar, but perhaps more complicated, board to show to Analog Devices. This will include more input sensors and a microcontroller, which will analyze the input signals and send output information to a laptop via USB or an RF transceiver.

2.2 Choice of Application

The Mini PCB Input Sensor and Display Circuit is project of choice. This decision has several distinct advantages over the others. A main advantage is that this project will have a clear purpose and an end result that will hopefully last for a while and be useful to the school. Also, the opportunity to learn about many different aspects of circuit design is available, including protoboard design and testing, analog design, microcontroller programming, input/output sensors, and information and signals processing, as well as some other potential subjects. Although the project has a set final product, there are many degrees of freedom to choose from during the design process. A strict budget will be enforced while designing this circuit in hopes that the circuit is very cheap to reproduce.

Because of these advantages, this seemed to be the optimal project choice. There will be a very diverse number of electrical engineering topics to work on and learn about during the course of the project, which will serve as an aid in becoming a better engineer.

2.2.1 Discussion of Potential Circuit Options

There are four circuit options that were deemed plausible. They are skin resistance, temperature, pulse oximetry, and an electrocardiogram. A brief introduction to each idea is given below.

Skin Resistance

The resistance of humans' skin has a wide degree of variance. It can change under certain circumstances, for example if a person's skin is wet, oily, or salty. These changes in skin resistance could potentially correlate with the user's mood or how nervous the user is.

The goal of this circuit would be to find use of this skin resistance variance and provide an output that correlates to something that could be of use, i.e. mood.

Temperature

Pulse Oximetry/Plethysmography

Electrocardiogram (ECG)

The electrocardiogram will use two surface mount electrodes that are built into the circuit. The user will grab each of these electrodes with their finger/thumb and hold them there. The main focus of this circuit will be to show the user's pulse, and not necessarily the entire heartbeat waveform (more on this later).

The output of the ECG will ideally be able to produce a pulsing LED corresponding to the user's pulse, and will provide a clear enough waveform to be seen on the PC.

The main focus of this design will be to implement the AD8235 chip: a newly released chip from Analog Devices that is the smallest low power instrumentation amplifier to date. However, the AD8236 will be used for this design; it is the exact same circuit as the AD8235, but is available in larger surface mount packages.

2.2.2 Plan of Attack

Brainstorming and Background Research

Prototyping PCB

Below in Figure 14 is the initial artist's rendition of the PCB that will be used to test the sensors and other vital components, and build circuits around them.

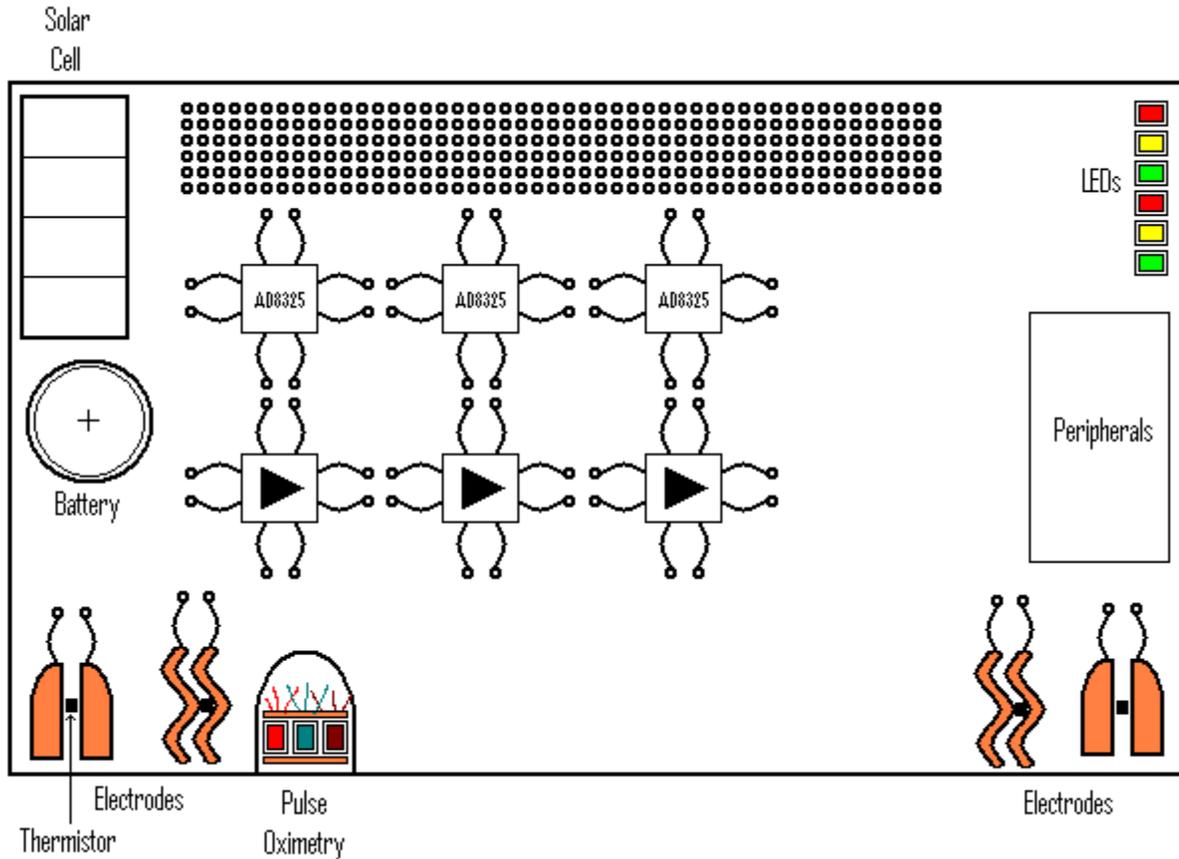


Figure 14 Artist's Rendition of testing PCB

The actual layout of the PCB was designed using Eagle⁶. A snapshot of the layout that was actually used can be seen below in Figure 15. This board will allow for the utilization and testing of many features including the AD8236 (top left of board), SOT23-5 and SOT23-8 devices (center left), several copper electrode configurations (bottom), thermistors, infrared LEDs, and phototransistors (between electrodes), through-hole LEDs (center), DIP sockets (center), output LEDs (center), the UART/USB configuration (center right), battery (top right), and many unconnected holes which can be used for new configurations on or off of the board. Each lead is attached to a hole, which will allow for wires to easily be soldered in.

⁶ <http://www.cadsoftusa.com/>

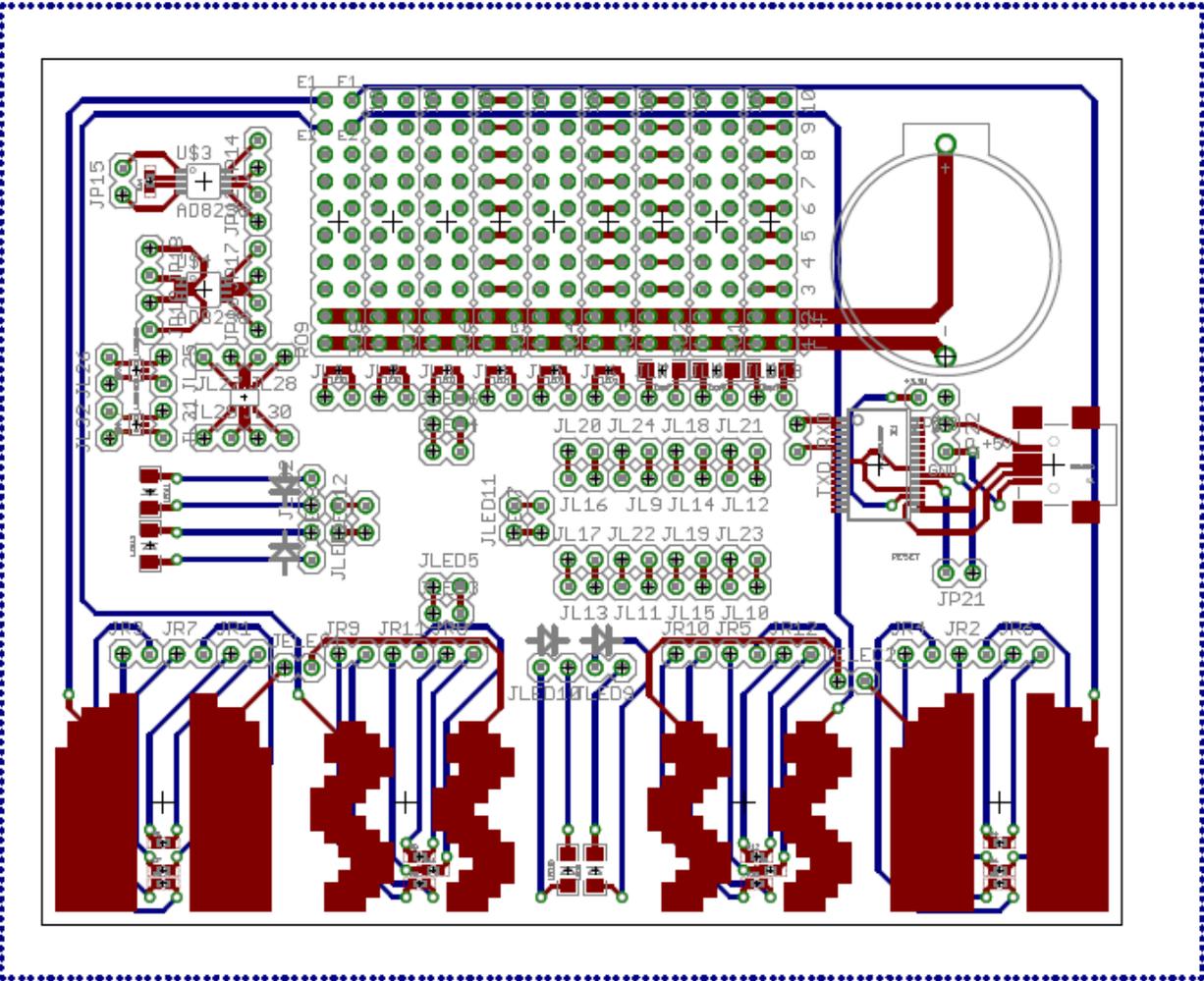


Figure 15 Layout of prototyping PCB using Eagle

3 Design Details

This section will go over the complete design of the circuits on the board. In the first section a general system level look of the design is discussed. Each circuit is represented as just a block in the overall diagram. This section also details the designs that are relevant to all of the circuits such as the power supply and circuit power switches. Following the overall section will be an in depth investigation into the design and component selection for each of the circuits. Each of these sections will also contain any and all necessary background information that will help in understanding how each circuit works.

3.1 Overall Design

This section will discuss the top-level design work involved in the design of this project. The first topic presented will be a top-level block diagram for the whole system. Next, the power supply will be discussed. The last topic discussed will be the automated switch mechanism.

3.1.1 Block Diagram

[block diagram and how the circuits are independent of each other]

3.1.2 Power Supply

It is clear that from the portable nature of this project the only option to supply power is with a battery. Batteries come in all sizes and capacities. However, only a small few can be considered for this project. At the forefront of consideration are the relatively flat coin cell technology of various diameters and the standard everyday cylindrical batteries. Of particular interest is the less common size of 1/2AA, which is, as expected, the same diameter as the

standard AA (or AAA for the corresponding 1/2AAA) but half as long. Once the battery is chosen, a holder will also need to be chosen. Preferably, the holder will be soldered to the board with the ability to remove the battery once installed. This will ensure even once the battery dies, a replacement can be installed. When comparing each setup (batteries and holders), the 1/2AA is nearly double the height (0.6in versus the 0.363in of the coin cell).⁷ Since one of the biggest constraints is to keep all the components as close to the surface of the PCB as possible, the possibilities of size and shape are narrowed down to just one style, the coin cell.

After choosing the type of battery to be used, the next step was to determine the technology and size to be used. In researching the technologies, many were discarded due to their primary purpose of being rechargeable. This left the lithium ion and the silver oxide technologies. Below is a table comparing the two technologies' minimum and maximum values in each category.

Table 1 Battery choice comparison

Ranges	Lithium Ion		Silver Oxide	
	3 V		1.55 V	
	Min	Max	Min	Max
Height (mm)	1.2	5	0.13	2.3
Diameter (mm)	10	24.5	4.8	11.6
Capacity (mAHrs)	34	620	8.3	200

Although the lithium ion batteries are much larger in diameter, the resulting capacity is also much larger. In a circuit where the output is heavily dependent on lighting LEDs, which consume between 10mA and 20mA, the higher capacity batteries will be more useful. Perhaps

⁷ Taken from datasheet of Keystone Electronics 108 (1/2AA) and 1066 (20mm) battery holders

the biggest difference is the nominal voltages. An LED also needs to have at least some specific forward voltage across it to even allow current to flow. This leaves the option of doubling the silver oxide batteries in series to create 3.1V nominal or to design some type of converter that can output a higher voltage from just the 1.55V input. The choice for this project was to go with the lithium ion technology.

In order to pick out the best size and capacity it is useful to look at the full range available. Below is a table showing the relevant information pertaining to the full range of active batteries produced by Energizer. All of the values were taken from the website and respective datasheets for each battery.⁸

Table 2 Lithium coin data

Name	Diameter (mm)	Height (mm)	Capacity (mAHrs)
BR1225	12.5	2.5	48
CR1025	10	2.5	30
CR1216	12.5	1.6	34
CR1220	12.5	2	40
CR1616	16	1.6	55
CR1620	16	2	79
CR1632	16	3.2	130
CR2012	20	1.2	58
CR2016	20	1.6	90
CR2025	20	2.5	163
CR2032	20	3.2	240
CR2320	23	2	135
CR2430	24.5	3	290
CR2450	24.5	5	620

⁸ <http://data.energizer.com>

In addition to the above data, commonality was also observed. This was done by simply going to a retail store and observing what was for sale. The motive behind this was that since this board is designed to be handed out to prospective WPI students, if the battery were to ever die, the board could be brought back to life without too much hassle.

The most common size from the table is 20mm, which matches the most common product sold in stores, the CR2025 or CR2032. Of the two, the CR2032 was chosen since it has a greater capacity, which will elongate the lifespan of the board.

3.1.3 Automatic Power Switch

[also include section of PMOS switch]

3.2 Skin Resistance

One idea for an input sensor on this device is a method to measure skin resistance. This would likely (and ideally) be done by using two electrodes that, when touched by the user, would be connected, forcing the user to act as a resistor. These electrodes would be made out of a good conducting material and would measure the skin resistance of the person touching them.

3.2.1 Background Research

Skin resistance can be affected by many different things. Some factors include: mood, cleanliness, sweat, and dryness. Skin resistance is measured using two electrodes on two different types of the body. The body and skin act as the resistor while each electrode acts as a wire lead. From this method a potentiometer with the human body can effectively be created.

Skin resistance varies widely depending on the amount of water, sweat, and oils on the skin. Each of these variables fluctuates from person to person, and from mood or temperature. Human skin can range from $1\text{k}\Omega/\text{cm}^2$ to $100\text{k}\Omega/\text{cm}^2$. Dry skin usually varies from $35\text{k}\Omega/\text{cm}^2$ to $50\text{k}\Omega/\text{cm}^2$, while wet skin has a much lower resistance.

Galvanic Skin Response (GSR)

The Galvanic Skin Response method for measuring skin resistance involves using two electrodes on two different parts of the body (usually two fingers). It measures the current and/or resistance between the two points. It can detect differences in skin and muscle tissue resistance due to internal and external stimuli. If calibrated correctly, the output will change depending on the user's skin resistance due to mood.

3.2.2 Experimentation and Design

Shown in Table 3 are measurements taken on three different subjects during an experiment. Each subject was tested having both dry and wet skin. Figure 16 shows the setup used to obtain these measurements.

Table 3 Skin resistance values

Subject	Resistance (MΩ)	
	Dry skin	Wet skin
Ian	3.5	0.18
Lena	1.2	0.23
Chris	1.2	0.14

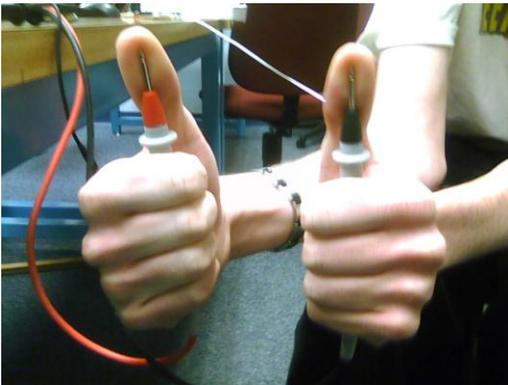


Figure 16 Using the DMM to find skin resistance

Next, a simple voltage divider circuit was built in order to convert the resistance values into something that can be used, namely a voltage. Two 10MΩ resistors were put in a parallel configuration to create a 5MΩ resistor. Then, two wires were configured in an open circuit fashion, so that when the subject grabs these two wires with each hand, the body acts as the resistor R_{body} , seen in Figure 17 (left). On the right of Figure 17 is the voltage, V_{out} , with respect to time for three different test subjects.

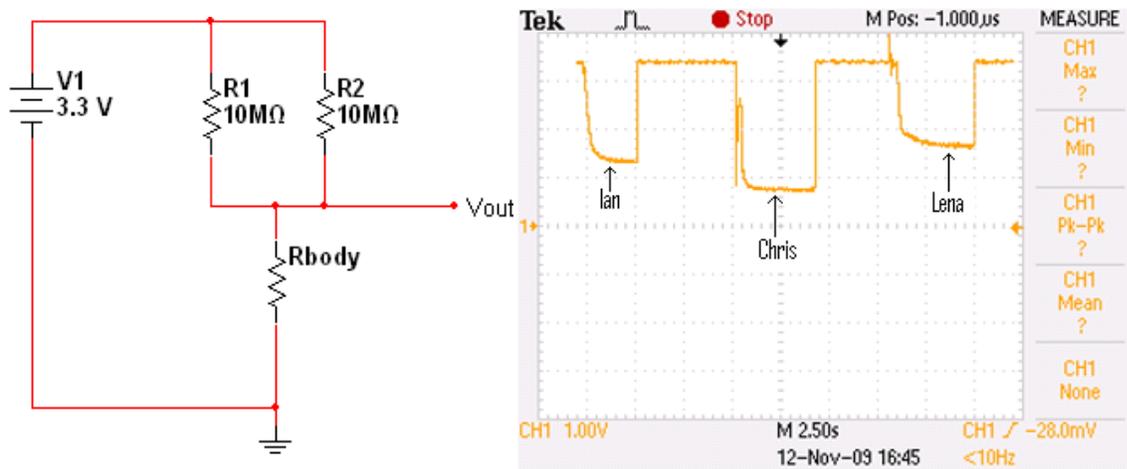


Figure 17 Circuit used for simulation (left) and Measured voltage values (right)

Surface Mount Electrodes

The proposed method for making and testing the surface mount electrodes used for measuring skin resistance will be discussed.

The most important element of the material used is that it be a good conductor. Using a good conducting material will ensure that the electrodes are sensitive enough to measure minute differences in resistance.

The least expensive and most conductive surfaces are metals. The most common of these is copper, which is used in many electrical engineering projects as the main conductive surface; therefore, copper will be used as the electrode material.

The next topic to consider is the shape and design of the electrodes. Due to the design limitations of this project, the electrodes shall be surface mounted, and ready-to-use (i.e. no electrode gel or any other material is required). This means it will not be possible to obtain the same accuracy as a typical electrode used in many medical applications. Listed below are two proposed electrode design strategies that may compensate for this inefficiency:

1. Large surface area

Two electrodes PCB with the largest possible surface area that matches our requirements will be mounted to the PCB. A picture representation can be seen in Figure 18.



Figure 18 Electrode with large surface area

2. Multiple contact points

This design will aim to have many contact points with the thumb of the person. This should allow for more accurate results, but may prove to be more complex than option

1. This design is shown in Figure 19.



Figure 19 Electrode with multiple contact points

Using this in the design

A simple voltage divider would be used to measure skin resistance by passing a small DC current through. Then the corresponding voltage due to the changing skin resistance would be measured.

One potential method of implementation would be to scale the skin resistance output voltage to correspond exactly to the thermistor output voltage, and then implement a switching mechanism to switch between the two sensors. This would allow for one circuit to have two functions, resulting in saved board space.

3.2.3 Reason for Rejection

Below are the major pros and cons for the implementation of this circuit.

Advantages

- There is a large variance in skin resistance, allowing for easy and distinct measurements.
- Very simple to implement in the final design.

Disadvantages

- The change in skin resistance does not have a clearly defined meaning.
- It would be difficult to provide an output that is relevant to the user.

Due to the fact that any output that could be produced would essentially be “pointless”, it was decided not to implement skin resistance as a feature in this design.

3.3 Temperature

3.3.1 Background Research

3.3.2 Progression of Design: Measurements and Results

3.3.3 Final Circuit Design

3.3.4 Component Selection

3.4 Pulse Circuit

This section describes the design process involved for the pulse circuit. It begins with some background information on how the circuit can work and the principles being utilized. This is followed by the circuit block diagram with a detailed description of each block following. As measurements were taken, the design to the circuit changed. These modifications are discussed as well. Since this circuit requires some particular parts in order to work, the last section describes the component selection process.

3.4.1 Background Research

In order to simply power a light emitting diode (LED) to the beat of one's heart, a great deal of research must go in to find out this can work. In general terms, this concept takes its roots in two fields that are more than slightly related: pulse oximetry and pulse plethysmography. The former uses two different wavelengths of light to measure blood oxygen levels, while the latter uses various means to determine how the blood flows through the body. The goal of this project is to draw on both ideas to use light as a means to capture the heart beats and to pulse an output LED to once the peaks cross a given threshold. It should be noted that since pulse oximetry relies on the flow of blood through the body, plethysmography is actually a subset in the oximetry process.

To better understand these concepts, each will be briefly described and only relevant information discussed. One commonality between both concepts is the non-invasive nature of testing. More specifically, the oximeter shines a red and an infrared light into the body (usually a thin, semi-translucent area, such as an ear lobe or finger) while the plethysmography utilizes a

variety of pressure measuring devices and optoelectronics (including air chambers for monitoring lung expansion and water chambers for monitoring circulatory systems in the extremities). (Medoff, 2008)

Therefore, in order to achieve the goal of monitoring one's heart beat, the idea of using the light to shine into a finger will be able to determine that beat since the blood flows in accordance with one's heart. So the end concept will borrow the idea of light absorption from the oximetry and the blood flow changes from the plethysmography. Since only one part of the pulse oximetry concept is actually being used (i.e. Not calculating the actual oxygen levels), a vast majority can be disregarded. However, it is important to know how the process works.

Pulse Oximetry

The goal of a pulse oximeter is to measure the blood oxygen level in the body. In layman's terms, some data is collected and based on an empirical formula, a number is found. For the purposes of this project, the oxygen levels are of no concern. The process by which the data is collected is the main focus.

"By taking advantage of the pulsatile flow of blood...the pulse oximeter tracks the change in light absorbance as the blood pulses. By tracking this peak-to-peak ac component, the absorbance due to venous blood or tissue does not have any effect on the measurement." (Farmer, 1997) This outlines the overall goal of using a pulse oximeter to obtain the beating heart and at the same time rejecting the common mode noise of the body. To accomplish this two different LEDs are used to shine light into the body. The first is a light within the red

spectrum of light and the second is within the infrared spectrum of light. It should be noted that the particular wavelength of light is a great factor as well.

Overview

Different types of blood will absorb these two wavelengths differently. The two types of blood that are being referred to are oxygenated hemoglobin and deoxygenated hemoglobin. The amount of oxygen in each blood cell determines how much of the light is absorbed and how much is reflected. In essence by shining the two different wavelengths into a given part of the body, a difference can be taken and thus the blood oxygen level can be calculated. Below is a graph that depicts how each type of blood absorbs and reflects the two different wavelengths. The extinction coefficient is plotted against the wavelength in nanometers. The extinction coefficient is talked about in more detail in the following section. As can be seen, at lower wavelengths, the deoxygenated hemoglobin (Hb) absorbs more light than the oxygenated hemoglobin (HbO₂). As the wavelength increases, the roles are reversed. Although this graph only shows absorption, the true measurements are taken from whatever light is left as it passes through the body. Therefore if more red light passes through than infrared light, it can be inferred that the blood is oxygenated.

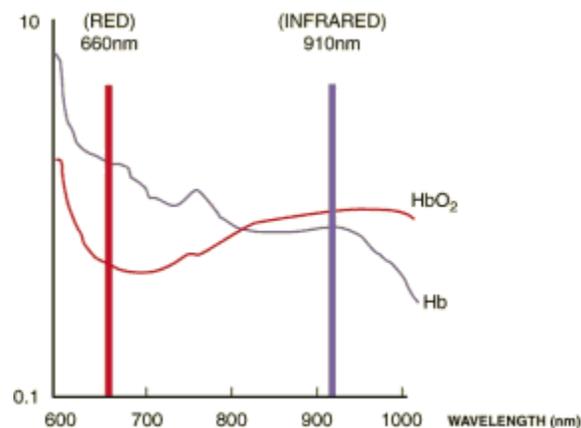


Figure 20 Light Absorption by Blood⁹

It is necessary to use two different wavelengths due to light scattering in the body. If two points are used, it increases the accuracy of the measurement. However, in the application of pulsing an LED, only one LED is needed as will be explained later on.

In order to receive the transmitted light, a few options are available. Since only two options were considered for this project, only those will be discussed, the photodiode and phototransistor. Both devices convert light into current. The biggest difference is that due to the natural behavior of the transistor, an automatic gain is applied to the current, thereby making the signal easier to work with. The choice between the two is explained in further detail in the design section. For now, it is sufficient to assume one of these devices is receiving the light that is not absorbed by the blood.

From this point, most pulse oximeters feed the data into a microcontroller where the signal is conditioned and the oxygen level number is computed based on the absorbance at the two wavelengths using CO-oximeter data to lookup the value for the S_pO_2 , an estimation of the actual oxygen level.(Farmer, 1997)

Light Absorption and Beer's Law

There is a lot of further research needed into how and why the different types of hemoglobin absorb light in two distinct patterns. This section provides a small background and explains one of the laws as to how light be absorbed and the basic math involved in determining absorption. This section will also discuss the optimum wavelengths to be passed through the body to achieve the greatest effects.

⁹ <http://www.oximetry.org/IMAGES/cpo.gif>

Beer's Law (also referred to as Beer-Lambert's or Bouguer's Law) provides an equation for determining how much of the signal is left after passing through some substance. (Wieben, 1997) The intensity of light received on the other side of the substance decreases exponentially with increasing distance. Using a monochromatic incident light of intensity I_0 , the received intensity, I , traveling through the substance can be modeled as

$$I = I_0 e^{-\varepsilon(\lambda)cd}$$

Equation 2 Received light intensity

where $\varepsilon(\lambda)$ is the extinction coefficient or "absorptivity" of the absorbing substance at a specific wavelength (expressed in $L \text{ mmol}^{-1} \text{ cm}^{-1}$), c the concentration of the absorbing substance which is constant in the medium (expressed in mmol L^{-1}), and d the optical path length through the medium (expressed in cm). (Wieben, 1997) The basic principle of Beer's Law is founded on the conservation of light, whereby the sum of the transmitted and absorbed light will equal the incident light. Therefore the transmittance of light, T , can be defined as the ratio of the transmitted light, I , to the incident light, I_0 .

$$T = \frac{I}{I_0} = e^{-\varepsilon(\lambda)cd}$$

Equation 3 Transmittance of light

The total absorbance of light, A , can be defined as the negative natural log of the transmittance. This yields the following equation.

$$A = -\ln T = \varepsilon(\lambda)cd$$

Equation 4 Light absorption

As can be seen from this latest equation, the absorption is directly proportional to the wavelength of light being passed through the medium. It is because of this behavior that the

two different lights can be used to determine the difference in absorption between the oxygenated and deoxygenated hemoglobin in the blood.

Choosing the correct wavelengths is rather simple when referring back to Figure 1. Any light below 600nm is of no use due to the red pigmentation of the skin, which absorbs a great deal of light. Therefore, when choosing the wavelengths it is ideal to choose two wavelengths that are spaced far enough apart as to give clear differences in extinction coefficients. Choosing a low wavelength of 660nm is a good choice since the difference between Hb and HbO₂ is greatest on the low end. Similarly, with the upper end, a choice of 940nm yields the greatest difference in the hemoglobin absorption. Another consideration is the relative flatness of the spectra. To prevent large errors, a flat spectra means a slight variation in wavelength will not greatly skew the results. It has been observed that other combinations of light will also provide better results based on a difference in saturation (735nm and 890nm for low saturation and 660nm and 990nm for high saturation). (Wieben, 1997)

Although the goal of this project is to only track the pulse of a human, it should be noted that Beer's Law makes many assumptions that would not carry over if an accurate pulse oximeter were to be built. First, Beer's law assumes monochromatic incident light. Given that the only practical option for this project would be to use an LED (a light source that does not emit monochromatic light) the actual absorbency as defined above, would have to be altered. Beer's Law also does not account for the scattering of light in the body. It is this actual behavior that serves as the principle concept in this project's overall effectiveness. This will be explained later in the next section dealing with transmission versus reflection measurements.

Transmission versus Reflection

Given what is already known about sending light through the body and measuring what comes out, there are two ways to go about this procedure. The first is used in most all applications since it is the most accurate, transmission. The other alternative is to not measure what passes through the body but rather what is reflected back towards the source. This method is less accurate for a few reasons. However each method has its own advantages and disadvantages.

The benefits of placing the receiver directly behind the medium and sending light through are that it is the easiest and most accurate method. There is minimal interference from scattered light and saturation as well as being able to truly measure all the light that is not absorbed by the hemoglobin. In many applications the probe can be constructed to go around a finger of a person with a small spring to keep tension on the device. Moving the probe will cause distorted data since the probe will now be looking into a different section of the body. As such, most probes of this nature use a clamp method with one side of the clamp housing the incident light and the other housing the receiver, as seen below.

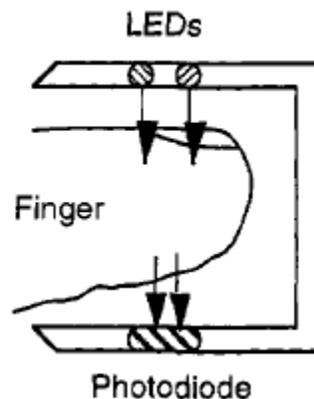


Figure 21 Transmittance probe diagram¹⁰

However, the downside to using this method is its bulky nature. It is a necessity to have access to both sides of the medium, be it a finger or an ear lobe for example. Unless a truly large probe was to be made, the oxygen levels in a larger part of the body could not be measured, such as a leg. It should be noted that many of these “disadvantages” are of no concern to the vast majority of applications where a medical patient is lying on a bed with a clamp on the finger. The relative size and immobility of the probe do not matter.

Using a reflectance probe has its own set of advantages as well. Based on the principle of measuring the backscattered light to determine blood oxygen levels, a reflectance probe can be placed anywhere on the body. The backscattered light consists of light that is not absorbed by the hemoglobin and bounced back as well as light reflecting off of the stationary tissue in the body. However, since the emitter and receiver are on the same plane, the probe has the ability to adhere to the skin, or for a finger to be pressed against the probe to get a reading. (Reddy, 1997) A diagram of this type of probe can be seen below.

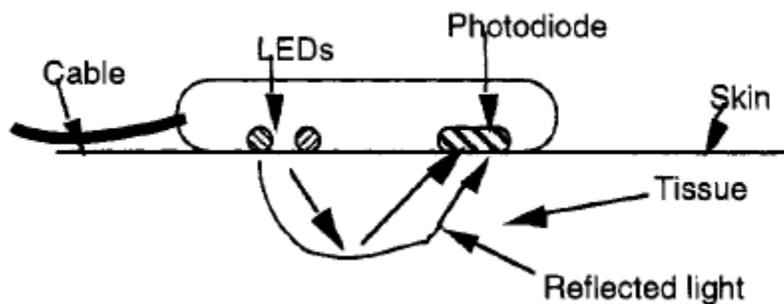


Figure 22 Reflectance probe diagram¹¹

¹⁰ Taken from *Design of Pulse Oximeters* page 87

¹¹ Taken from *Design of Pulse Oximeters* page 88

With the many advantages of using a reflectance probe, the relative inaccuracies involved have limited its widespread use. One of the biggest design obstacles is the distance between incident light and receiver. The biggest issue with this is that the probe may become too saturated with the incident light as it scatters throughout the body. To combat this issue, two steps can be taken: increase the light intensity to provide a better contrast between AC component and the DC component of the surrounding tissue, or to place the receiver relatively close to the boundary of total saturation and peak receiving. This produces a proportionality relationship between increasing light intensity and keeping large distance or keeping a lower constant intensity and moving the components closer together. (Reddy, 1997)

Mendelson and Ochs (as cited in Reddy, 1997) explored the effects of skin temperature on pulse measurements. By increasing the skin temperature by 1°C (from a range of 34°C to 45°C), they were able to see a five-fold increase in pulse amplitude. In addition to the temperature sensitivity, it must be noted that due to the property of reflection, only a fraction of the light intensity will ever be measured, which instantly means the amplitude of the pulse will automatically be less than that of transmittance probes.

Common errors to either type of probing technique include ambient light interference, optical shunting, and edema. The ambient light from the environment is already lighting the tissue and being absorbed. This causes the probe to detect the actual signal buried within some noise and false readings. The obvious and easy solution in most cases is to cover the probe in some opaque material. Optical shunting happens when the incident light shines directly through the medium into the detector. This can happen if the probe is too large or

possibly if the probe is moved while trying to take measurements. Lastly, edema refers to the effect of placing the probe over an area that happens to have an excess of fluid built up causing the body to swell. The fluid in the body at this location will give false readings since normal blood flow is being altered. (Reddy, 1997)

Plethysmography

Where the oximeter circuit is trying to neutralize the common mode AC component to measure an accurate blood oxygen level, the purposes of this project will be trying to keep only this change. Since the data will be directly related to the heart beating, the goal of this system will be to measure these changes and use the new data to plot the pulse of a given person. The next section briefly explains plethysmography and how it relates to the overall project goals.

As mentioned before, the area of plethysmography can be thought of as a subset of pulse oximetry. The pressure of the blood as it flows throughout the body is directly related to the beating of the heart. At each beat of the heart, a surge of blood runs through the veins, causing the veins to slightly expand. As the veins expand and more blood rushes past a given sample area, the pressure changes are recorded. A very common application using this technique is measuring one's blood pressure by compressing the limb with a strap and listening to the pulse using a stethoscope as practiced by most all medical facilities. However, since the oximeter uses two light sources in the same area, the increase in pressure and blood flow will increase the amplitude of the pulse as seen by the photodetector.

Blood pressure is not the only type of plethysmogram observed today, although it is the only concept pertaining to this project. Very common other applications include the amount of

air in one's lungs and differences in readings between arms and legs. The former utilizes a large body chamber to measure the air pressure changes when the patient takes a deep breath. This procedure measures how much air the patient can hold in his or her lungs. (Medoff, 2008) The latter test involves taking plethysmograms of both the arms and leg. In this case, the differences between the two measurements are observed. If there are any great discrepancies, it can be inferred that there is a blockage somewhere in the body. (Lee, 2009)

Summary

By combining the two concepts of plethysmography and pulse oximetry, an interactive application for this project came to mind. In order to pulse an output LED to the beat of one's heart only one incident light source is needed since the purpose of using two is to take a difference and let one act as an "anchor" or a point of reference. The only purpose of this circuit is to measure the blood flow past a certain point in the body. To achieve this, only one LED and one photodetector will be needed to measure the plethysmogram of the blood pressure. From this reading the signal will then be conditioned and the end result will be an output LED pulsing to the pressure changes in the blood. For further reading on building pulse oximeters, please see *Design of Pulse Oximeters*, which is a collection of papers written by experts in the field edited by J.G. Webster.

3.4.2 Circuit Design

Below is the circuit block diagram for the pulse circuit (following the signal path).

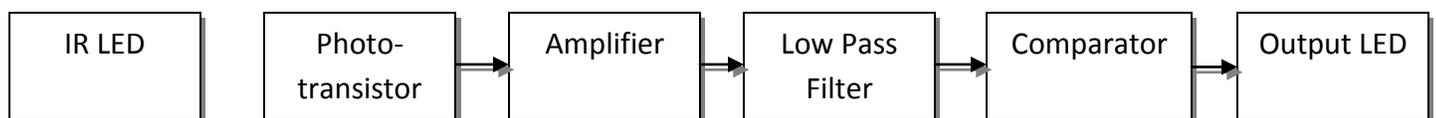


Figure 23 Pulse Circuit Block Diagram

Infrared LED

As mentioned in the background information, the two types of light that are used to shine into the body to measure the blood oxygen level are red and infrared light. Furthermore, the optimal wavelengths to choose from are 660nm (red) and 940nm (infrared). For this circuit, infrared was chosen for a few reasons:

1. There is less of a difference between the two types of hemoglobin at this wavelength, which will result in less "echoing" where the same signal will be received at different amplitudes (one signal from the Hb and the other from HbO₂).
2. On average, an infrared LED will have a lesser forward voltage drop than red LEDs. Typical values of infrared are around 1.2V whereas typical red LEDs operate around 1.8V or higher. Since this circuit has power constraints, a lower voltage is better.
3. Infrared light is invisible to the naked human eye. This allows more of a "wow" factor when people place their finger on the board as they wonder how it works.
4. There is a chance that by using red light, the natural pigmentation of a given person's skin may absorb more light than designed for, which will attenuate the signal. By using infrared, this possibility is decreased.

As stated in the project goals section, one of the constraints is to make the board as flat as possible. This means that whenever possible the path of less height is chosen. As such, the infrared LED and corresponding photodetector can be set up side by side on the same plane, which will take advantage of the reflectance principle. Although there are advantages and

disadvantages to using this approach, the ultimate goal is to successfully design the system so that there is as little components protruding from the board as possible.

By comparison, the transmittance approach would require some outlandish design work. The LED and photodetector would have to be placed in direct line with each other with the ability to place a finger in between. A possible idea that was looked at was to use right angle components and cut a hole in the board so the light may be passed through the finger. Another idea was to mount the LED on the board facing up, and using some sort of clamp type assembly, mount a photodetector above the finger. However, both ideas were too bulky and did not agree with the defined project goals. This left only the reflectance idea as a viable option.

In order to drive the LED a simple circuit is implemented. At first the idea was to keep the LED at a constant 20mA to provide optimal light intensity. This, in turn, means more light enters the finger, and more light is reflected back yielding a higher amplitude and more distinct waveform. Throughout the course of the design process, this drive circuit changed to a pulsing LED, which is described in more detail in the power design section. However, due to restraints by other components in the circuit, the circuit had to revert back, albeit with a smaller current to conserve battery life.

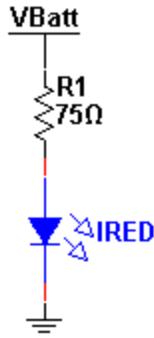


Figure 24 Infrared LED drive circuit

In this setup, the IRED has a 1.2V drop across it. R1 is set to limit the current through the LED at 18mA (with a 1.35V drop across R1). Although the nominal voltage of the battery used in this project is 3V, due to the high current drain and series resistance, only 2.55V appear at the terminals. This is described in more detail under the power design section below.

Phototransistor

In choosing the proper photodetector, two options are available: the photodiode and phototransistor. Both components convert light into current. However, the main difference is in the actual construction of the two devices. The photodiode is just like a standard diode except its sensitive junction is exposed to light. As light strikes the diode, an electron is excited, which causes current to flow. More sensitive photodiodes utilize a PIN junction as opposed to a standard PN junction. In a PIN junction, a near intrinsic semiconductor is placed between the p-type and n-type regions.

The phototransistor is quite similar to the standard bipolar junction transistor except that it is only a two terminal device. The base terminal of the transistor is left open to receive the incoming light. The current through the base-collector junction is then amplified by the

natural gain of the BJT. In comparison to the photodiode, the same amount of light in each device will provide more current at the output to the phototransistor due to this gain. Since this circuit is utilizing the reflectance principle where less light is being received, the phototransistor will be the better match.

Since the phototransistor is the front end to the signal stage, the current must be converted to a voltage. This is accomplished by choosing a resistor tied to the supply rail. As the current varies from the phototransistor, the current through the resistor will vary. Since the current measured from the phototransistor is still quite small (on the order of a few micro amps), even with the initial amplification from the BJT, a value of $100\text{k}\Omega$, R2 below, will be used to increase the signal to a few milli-volts. Below is the phototransistor, Q1, along with the regulated DC operating point.

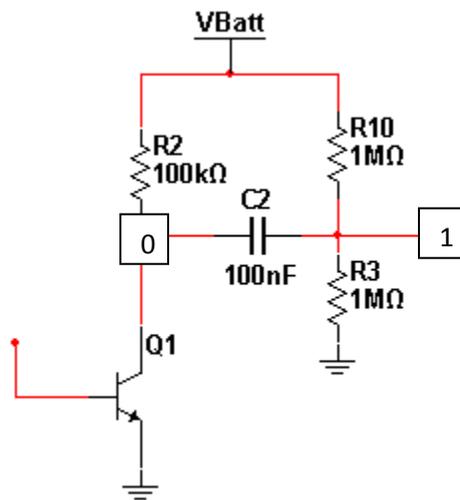


Figure 25 Front end of signal path

Moving beyond the phototransistor, the $0.1\mu\text{F}$ capacitor, C2, is AC coupling the signal so only the pulse signal makes it through (strips all DC components). The next section sets the DC operating point for the signal when it goes through the amplifier stage. By using a voltage

divider where both R10 and R3 are equal, the operating point is set to be centered between the positive rail and ground. This allows for maximum dynamic range for the signal to be amplified. Since current draw is a constraint (using a battery with finite capacity), the value of $1\text{M}\Omega$ is used so that the current draw is quite low at $2.55\mu\text{A}$. The figure below depicts what is happening when the circuit is "on," a finger is placed across the LED and phototransistor, and the output taken at node 1 as seen in Figure 25 above.

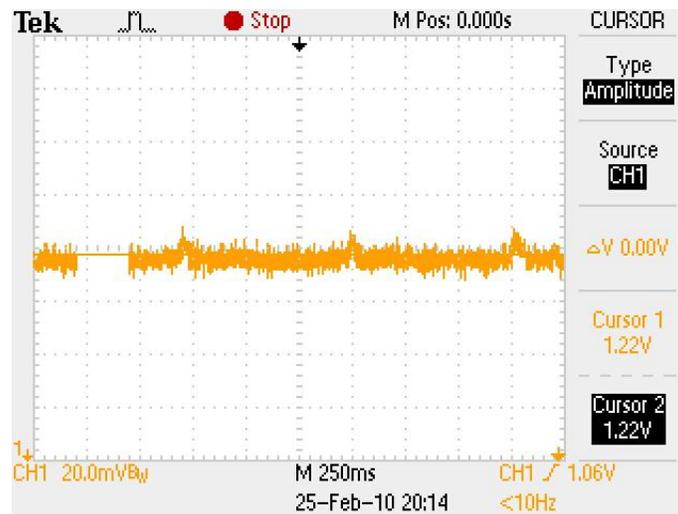


Figure 26 Pulse signal centered between rails schematic

Amplifier

The goal of this block is simply to amplify only the signal and keep the same operating point midway between the rail and ground. This can be done using an op-amp in the non-inverting gain configuration. On the first attempt, a simple op-amp with a resistive feedback network was used. Based on the input signal measuring about 10mVpp as seen in Figure 26¹² and the desired output to swing 1Vpp , the necessary gain is 100 V/V . To achieve this, the following standard equation for a non-inverting gain configuration is used:

¹² Highest resolution on Tektronix TDS 2004B is 20mV/Div

$$G = \frac{V_{out}}{V_{in}} = \frac{R4 + R5}{R5}$$

Equation 5 Non-inverting gain

Keeping currents low led to the decision that $R4 = 1\text{M}\Omega$, which causes $R5 = 10\text{k}\Omega$. Using this setup, the output waveform was taken at node 2 as depicted in the schematic below.

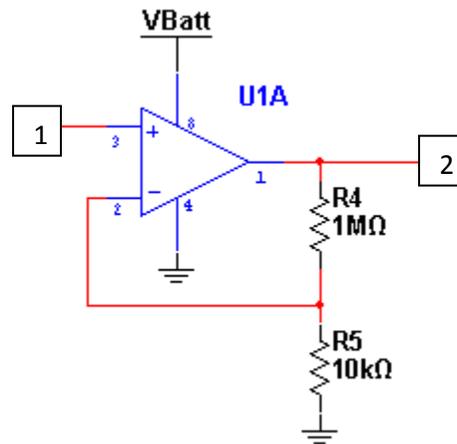


Figure 27 Non-inverting gain of 100V/V

When viewed on the scope, the output was nothing more than the positive rail. In addition to amplifying the signal, the offset was amplified. One option to fix this is to add in another coupling capacitor and reset the operating point. Although this is not a practical solution since the extra components will only crowd the final board and increase the total cost. After researching negative feedback amplifiers, a new solution presented itself.

In order to make sure the DC offset does not get amplified, a capacitor is placed in the feedback network. Since adding in the capacitor will change the impedance of the load, this equation needs to be modified to take into account the new impedance. The resulting equation is:

$$G = \frac{R4 + R5 + \frac{1}{j\omega C4}}{R5 + \frac{1}{j\omega C4}}$$

Equation 6 New gain equation with C

The heart at rest beats on average 70 times per minute, or at 1.17Hz.¹³ Therefore, $\omega = 7.35\text{rad/sec}$. It is determined that to keep the current draw low, $R4 = 2.5\text{M}\Omega$ and $R5 = 10\text{k}\Omega$. Based on Equation 6 and that the gain equals 100 V/V, the resulting $C4 = 10\mu\text{F}$. Using these values, the schematic of this block can be seen in Figure 28. Since the $2.5\text{M}\Omega$ resistor is not a common value within the standard lab kits, the circuit was built around the values used for a standard gain of 100 (where $R4 = 1\text{M}\Omega$) as in Figure 27. This only yields a gain of 43.4V/V. Final scope images of each node on the final board can be found at the end of this section.

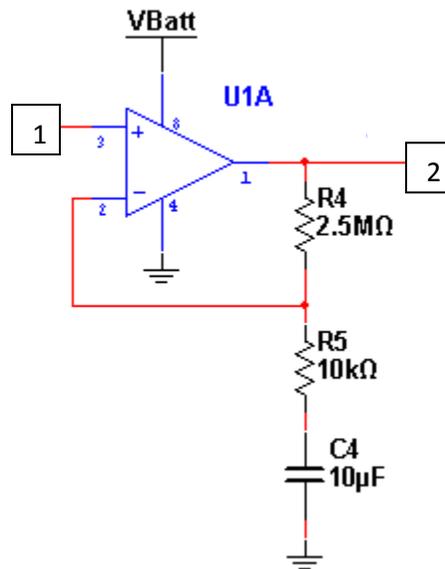


Figure 28 Amplifier stage schematic for final board

¹³ By taking pulse for 60 seconds on own body

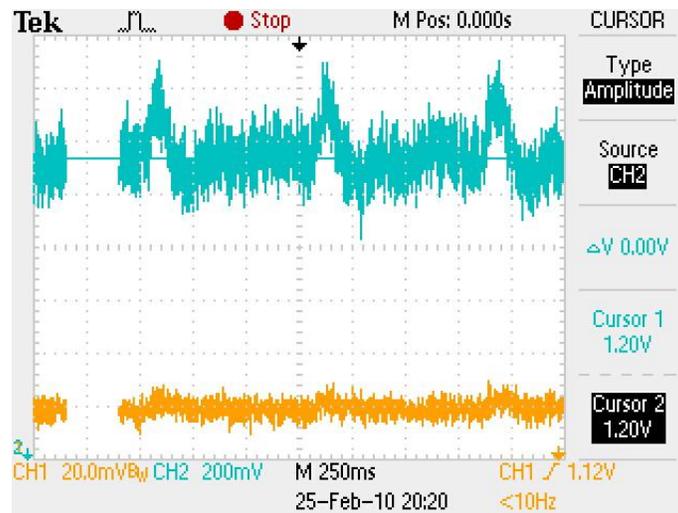


Figure 29 New pulse signal with capacitor (gain of 43.4V/V)

The last big step was choosing the appropriate op-amp. The schematics and scope images above are utilizing the OPA2337 dual op-amp package, single supply op-amp from Texas Instruments. The requirements of this project narrowed the search considerably. Since the design calls for an amplifier and a comparator, the circuit will utilize a dual package op-amp setup, one as a non-inverting amplifier, and the other as a comparator. It needed to have low power dissipation, low supply voltage minimum and be able to run with a single supply, all due to using a battery as the supply voltage. It also needed to be able to swing the output close to the rails to make the most of the limited range of the supply (other op-amp possibilities only swing to within 1.5V of the rail).

Since the choice of the right op-amp has been narrowed, the best way to choose one is to pick the candidates that meet the most requirements and test them in the circuit. This is particularly useful for the op-amps that are presented as low noise and have internal filtering to see how much better the signal will look. The relative low frequency of the entire circuit also

leaves a few variables in the air such as slew rate limiting and gain-bandwidth product. The various choices are described in more detail in the component selection section.

Low Pass Filter

The next block is a very simple, yet effective low pass passive filter. The objective of this filter is to mostly filter out all of the 60Hz noise in the surrounding air or from the body that has latched onto the signal. Since the cutoff frequency,

$$f_{3dB} = \frac{1}{2\pi RC}$$

Equation 7 Filter cutoff frequency

needs to be anything above the signal yet below the 60Hz, a wide range of possibilities is available. However, since this circuit is using a simple single pole passive filter (also known as a Butterworth filter), the cutoff should not be too close to the desired signal. To make the circuit easier to read and duplicate, the cutoff can be chosen with resistor and capacitor values that are already being used within the circuit. Since power consumption is always a concern, a high resistance is needed. Therefore, a value of 100kΩ is chosen for R6 and the corresponding capacitor value will be 0.1μF for C6. These values correspond to a cutoff frequency of 15.9Hz. This will ensure that the heart signal is not attenuated by the roll off. Figure 30 below depicts the filter where the input at node 2 is the same as the output node 2 from Figure 28.

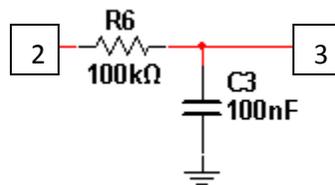


Figure 30 Low pass filter

The resulting output, taken at node 3, can be seen on the following scope graph. The input is plotted as well as the output to show the filtering success.

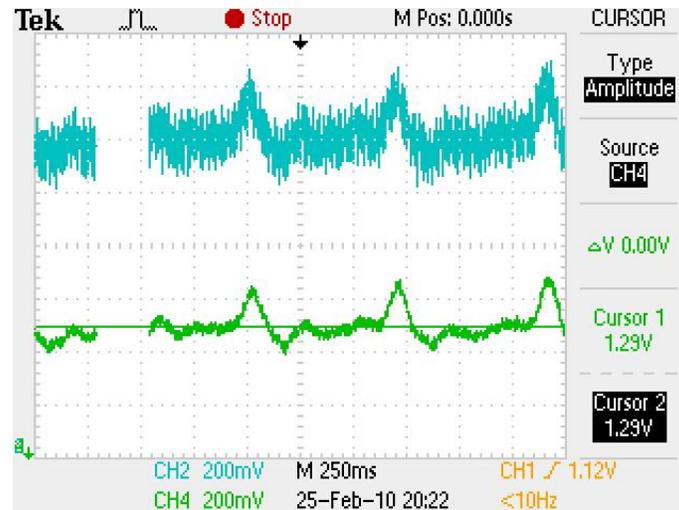


Figure 31 Filtered pulse signal

At this point in the circuit, the output waveform represents the end of signal conditioning. Almost all of the noise has been stripped from the signal, and the amplitude is high enough to warrant good threshold voltage values that will not be drastically affected by the inaccuracies of the 5% tolerance resistors that will be used.

Comparator

This next design section will convert the analog input wave of the heart beat into a “digital” signal. This means the output will either be ground (value of ‘0’) or the positive rail (a value of ‘1’). When the comparator outputs the high signal, the LED will turn on. Therefore it is imperative to turn send the output high only once per pulse beat and also to keep the output high enough so that the human eye can detect the light. These issues derive from the setting of the threshold levels. If the threshold is too high, only the tip of the pulse will break the threshold, so the comparator will only be on for a very brief time. On the other hand, if the

threshold is too low, the output will go high for not only the primary spike of the pulse but the secondary and tertiary spikes as well. An output of this nature will just seem like a malfunctioning device where the LED turns on all the time.

The solution chosen for this application was to use the scope to determine the threshold values. By monitoring the output wave, the cursor function of the oscilloscope was arranged so the voltage value that best fits the above description can be found. Figure 32 shows the wave and measured value.



Figure 32 Determining threshold values

In order to set this value as a constant DC source, a voltage divider network is implemented. Since there will always be a voltage across this network, the current draw needs to be in the low micro-amp range. Based on the following equation, it is determined that $R9 = 775K\Omega$ and that $R8 = 1M\Omega$, given that the supply voltage at this point of measure was 2.4V from the battery and the desired threshold value is 1.35V.

$$V_{th} = V_{Batt} \frac{R8}{R9 + R8}$$

Equation 8 Voltage divider for threshold

To make the output remain at 0V until the pulse wave breaks the threshold, the voltage divider network will be placed so V_{th} is at the inverting input to the op-amp. This will cause the op-amp to remain at the negative rail since the op-amp is configured with an open loop. When the pulse breaks the threshold, the op-amp will amplify the positive difference by the open loop gain, sending the output to the positive rail. This system block is depicted in the schematic below along with a scope image depicting the signal input from node 3 with an overlay of V_{th} from node 4, and the comparator output from node 5.

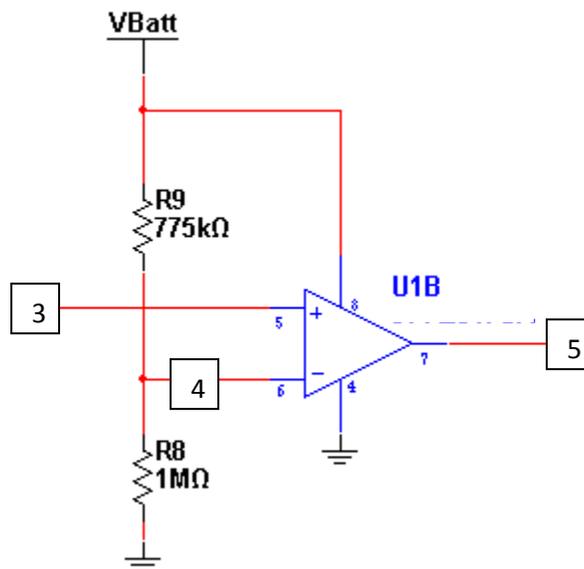


Figure 33 Comparator with threshold network

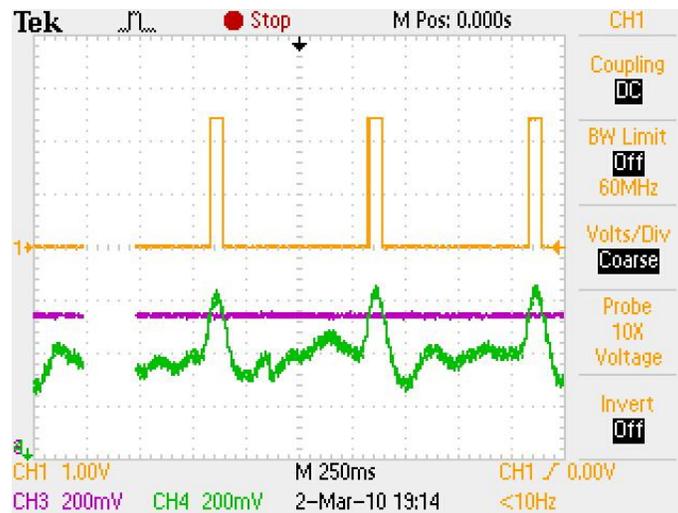


Figure 34 Comparator inputs and output

Output LED

The final stage of the pulse circuit is the output LED. Using the signal from the comparator like an On/Off switch, the LED will switch on in accordance with the pulse rate. Although the drive circuit for the output should be quite similar to the drive circuit for the infrared LED, this posed a few problems for the battery and op-amp. With each current pulse, the battery voltage drops due to the series resistance of the battery, which caused a few problems overall. However, since this subject is quite in depth, it is described in much greater detail in its own section later. The op-amp issue was easily solved. The amount of current to successfully light the output LED so that it could be detected far exceeds the amount of current that can be sourced by these low power op-amps. As a result, a new design element is added to the drive circuit.

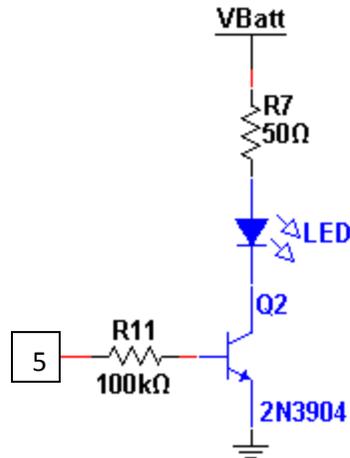


Figure 35 Schematic of output stage

By using a NPN bipolar junction transistor (BJT), Q2, the current can be sourced directly from the battery. The BJT only acts as a switch that allows current to flow from the collector terminal to the emitter¹⁴ when the voltage at the base terminal puts the device into saturation mode. Since the comparator is swinging from ground to the positive rail, each time the signal switches, the BJT turns on and allows current to flow through the LED. Therefore this is the same desired output as if it were connected directly to the op-amp output. Since the only use of Q2 is for its switching capabilities, a very common and cheap NPN can be used. Here it is chosen to be the 2N3904, a common BJT in the ECE lab kit. It should be noted, that the current limiting resistor, R7, and the LED could be placed at the output of the emitter, rather than the collector, however there is a 0.7V drop across the base-emitter terminals. This will then drop the voltage across the LED to just above its turn on voltage of 1.8V causing the LED to decrease in luminous intensity. In this configuration, the drop across the collector-emitter terminals is only 0.2V. A 100kΩ resistor, R11, is added between the output of the op-amp at node 5 and the base terminal for protection. This will ensure a massive surge of current will not occur, and

¹⁴ In this orientation, from power to ground

affect any of the components. There is no voltage drop across the resistor since it is not put to ground, so the voltage output from the op-amp is still seen in its entirety at the base terminal. R11 will keep the current running through the op-amp around $25\mu\text{A}$, at the most, only when the output goes high.

3.4.3 Difficulties

In this section, the various difficulties and obstacles in designing the above circuit will be discussed. Not every topic in this section is a problem. Some were attempts to improve the circuit for various reasons, such as power savings. This section will start with various power issues and how the battery supply affected many functions of the circuit and continue to power savings and photodetector placement.

Power Design

One of the constraints for this project was to keep all the components as flat to the board as possible. It was also abundantly clear that whatever the application was decided, it would run off a battery supply. As discussed above, the chosen battery is a 3V nominal CR2032 lithium ion coin cell with a measured series resistance of 29.6Ω . Since the pulse circuit will be drawing a constant current at the infrared LED and a pulse for the output LED, for the brief time both are on, the battery will have to supply on the order of 28mA (18mA from the former and 10mA from the latter).

With this much current flowing through that series resistance, the supply voltage drops. This drop in voltage caused a variety of circuit changes. In the original design, the desired current draws by the IRED and LED were 20mA and 15mA respectively. However, due to this great draw on the supply, the drive circuits were modified to run on minimal current while still achieving the desired effect. The input was able to sacrifice 2mA and not lose the pulse signal while the output was able to shave 5mA and still be able to brightly light the LED.

Before the final op-amp was chosen and the use of Q2 as a switching transistor was installed, the OPA2344 dual op-amp package, low power op-amp was used to drive the output LED. Although when connected to the bench power supply the circuit had no problems, once the battery was installed, the dropping supply voltages caused the op-amp to oscillate at a varying frequency of 10-15Hz. Once the op-amp began to oscillate the entire circuit became unstable and began to oscillate as well. In the below left image, from top to bottom using the nodes as depicted in the above schematics, the waves correspond to nodes 0, 1, 2 and 3. Below right from top to bottom correspond to V_{Batt} , node 3 (for reference), node 4 and 5.

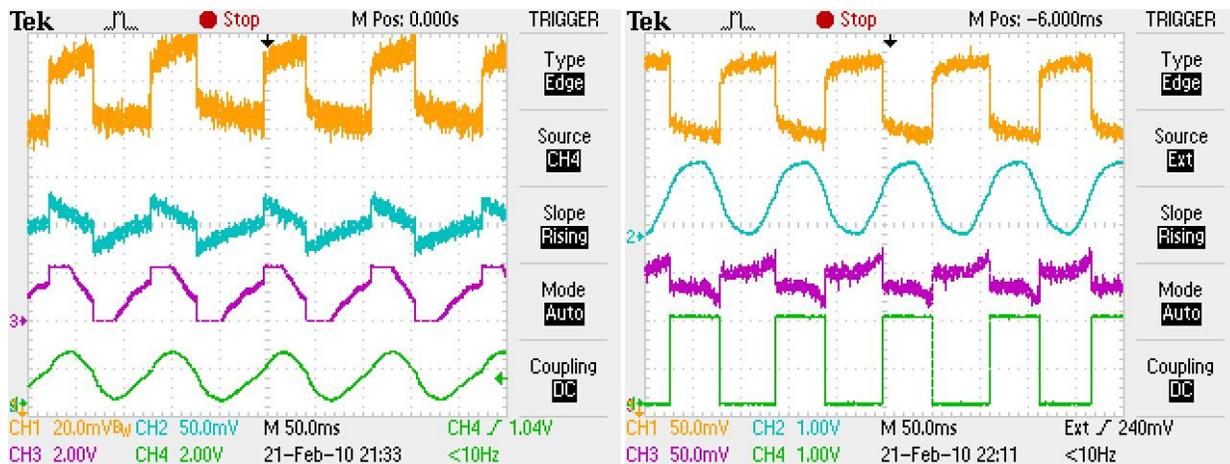


Figure 36 Oscillating system

After switching to the OPA2337, the oscillations ceased to exist. However, the true solution was to redirect the surging current for each pulse at the output away from the op-amp. This allows the op-amp to keep a high impedance output and not need to source so much current. With this problem solved, the slight dip in supply voltage was able to be compensated for by the op-amp even when the original OPA2344 was installed.

Pulsing IRED

As a way to conserve battery life, the idea of pulsing the IRED was investigated. In principle, the pulsing IRED will act as a sampler on the analog signal that is one's pulse. As long as the IRED turns on at twice the heart beat, or at the Nyquist frequency, the full waveform will be able to be reconstructed and the circuit will work to specification.

In order to achieve this, a timing IC was used: the LM555CN. Similar to the standard 555 timer, the 555C is the low power CMOS version. Taken from the LM555CN datasheet, the frequency of oscillation in the astable mode and the duty cycle can be calculated using the following equations:

$$D = \frac{R_1}{R_1 + R_2} \qquad F = \frac{1.38}{(R_1 + 2R_2)C}$$

Equation 9 Duty cycle (left) and frequency (right)

Also from the datasheet, the circuit is to be connected such that the above resistors correspond to the schematic as seen below. The duty cycle was chosen to be at 10%, to make the average power used be just 1/10th of the continuous current, thus elongating the battery life by a factor of 10. The frequency was set at 100Hz to ensure the full waveform including the non primary pulses were able to be sampled correctly with some oversampling. These specifications resulted in some rather exact resistor values that were able to be recreated due to the 5% tolerance.

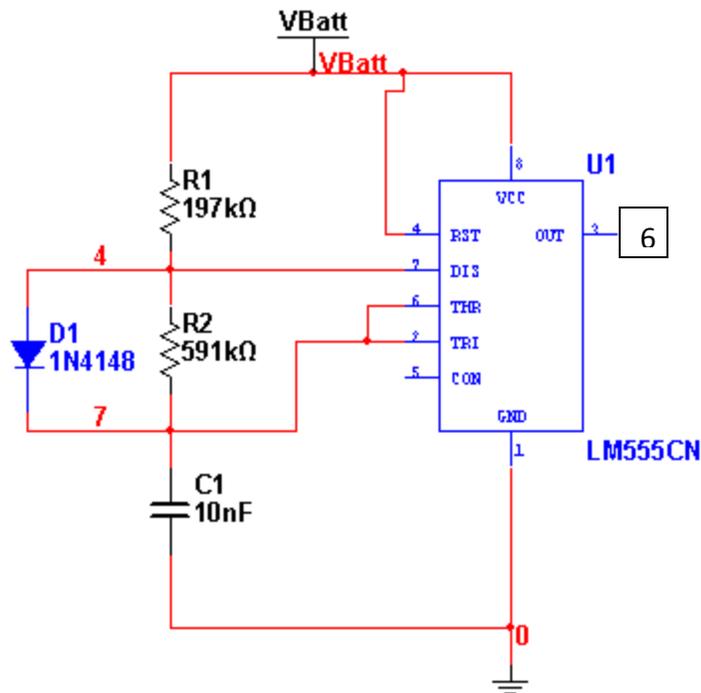


Figure 37 Oscillating circuit

Although the output at node 6 above is the desired 10% duty cycle at 100Hz, when inserted into the circuit, another component prevented it from solving the power issue. When a finger is first pressed against the IRED and phototransistor, the 10 μ F capacitor in the amplifier feedback network, C4, takes time to acquire the AC signal of the pulse from the constant DC ambient light. Due to the size of the capacitor and the length it takes to charge (greater than one second), the circuit is never able to charge that capacitor and condition the pulse signal before the LM555CN output drops to 0V. The resulting image depicts the output from node 6 above as well as the waveform as measured from node 3 in the above schematics. The signal waveform can be seen riding the rail until the pulse comes. At this point the signal wave begins to acquire, but the output switches immediately. For this reason, this idea was rejected as a viable option, and further pursuit of saving battery life from this angle was ceased.

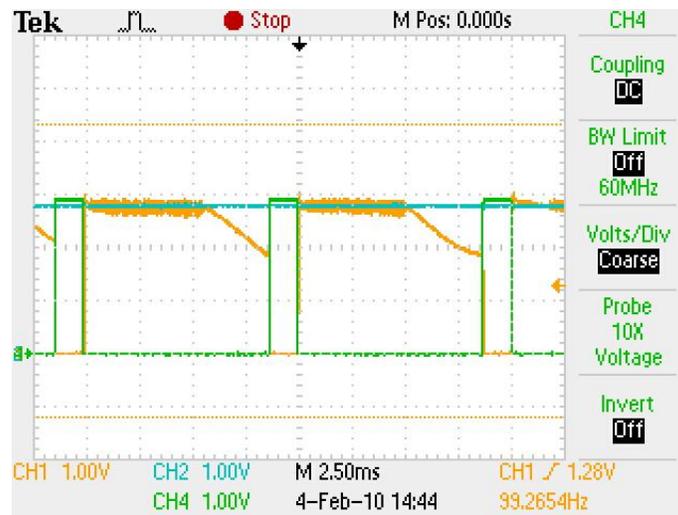


Figure 38 Effects of oscillating input

Phototransistor Placement

As mentioned in the background research section, the position of the phototransistor with respect to the incident light has a great effect on the type of results produced. A big concern is saturating the phototransistor with some much light that the pulse signal gets lost in noise. There were two ideas for the arrangement of the devices. Both were in the same package, two terminal surface mount rectangles measuring 3.2mm by 1.6mm. The two possible configurations can be seen below.

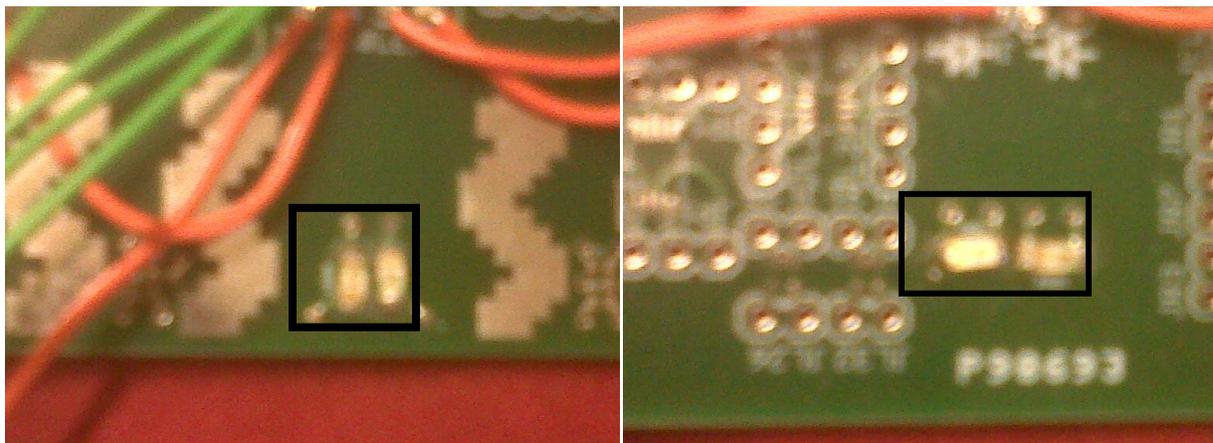


Figure 39 Side by side (left) and end to end (right)

Since this decision had to be made very early in the circuit design, many of the parameters were not set to optimal values. The op-amp being used at this stage, while the low power, rail-to-rail OPA range of op-amps was being ordered, was the LM358. This is also a dual packaged, single supply op-amp as well. Regardless of this fact, the comparisons were made using the same initial conditions so the test was fair. The output signal at node 3 was observed using both methods.

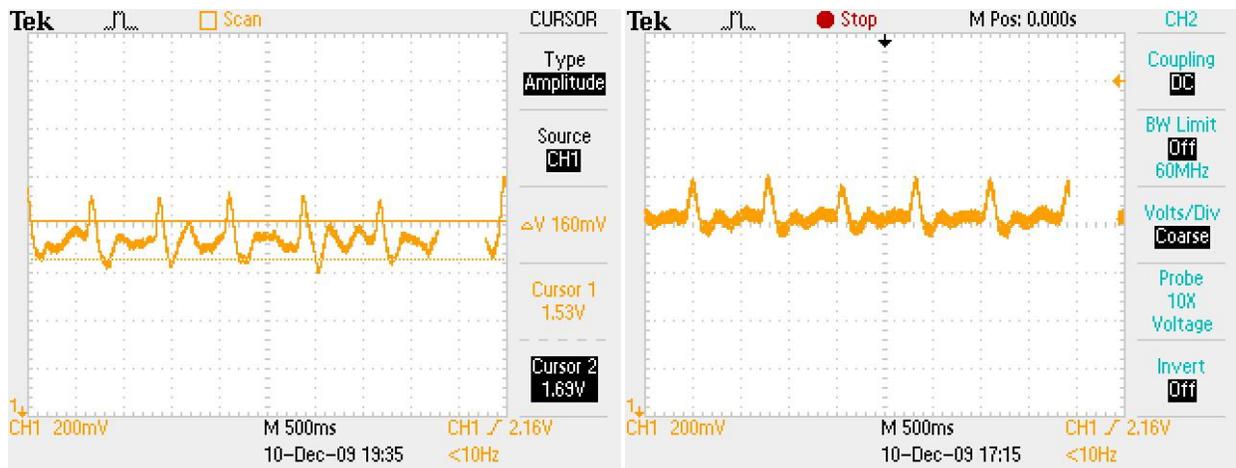


Figure 40 Side by side (left) and end to end (right)

Since these scope images were taken after the filter stage, it was decided to go with the side by side configuration due to the more defined signal with greater amplitude as well as less noise attached to the signal.

3.4.4 Component Selection

3.4.5 Measurement and Results

3.5 Electrocardiogram (ECG)

This section will explain the electrocardiogram design details, including prior art and background research, a detailed explanation of the measurements and results will guide the reader through the progression of the design process, and then lead to an explanation of the final design of the circuit. The last section details the selection of components for the circuit.

3.5.1 Background Research

Before beginning any design work, it is important to conduct research on the background of the design. The following section reviews electrocardiograms in general, as well as other existing products that are similar to this project.

3.5.1.1 Electrocardiogram

An electrocardiogram is a device that detects and displays the electrical signals of the heart. Using an ECG allows a person to see the exact heartbeat of a user. Measurements are taken using a device called an electrode. Electrodes are placed on the user's skin and can detect extremely small changes in voltage.

Most electrocardiograms today use three electrodes: two placed across the heart to obtain its signal, and a third placed on the lower part of the leg to send a ground signal back through the user. The design of the ECG in this project is unique in that it will only use two electrodes, one on each thumb.

Human Pulse

The human pulse, shown in Figure 41, is characterized by five points on the wave, better known as the PQRST points. The actual "beat" of the heart is the QRS wave. This signal is

typically $\sim 17\text{Hz}$ ^{15,16,17}. For the purpose of this project, we will focus only on the QRS complex, ignoring the P and T waves. Although the entire waveform of the heartbeat will not be seen, each pulse will still be able to be detected.

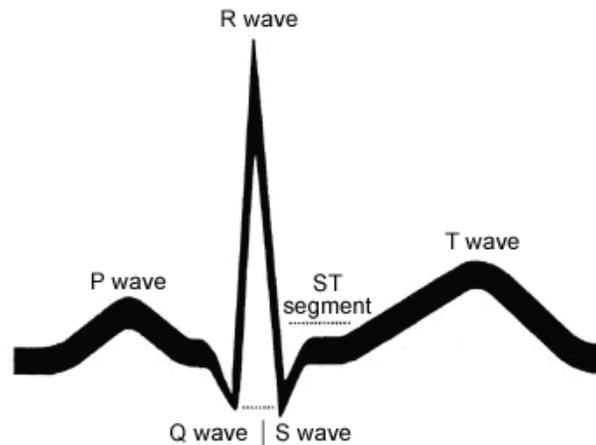


Figure 41 Typical human pulse¹⁸

3.5.1.2 Existing Products

There are not many commercial products on the market that use the two-electrode configuration. The following is a brief report on the most concrete data on this subject.

Pulse Sensors on Treadmills

Heart rate monitors that are on treadmills detect signals through the hand area. A pulse rate can be sensed in the palm and finger tips. The treadmill pulse sensor consists of wireless hand grips and a receiver module. The hand grips sense the electrical signals generated by the heart. For each pulse detected, a signal is transmitted to the receiver module, and the individual's pulse rate is calculated. This type of hand-grip heart rate monitor includes one

¹⁵ http://www.mathworks.com/access/helpdesk/help/toolbox/signal/qr_filtered.png

¹⁶ http://www.scienceprog.com/wp-content/uploads/2007i/Wiener/ECG_signal%20model.jpg

¹⁷ <http://www.swharden.com/blog/images/ecg2.jpg>

¹⁸ <http://www.a-fib.com/images/PQRST%20Wave%20graphic%20JPEG%20Complete.jpg>

transmitter and one receiver. This way of measuring heart rate and pulse is not the most accurate. However, the more one's skin is conductive (sweaty) the more accurate the reading will be. Although treadmill pulse sensors work the same way as ECGs, nurses have the ability to put conductive material (gel) on a patient before using equipment. Electrocardiography is a transthoracic interpretation of the electrical activity of the heart over time and externally recorded by skin electrodes. Electrical impulses in the heart originate in the sinoatrial node and travel through the intrinsic conducting system to the heart muscle. The impulses stimulate the myocardial muscle fibers to contract and thus induce systole. The electrical waves can be measured at selectively placed electrodes (electrical contacts) on the skin. Electrodes on different sides of the heart measure the activity of different parts of the heart muscle. An ECG displays the voltage between pairs of these electrodes and the muscle activity that they measure from different directions, also understood as vectors. This display indicates the rhythm of the heart and any weaknesses in different parts of the heart muscle. These are very accurate.

AD8236 Datasheet

On page 19 of the AD8236 datasheet¹⁹, Analog Devices suggest that if only two electrodes are used, one of them can simply be grounded to obtain an accurate signal.

3.5.2 Progression of Design: Measurement and Results

This section will discuss the details and steps follow that led to the final design. It will increment through each analysis in chronological order, as done by the designer. If the reader wishes to read about the final design, skip to section 3.5.3 Final Circuit Design.

¹⁹ http://www.analog.com/static/imported-files/data_sheets/AD8236.pdf

3.5.2.1 Initial Brainstorming

The first step in the design process is to brainstorm circuit configuration ideas. To aid in this process, an initial top-level block diagram is constructed, as seen below in Figure 42.

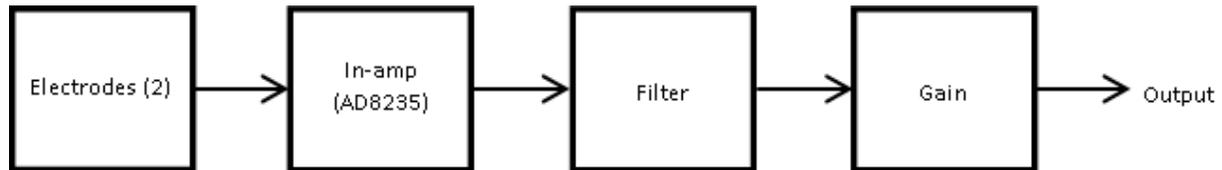


Figure 42 Initial ECG block diagram

Filter Design

The most important part of an ECG is the filter. A well-designed filter allows for the engineer to choose exactly which frequencies will pass through to the output. The pulse of a heart has a very precise frequency, and any muscle movement may hinder the visibility of the pulse. Therefore, a very accurate filter is a necessity.

Bandwidth and Q Factor

The filter is the most vital part of the ECG. A well designed filter will allow for a clean pulse signal with minimal noise. For this design, a bandpass filter that is centered at 17 Hz is best. Experts say that the best band-pass Quality Factor (Q) value for QRS detection centered at 17 Hz is $Q = 5^{20}$. Referencing the definition of the quality factor,

$$Q = \frac{f_r}{BW}$$

Equation 10 Quality Factor, f_r = resonant frequency, BW = bandwidth

a bandwidth of 3.4 Hz is needed. Therefore, the high-pass cutoff frequency is 15.3 Hz and the low-pass cutoff frequency is 18.7 Hz. Since this design requires such a precise bandwidth, it is

²⁰ Thakor et al. and Valtina X. Afonso

important to have a filter that is as close to ideal as possible. An ideal band-pass filter with a Q of 5 implies that the high-pass and low-pass filters must have a mathematically flat frequency response ($Q = \frac{1}{\sqrt{2}}$). This is why a Butterworth filter is the best choice.

NOTE: For more information on Q Factor: <http://www.beis.de/Elektronik/AudioMeasure/UniversalFilter.html>
For more information on Butterworth filters: http://www.electronics-tutorials.ws/filter/filter_8.html

Sallen-Key Second Order Butterworth Filter

A second order filter will provide a frequency attenuation of ± 40 dB/dec instead of ± 20 dB/dec for a first order filter. The Sallen-Key topology uses only four passive components (two capacitors and two resistors) and one active component (an op amp). The generic topology for this filter is displayed in Figure 43.

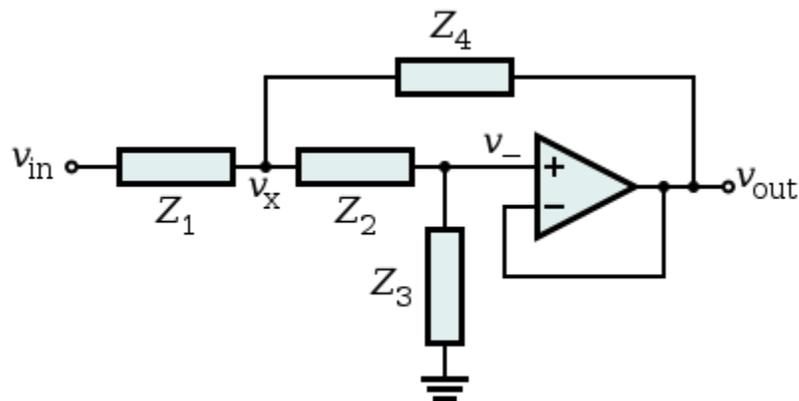


Figure 43 Sallen-Key circuit topology²¹

In this design, two Sallen-Key filters will be used: one as a high-pass filter and one as a low-pass filter. This configuration is intended to block out every frequency except the one we need: 17 Hz. To act as a high-pass filter, Z_1 and Z_2 are capacitors, and Z_3 and Z_4 are resistors. For a low-pass filter, the opposite configuration is needed.

²¹ http://en.wikipedia.org/wiki/File:Sallen-Key_Generic_Circuit.svg

Design of High-Pass Filter

The Sallen-Key topology allows for the simple design of a second order Butterworth filter. Figure 44 below shows the Sallen-Key second order high-pass filter configuration.

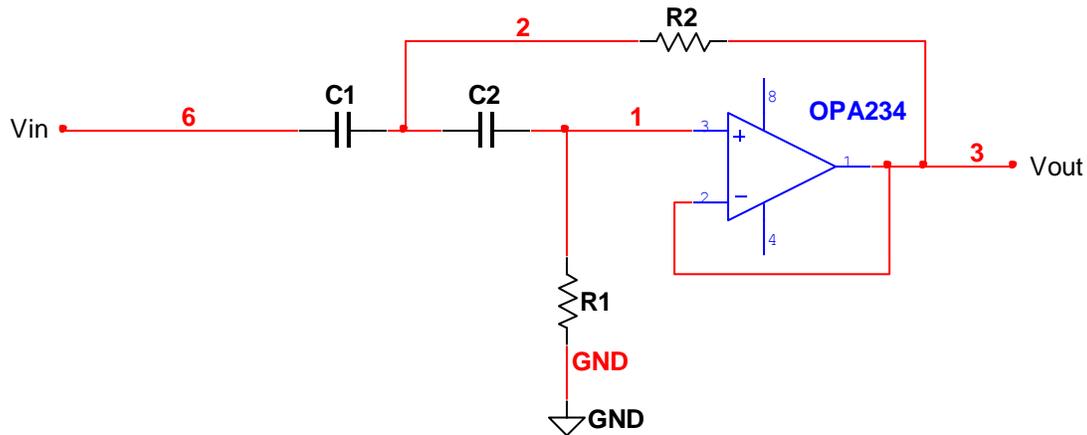


Figure 44 High-pass Sallen-Key second order filter

Equation 11 is used to calculate the cutoff frequency:

$$f_c = \frac{1}{2\pi\sqrt{R_1 R_2 C_1 C_2}}$$

Equation 11 Sallen-Key filter cutoff frequency

Equation 12 is used to calculate the Q Factor for the high-pass filter:

$$Q = \frac{\sqrt{R_1 R_2 C_1 C_2}}{R_2 C_2 + R_2 C_1}$$

Equation 12 Sallen-Key high-pass filter Q Factor

For a complete derivation of Equation 11 and Equation 12, refer to Appendix A – Derivation of Cut-off Frequency for Sallen-Key Filter.

In order to make this into a Butterworth filter, a Q of $\frac{1}{\sqrt{2}}$ is needed. This can be accomplished by setting $R_1 = 2 * R$, $R_2 = R$, $C_1 = C$, and $C_2 = C$. Using these ratios, we

can now plug R and C values into Equation 11 to achieve a cutoff frequency of 15.3 Hz. The actual component values used in this project can be seen below in Figure 45.

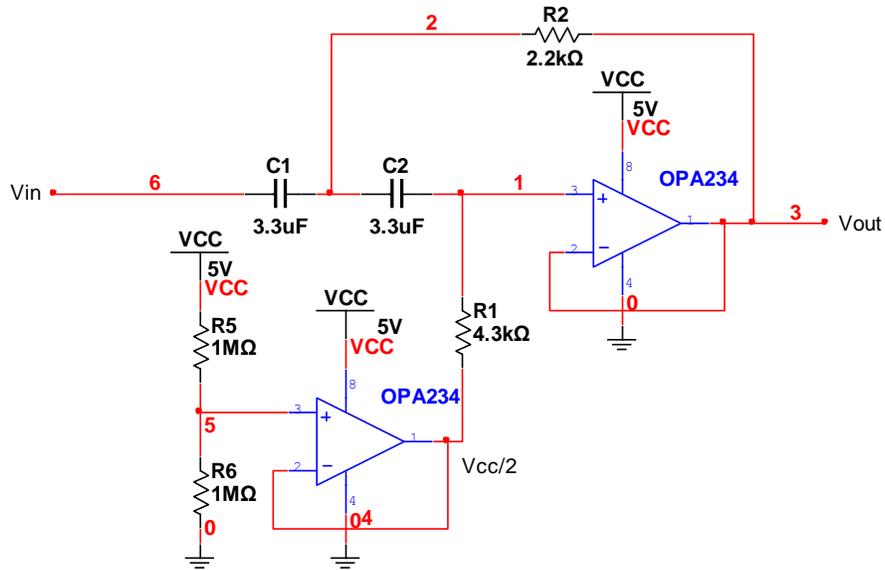


Figure 45 High-pass filter used in design

It is important to note that $\frac{V_{CC}}{2}$ was substituted for ground in the filter in order to account for the single-supply op amp. Doing this allows the calculations to remain equal to that of a dual-supply configuration.

Design of Low-Pass Filter

Figure 46 below shows the Sallen-Key second order low-pass filter configuration.

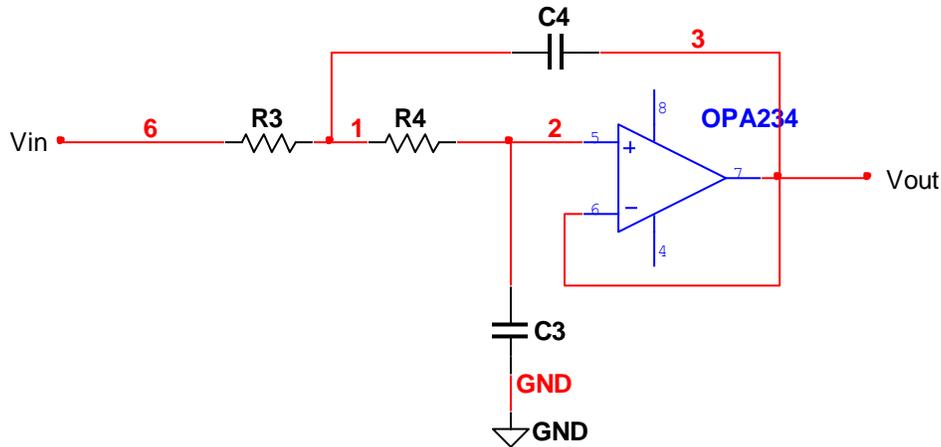


Figure 46 Low-pass Sallen-Key second order filter

The equation for the cutoff frequency is the same as for the high-pass, so Equation 11 is still used.

Equation 13 is used to calculate the Q Factor for the low-pass filter:

$$Q = \frac{\sqrt{R_1 R_2 C_1 C_2}}{R_1 C_1 + R_2 C_1}$$

Equation 13 Sallen-Key low-pass filter Q Factor

For a complete derivation of Equation 11 and Equation 13, refer to Appendix A – Derivation of Cut-off Frequency for Sallen-Key Filter.

In order to make this into a Butterworth filter, a Q of $\frac{1}{\sqrt{2}}$ is needed. This can be accomplished by setting $R_1 = R$, $R_2 = R$, $C_1 = C$, and $C_2 = 2 * C$. Using these ratios, R and C values can be plugged into Equation 11 in order to achieve a cutoff frequency of 18.7 Hz. The actual component values used in this project can be seen below in Figure 47.

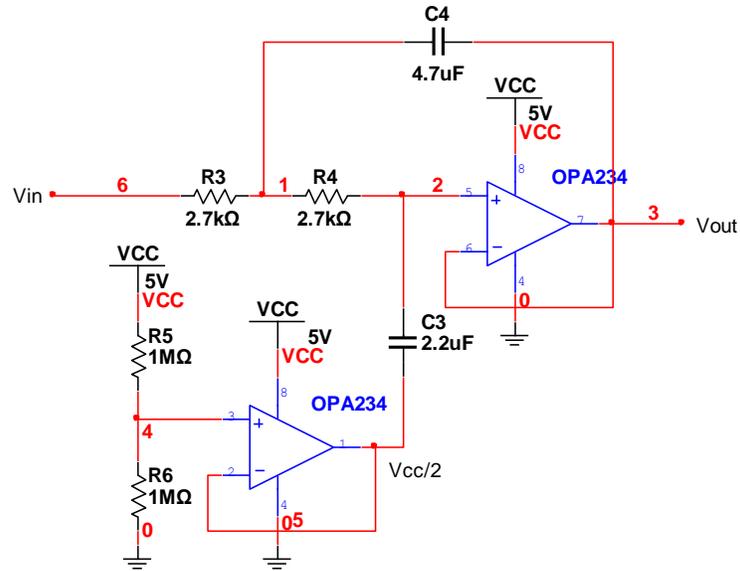


Figure 47 Low-pass filter used in design

It is important to note that $\frac{V_{CC}}{2}$ was substituted for ground in the filter in order to account for the single-supply op amp.

Complete Filter

The next step is to combine the high-pass and low-pass filters to create a bandpass filter. Figure 48 shows the complete filter used in this project.

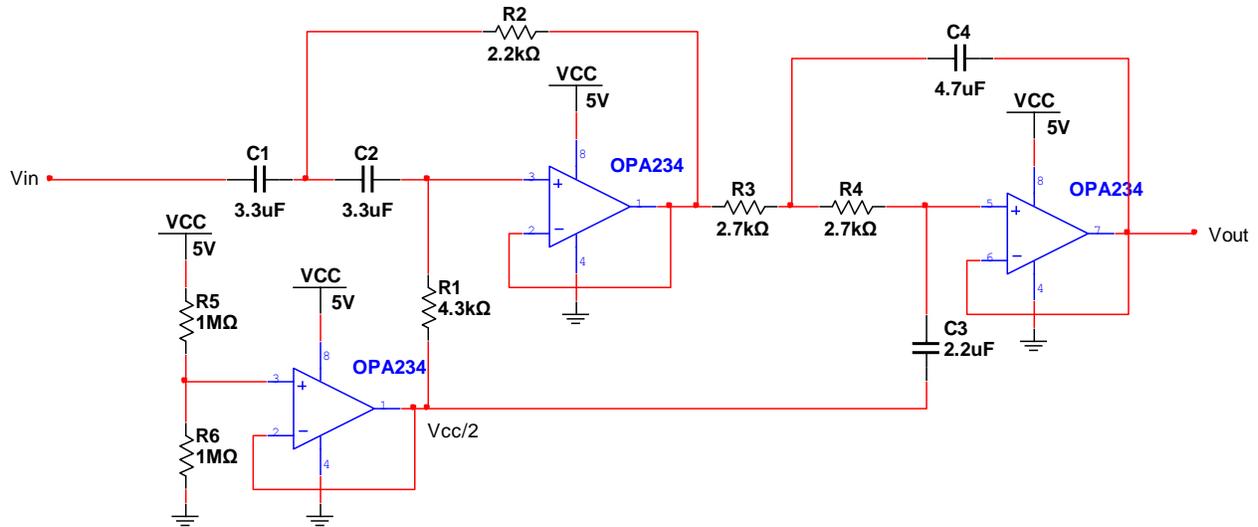


Figure 48 Complete Sallen-Key second order bandpass Butterworth filter

Simulation of Sallen-Key Second Order Bandpass Butterworth Filter

Before any physical circuits were built, the bandpass filter shown in Figure 48 was tested using NI Multisim as a simulation tool. A 5Vpp AC voltage source with an offset of 2.5V was attached to node Vin for the simulation. The results are seen below in Figure 51, Figure 50, and Figure 51.

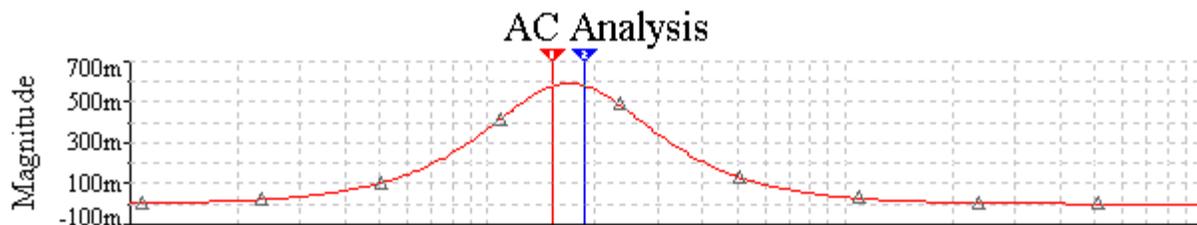


Figure 49 Linear frequency response of bandpass filter

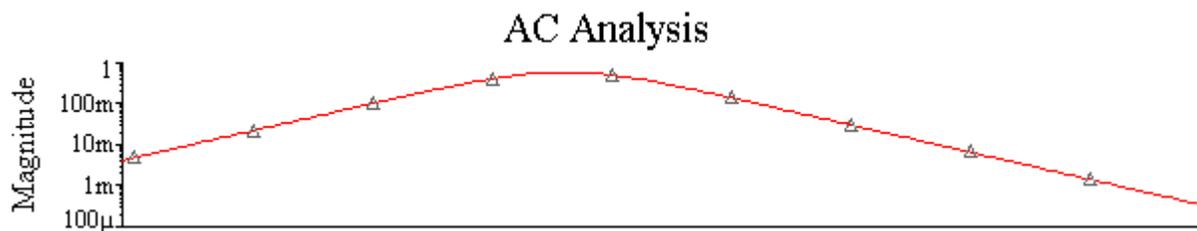


Figure 50 Bode plot of bandpass filter (dB)

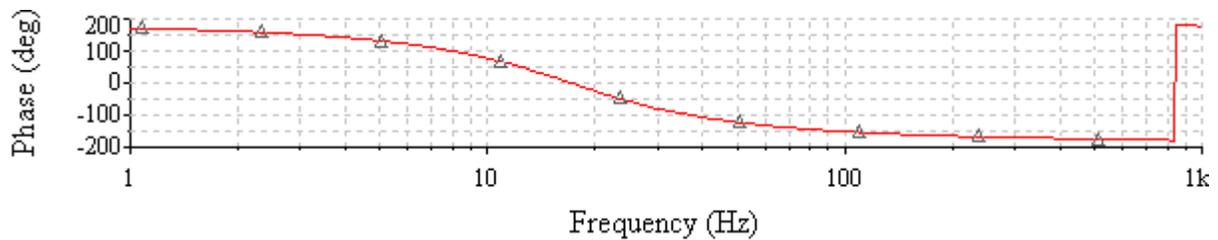


Figure 51 Phase versus frequency of bandpass filter

The simulated filter behaved as expected. Although it is not a perfect filter, it is anticipated that it will eliminate most of the unwanted frequencies in the circuit.

3.5.2.2 First Prototype

The first ECG circuit tested had two disposable electrodes going into an instrumentation amplifier with programmable gain, followed by the bandpass filter seen in Figure 48. The first circuit (with the AD624), seen in Figure 52, was built on a breadboard using a $\pm 5V$ dual supply. Two LM741 op amps were used for the filter. The second circuit (with the AD8236), seen in Figure 57, was soldered onto the prototyping board (Figure 15) and the OPA2348 low power single supply dual op amp in an SOT23-8 package was used for the filter. Both circuits were then amplified using a non-inverting op amp configuration in order to increase the visibility of the signal.

AD624

Figure 52 below shows the breadboarded circuit with the AD624 (circled in red) at the input.

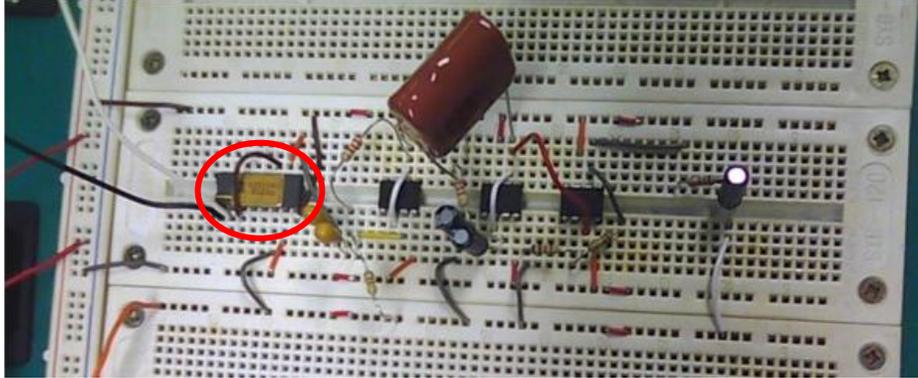


Figure 52 First ECG circuit, using the AD624

The first stage of this circuit was the AD624 instrumentation amplifier. The human heartbeat is estimated to have a voltage between 0.5 and 4mV²². A safe approximation of 8mV was used in the calculation for the in amp amplification. The highest pin-programmable gain on the AD624 of $500 \frac{V}{V}$ was used. This gives a maximum in amp output signal of $0.008V * 500 \frac{V}{V} = 4V_{pp}$. This value is close to the 5Vpp used in simulation.

This in amp output signal was sent directly into the filter. According to simulation, the filter's output using a 5Vpp input is 500mVpk, or 1Vpp. This is an attenuation of $\frac{1V}{5V} = 0.2 \frac{V}{V}$ for the filter. Therefore, the output signal from the breadboarded circuit is expected to be $4V_{pp} * 0.2 \frac{V}{V} = 0.8V_{pp}$. Hence, a gain of $\frac{5V}{0.8V} = 6.25 \frac{V}{V}$ was applied using the non-inverting op amp configuration.

The following pictures were taken from the amplified output with the electrodes in three different configurations: across the heart, on the back of each hand, and on each thumb.

²² Webster, John G., Medical Instrumentation

There was difficulty at first with reading the signal. In order to achieve the signals seen below, the user had to remove his shoe and ground his foot by touching it to a nearby metal frame. Without taking this precaution, only noise was seen.

Although some noise was seen, the signal from the electrodes across the heart produced a very clear pulse, shown in Figure 53.

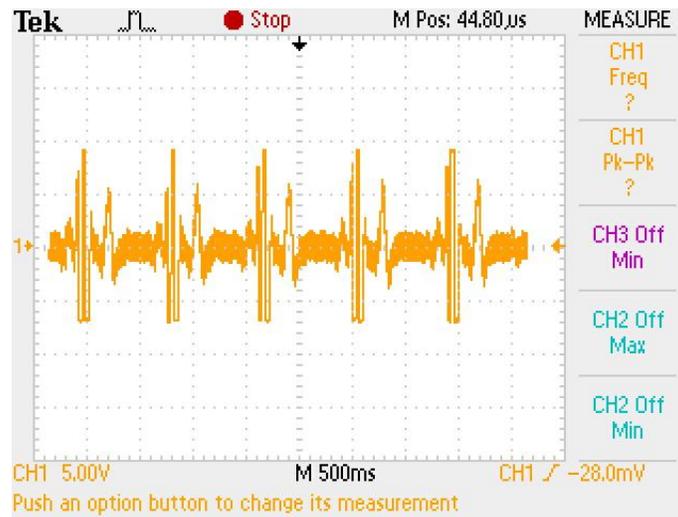


Figure 53 ECG output signal across heart

When the electrodes were placed on the back of the user's hands, the pulse was much harder to see than the initial trial; although it was still visible. This is shown in Figure 54.

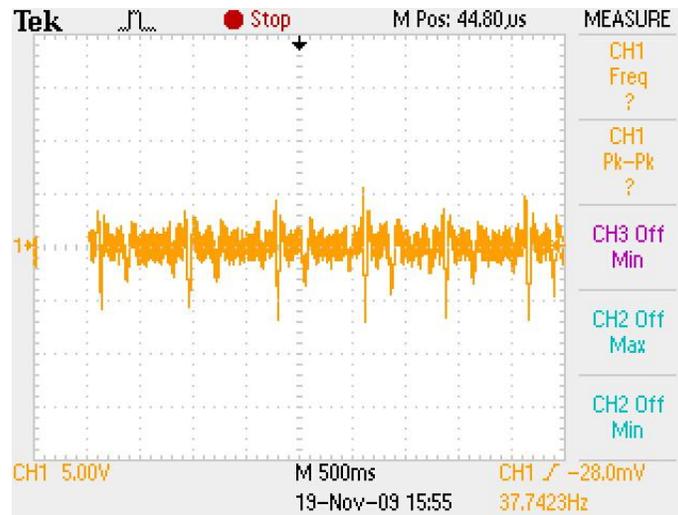


Figure 54 ECG output signal on back of hands

When the electrodes were in the configuration across the user's thumbs, a much smaller signal was seen; therefore, the gain of the non inverting amplifier was increased by a factor of 5. After this increase in voltage, the pulse is slightly visible to the human eye, although there is a significant amount of noise present. The signal is shown in Figure 55.

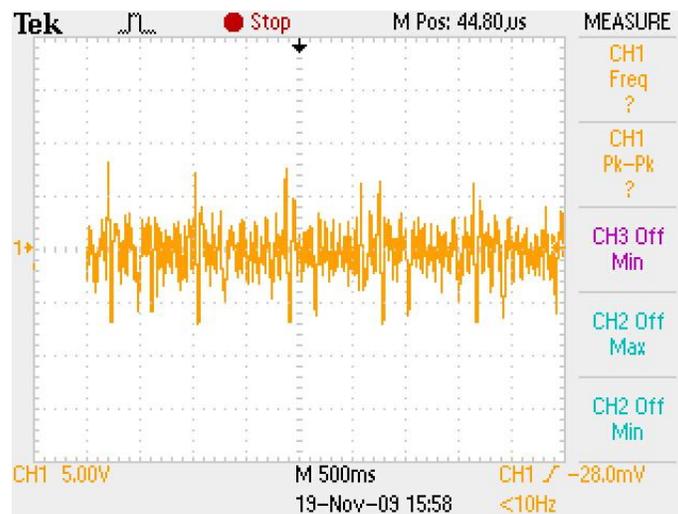


Figure 55 ECG output signal on thumbs

Figure 56 is the same signal as above, zoomed in to show each pulse more clearly.

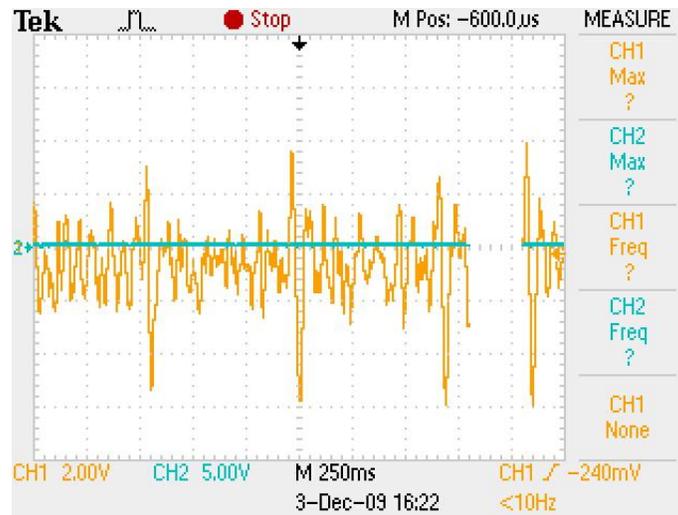


Figure 56 ECG output signal on thumbs zoomed in

AD8236

The next circuit used the same configuration, but with different components. The AD624 was swapped with the AD8236, and the LM741's were replaced by the OPA2348. This made it possible for the entire circuit to be soldered onto the prototyping PCB (Figure 15), and to be powered using a single supply configuration. The physical layout of the circuit is shown in Figure 57, with the AD8236 circled in red and the OPA2348 circled in blue on the left side, and the filter on the right side. The DIP package in the photo on the right was used to set the reference voltage V_{REF} for the filter.

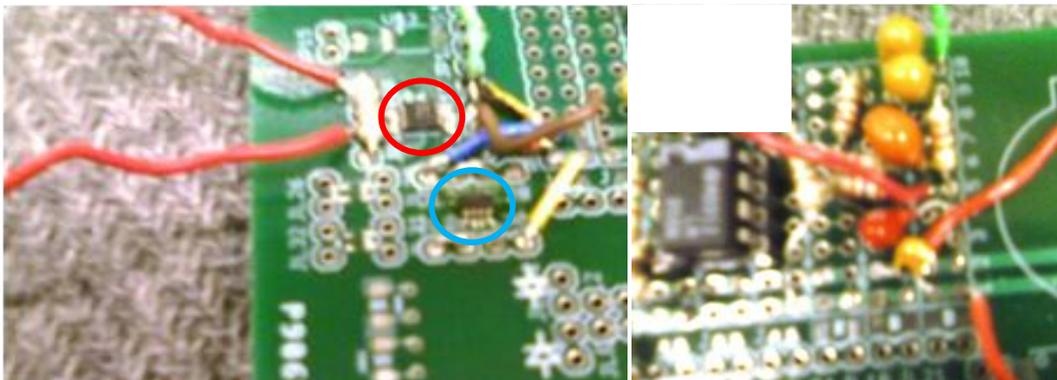


Figure 57 Second ECG circuit using the AD8236

The AD8236 has a built-in programmable gain function. This feature is used by adding a resistor, R_G , across pins 2 and 3. For this circuit, a 3.3V single supply voltage is used in order to simulate the coin cell battery we plan to use on the simple circuit (3.1.2 Power Supply). Using the maximum safety value of 8mV for a human heartbeat, this yields a gain of $\frac{3.3V}{0.008V} = 412.5 \frac{V}{V}$. However, according to Table 6 of the AD8236 datasheet²³, the maximum gain that can be achieved while avoiding severe gain error and drift is $G = 200.3 \frac{V}{V}$. This is using a 2.15k Ω gain resistor, calculated using Equation 14:

$$R_G = \frac{420k\Omega}{G - 5}$$

Equation 14 Gain equation for the AD8236

The resistor used in this project is 2.2k Ω , resulting in a gain of $G = 196 \frac{V}{V}$. This will yield a maximum in amp output signal of $0.008V * 196 \frac{V}{V} = 1.57V$.

The AD8236 circuit did not produce a very accurate pulse. The only electrode configuration that allowed for a visible pulse signal was across the heart. This signal is seen in Figure 58.

²³ http://www.analog.com/static/imported-files/data_sheets/AD8236.pdf

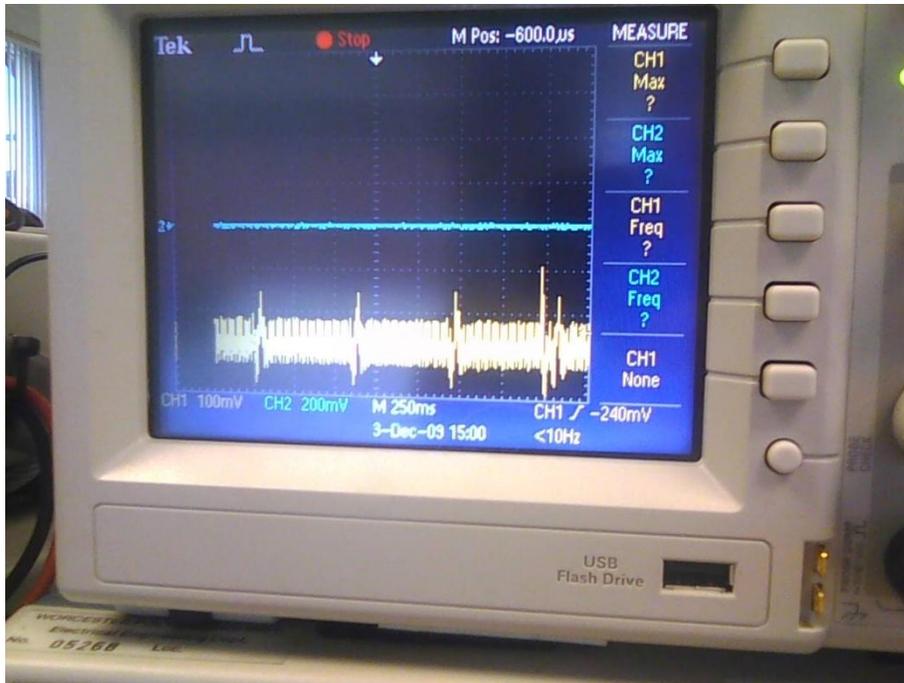


Figure 58 ECG output signal across heart

It can be clearly seen that there is a significant amount of noise that is altering the desired signal from the heart. In order to find the source of the problem, the oscilloscope probe was moved directly to the output of the AD8236, with the electrodes still placed across the heart. Figure 59 displays this signal.

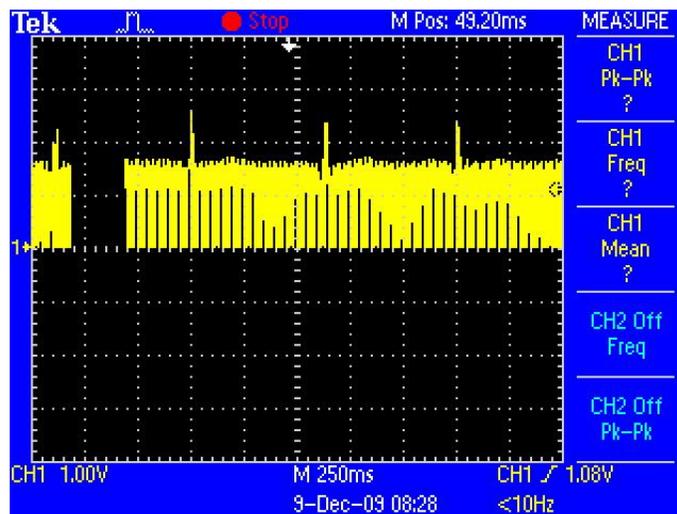


Figure 59 AD8236 output signal across heart

In the figure above there appears to be a repeating (perhaps sinusoidal) waveform. The next picture (Figure 60) shows this repeating waveform on a much smaller time scale.

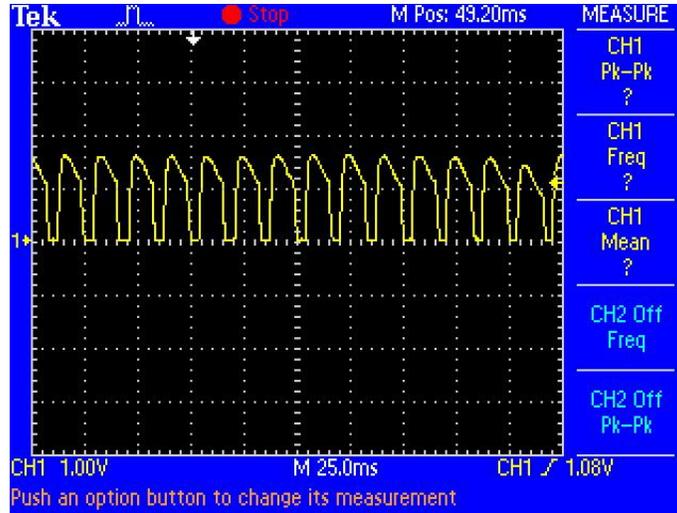


Figure 60 AD8236 output signal across heart (zoomed in)

Figure 60 shows a precisely repeating signal. Figure 61 is this same signal, zoomed in even further, and showing a single pulse, which is represented by the highest voltage in the signal (center of the snapshot).

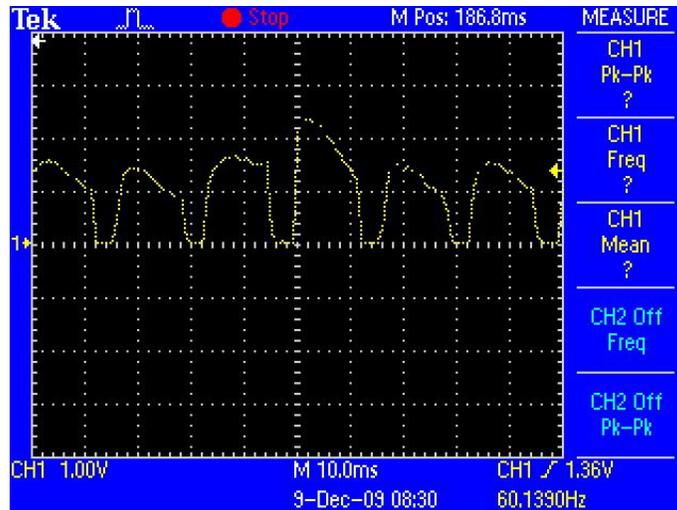


Figure 61 AD8236 output signal across heart (greatly zoomed in)

The same noise was also seen when the electrodes were placed on the thumbs, as seen in Figure 62.

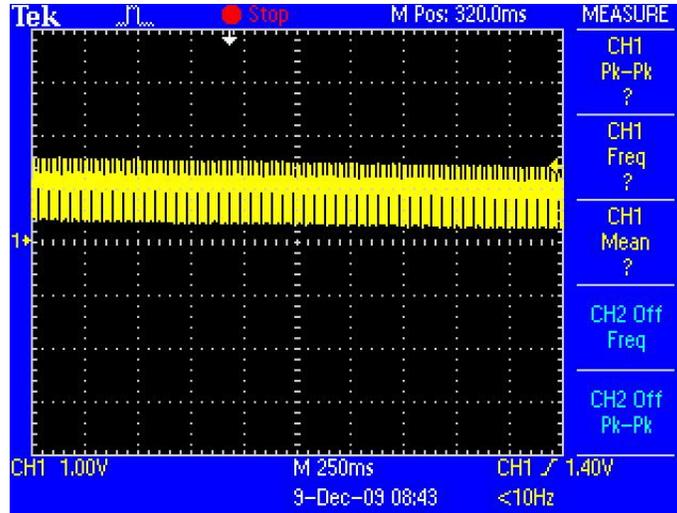


Figure 62 AD8236 output signal on thumbs

This signal is seen on a smaller time scale in Figure 63.

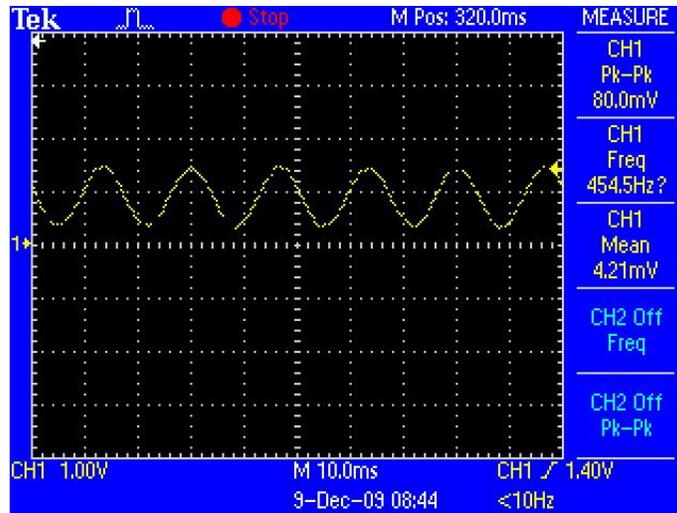


Figure 63 AD8236 output signal on thumbs (zoomed in)

The typical period of this noise is $T = \sim 17.5ms$. The frequency can be found using the frequency/period relationship, $f = \frac{1}{T}$: $f = \frac{1}{0.0175s} = 57.14 Hz$. This can be assumed to be 60 Hz noise. This 60 Hz noise is the main cause of the pulse signal distortion.

The next step in the design process is to eliminate this 60 Hz noise from the output, with the goal of achieving a cleaner signal.

60 Hz Notch Filter

A notch filter aims to eliminate a single frequency while allowing every other frequency to pass through. There are many ways to design a notch filter; however, for this design, the Twin T configuration is the most practical and economical.

Twin T Configuration

One of the most commonly used notch filters is the Twin T Notch Filter. This filter can be constructed in either a passive or an active configuration. Since a high Q will not provide a substantial benefit to the overall ECG filter, this design will focus on the passive configuration, which can be seen in Figure 64.

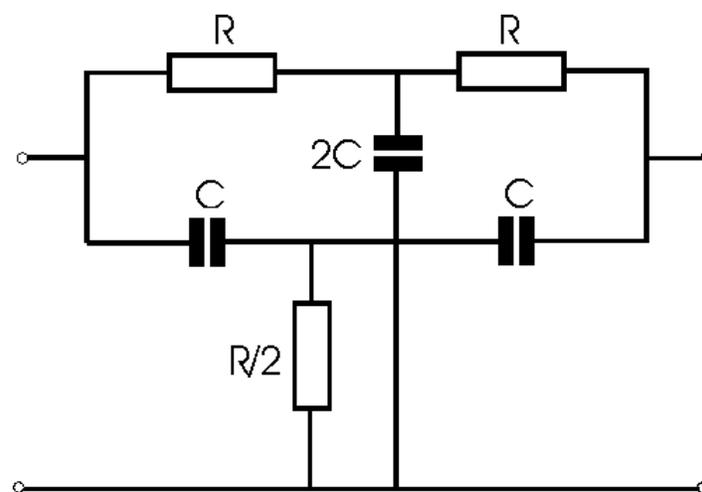


Figure 64 Passive Twin T configuration²⁴

There are a few benefits to this type of filter. The first advantage is that it can be implemented on any signal with a low current and not affect the signal's DC bias value. This

²⁴ http://www.radio-electronics.com/info/circuits/rc_notch_filter/rc_twin_t.gif

means that the filter can use the common ground instead of the virtual ground (i.e. $\frac{V_{CC}}{2}$) used in the Sallen-Key filters. The second advantage is that it can be implemented using only passive components.

Choosing Component Values

Using the R and C ratios given in Figure 64, the center frequency of the notch filter is given by:

$$f_n = \frac{1}{2\pi RC}$$

Equation 15 Center frequency for notch filter

NOTE: For more information on the Twin T notch filter including a derivation of the transfer function and notch frequency: <http://www.drp.fmph.uniba.sk/ESM/twin.pdf>

In order to keep cost down and save on board space, it is good to use small capacitor values. To obtain a notch frequency of ~60 Hz, this filter uses $C = 0.01\mu F$ and $R = 270k\Omega$. The resulting circuit is seen in Figure 65.

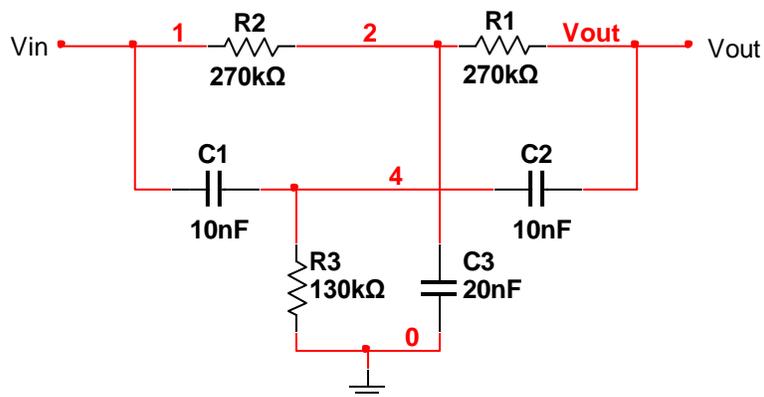


Figure 65 60 Hz Twin T notch filter used in design

Simulation

To ensure that this circuit works properly, a 2Vpp AC voltage source with an offset of 1V was attached to node Vin and an AC analysis was done. Figure 66 shows the voltage magnitude versus frequency response in a linear and logarithmic fashion as well as the phase plot of this filter.

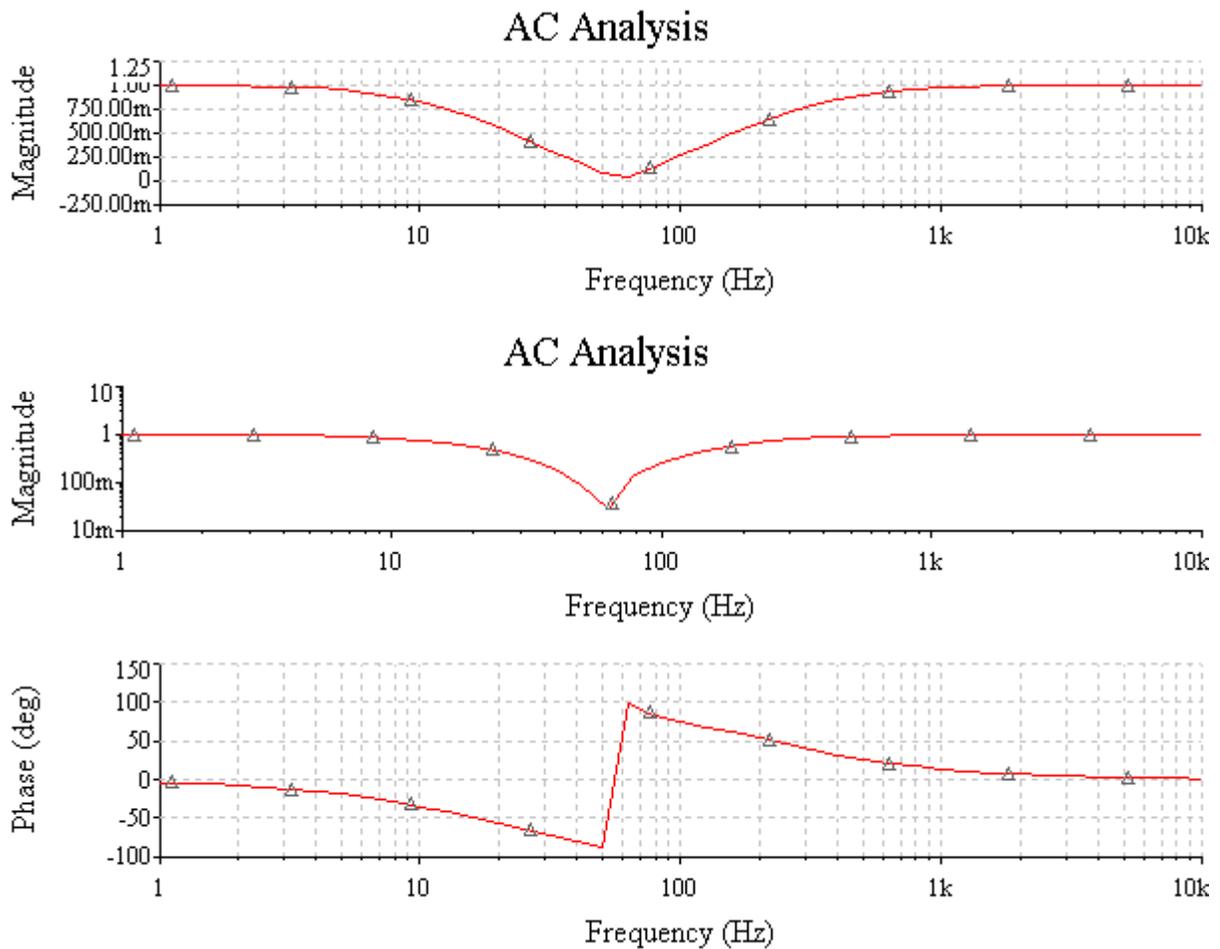


Figure 66 Frequency and phase plot for 60 Hz notch filter

This filter is centered accurately at 60 Hz. Although there is a slight attenuation at 17 Hz due to the low Q value, it will not affect the over performance of the circuit. All of these factors led to the conclusion that a passive Twin T notch filter can be effectively used to stop the 60 Hz noise in the circuit.

3.5.2.3 Second Prototype

The next circuit constructed was the same as the first prototype seen in the previous section (3.5.2.2 First Prototype), but with the 60 Hz notch filter (Figure 65) added to the output of the bandpass filter (Figure 48). The resulting filter is seen in Figure 67. The power supply was increased to 5V in order to replicate the USB supply voltage.

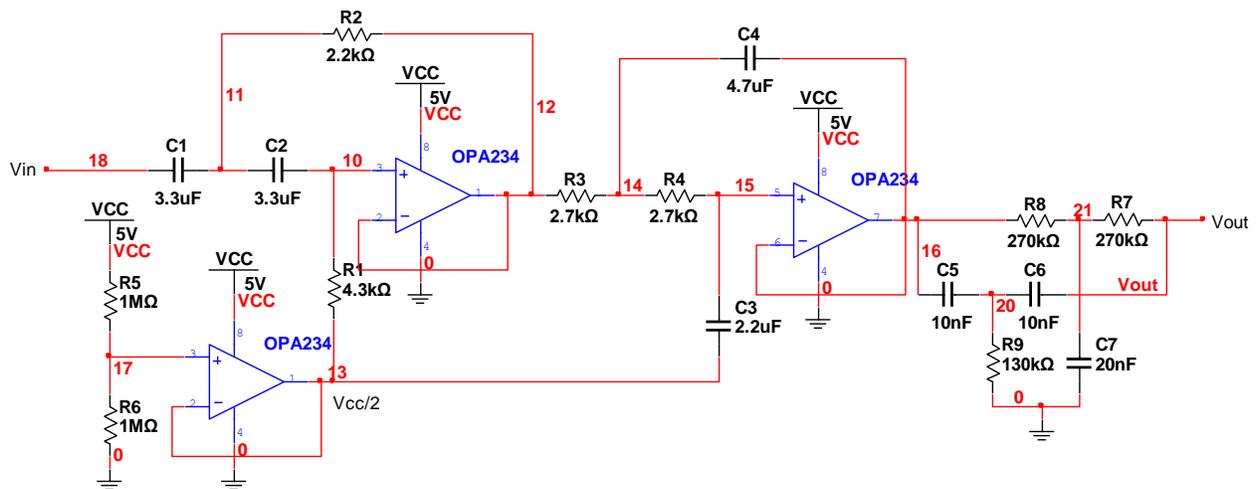


Figure 67 Complete filter for second prototype circuit

Simulation of Filter

The first step taken was to simulate the filter seen above. A 5Vpp AC voltage source with an offset of 2.5V was connected to node Vin for the simulation. The results seen below are the linear output magnitude versus frequency, Bode Plot, and phase plot (Figure 68).

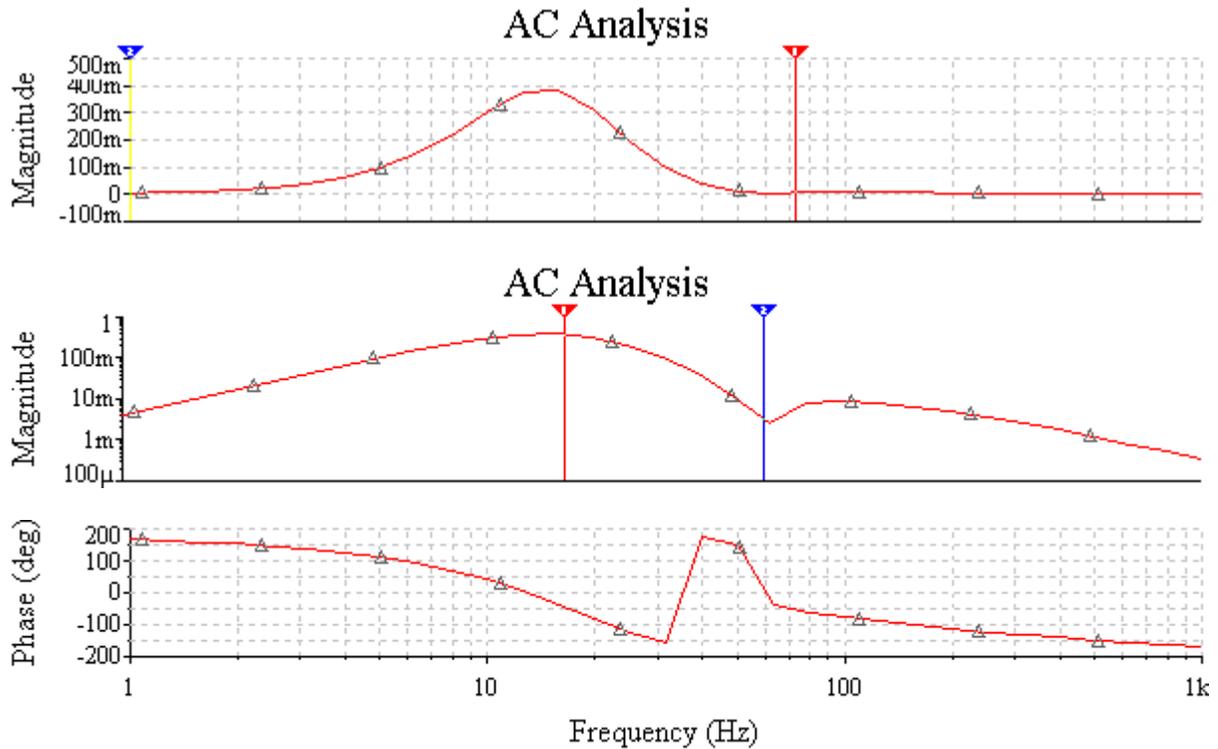


Figure 68 Frequency and phase response of filter

The simulation behaved as expected. As seen clearly above, the 60 Hz frequency was drastically diminished; the blue marker lies on 60 Hz and the red marker on 17 Hz.

Filter Improvement

This section will use simulation tools to compare the original filter to the filter with the 60 Hz notch attached.

Frequency Response Comparison

Shown below are the Bode Plots for the first filter circuit containing the two Sallen-Key Butterworth filters (Figure 48) and the second filter circuit, which added the 60 Hz Twin T notch filter (Figure 67). The response of first circuit is seen in Figure 69 via the blue trace and the second filter is the red trace.

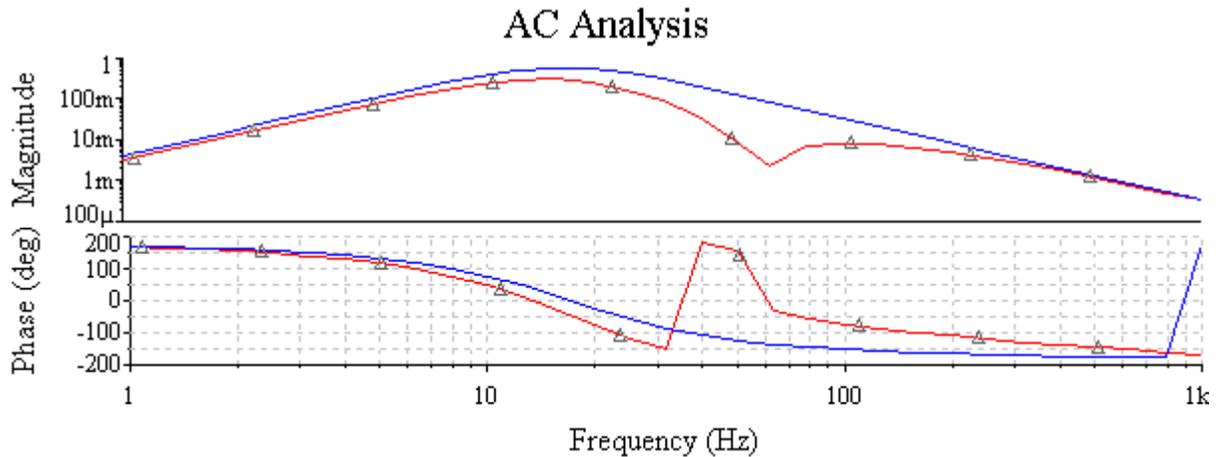


Figure 69 Comparison of first filter (blue) to the second filter (red).

This comparison shows excellent progress. Ideally, the 60 Hz noise seen when the AD8236 is used should be eliminated.

Simulated Virtual Heartbeat Input Comparison

A simulated signal that replicates the output of the AD8236 was used as the input for each of the two filters. This input signal was calculated from the signal seen in Figure 59, Figure 60, and Figure 61. It is two voltage signals added together. The first signal is the representation of the 60 Hz noise: a 1.7Vpp 60 Hz sine wave with an offset of 0.425V. The second replicated the QRS complex of the heartbeat: a 0.7V pulse that sits at a DC value of 0.7V. The pulse is ~ 17 Hz, consisting of a 20ms rise time followed by a 32ms fall time. The pulse beats every 0.4s (which is faster than an actual human pulse) for the sake of simulation.

Shown below are the transient responses for both of the circuits compared above. Figure 70 shows the simulation for the first circuit (without the notch filter), and Figure 71 shows the simulation for the second circuit (with the notch filter).

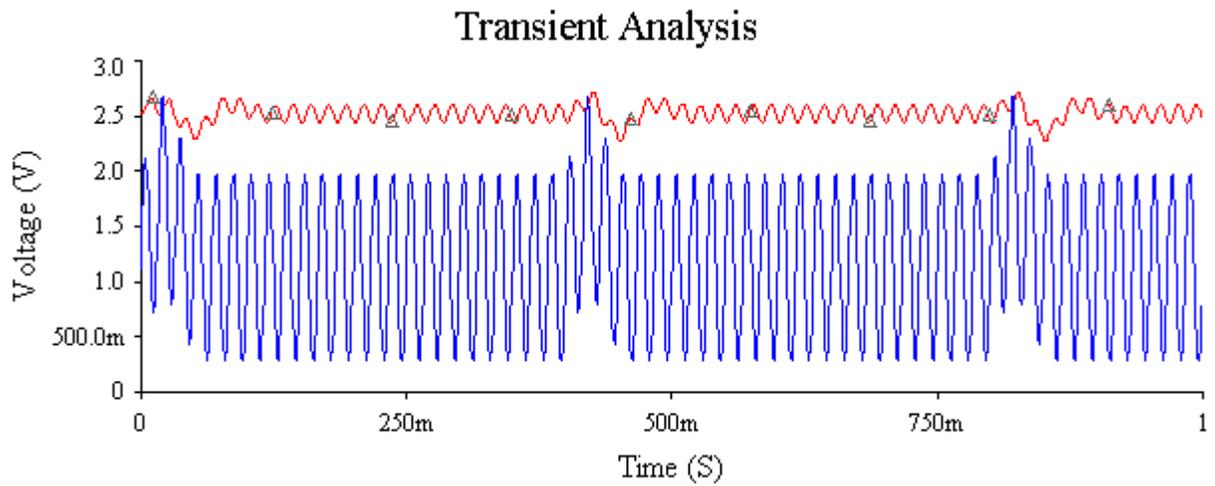


Figure 70 Transient response for simulated bandpass filter circuit

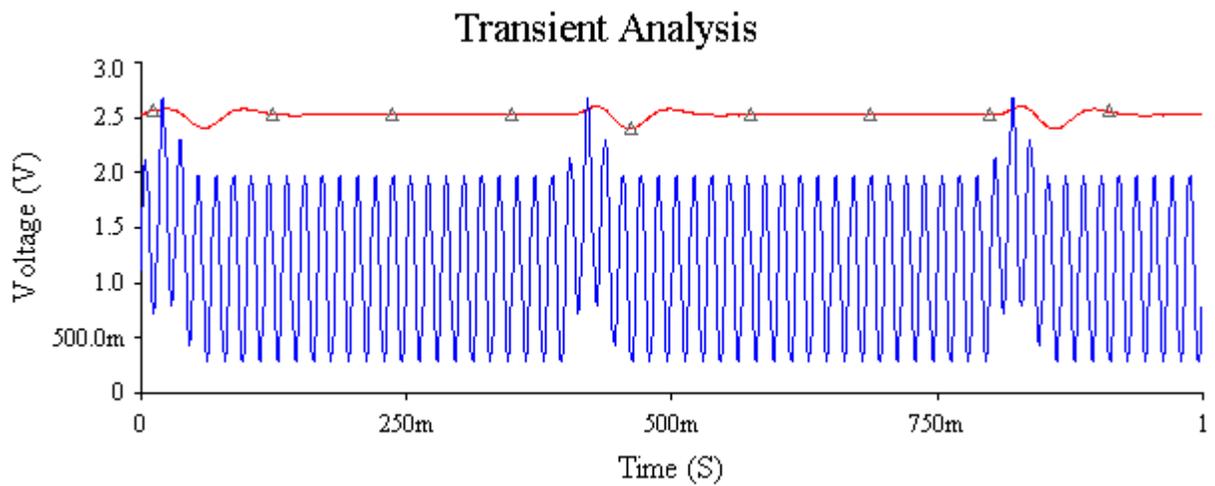


Figure 71 Transient response for simulated bandpass and 60 Hz notch filter circuit

This is a great response. The analysis of the first circuit showed a pulse with a small amount of 60 Hz noise. The second circuit showed a very clean pulse. The next step is to build this circuit and test it with real components.

AD624

The 60 Hz notch filter was soldered to the prototyping PCB. To fit the AD624 chip, a DIP socket was also soldered onto the board. This was designed to allow for all components to be soldered onto the same PCB. The AD624 requires a dual power supply, so this was

accommodated for. The rest of the components only require a single supply. A picture of the circuit can be seen below in Figure 72. The AD624 was placed in the 16-pin DIP package on the bottom right side of the photograph, but is not seen below. The notch filter is circled in yellow.

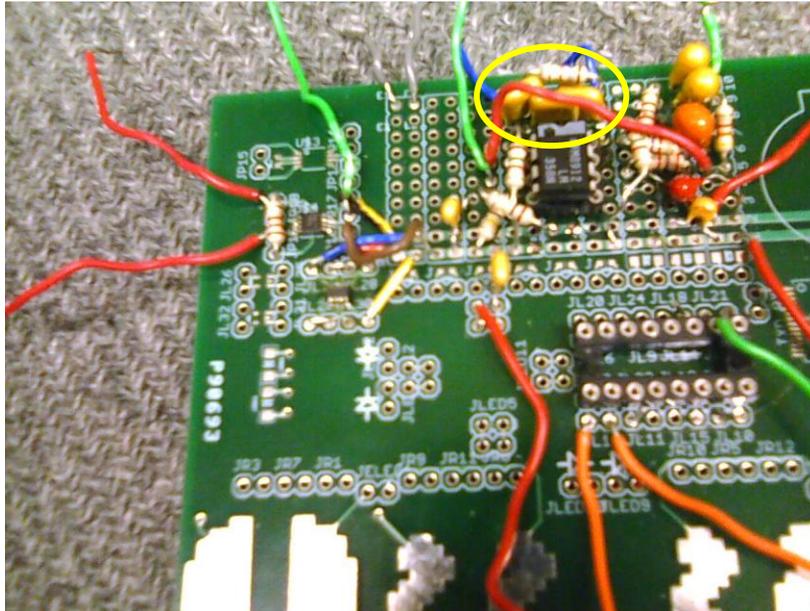


Figure 72 Second ECG circuit, using the AD624

First, the frequency response of the filter was taken, as seen below in Figure 73.

Channel 3 shows the input signal and channel 1 shows the output signal.

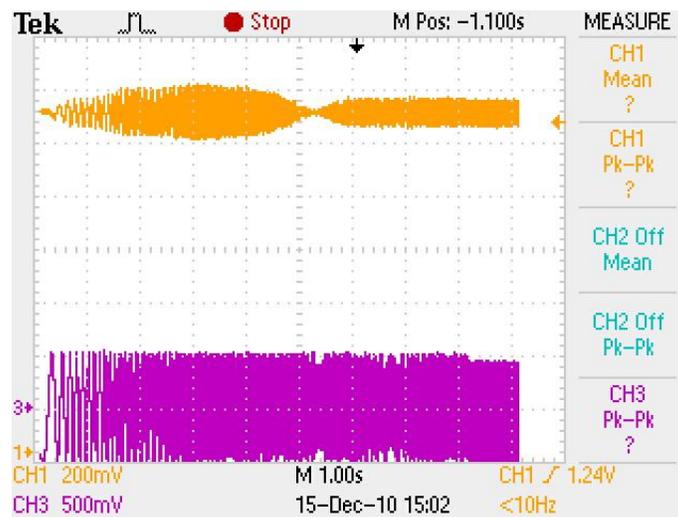


Figure 73 Frequency response of filter, 1 to 1 kHz

It is clear from the figure above that the filter worked, although not flawlessly. The highest attenuation of the output signal was seen at 60 Hz.

When the entire circuit was hooked up, the user did not need to ground his foot to obtain a pulse reading. The signal before (ch1) and after (ch2) the 60 Hz notch filter is shown in Figure 74. The electrodes were placed across the heart.

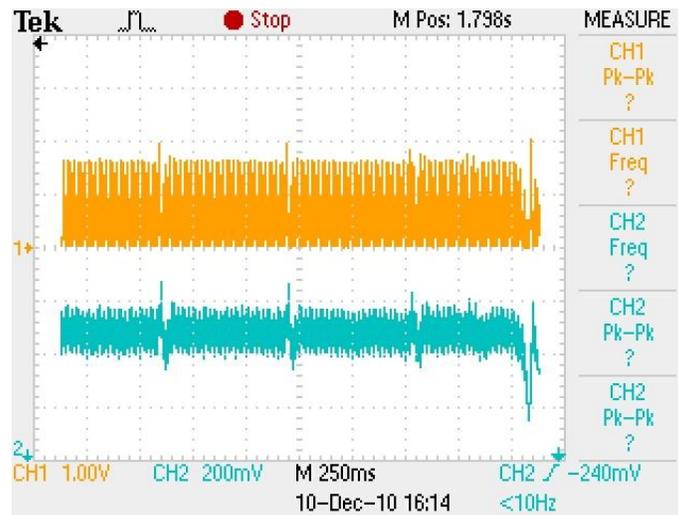


Figure 74 Output pulse before (ch1) and after (ch2) notch filter

The graph above shows two significant improvements. First, the 60 Hz notch filter works well, and second, a pulse can be seen without the user grounding his foot.

For the next experiment, the user grounded his foot. The output signal was amplified and a comparator and an LED were attached to the output. The result is seen in Figure 75, as well as a description of what each channel represents.

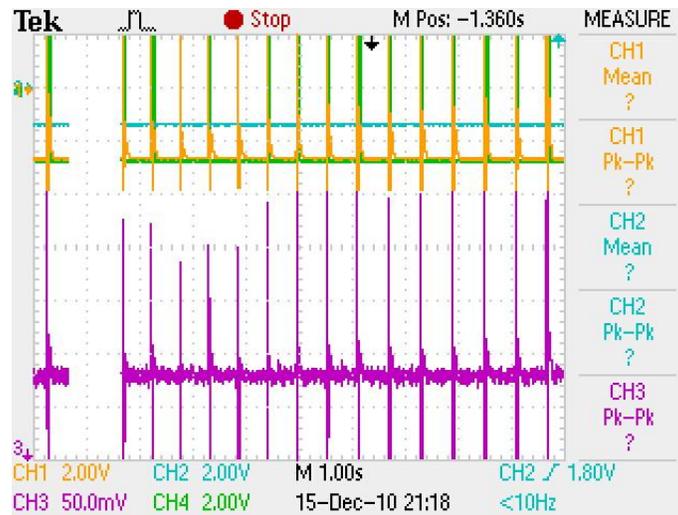


Figure 75 Output pulse across heart, ch1 = amplified output, ch2 = threshold, ch3 = unamplified pulse, ch4 = LED

Next, the user put one electrode on each thumb. The output is seen in Figure 76 on channel 1. Channels 2 and 3 can be ignored.

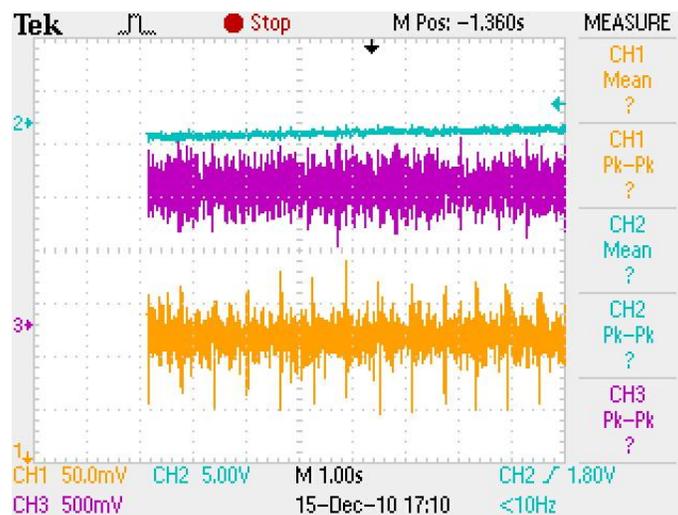


Figure 76 Output pulse on thumbs (ch1)

This is the cleanest pulse reading seen with the thumbs so far. Below in Figure 77 is the same signal zoomed in.

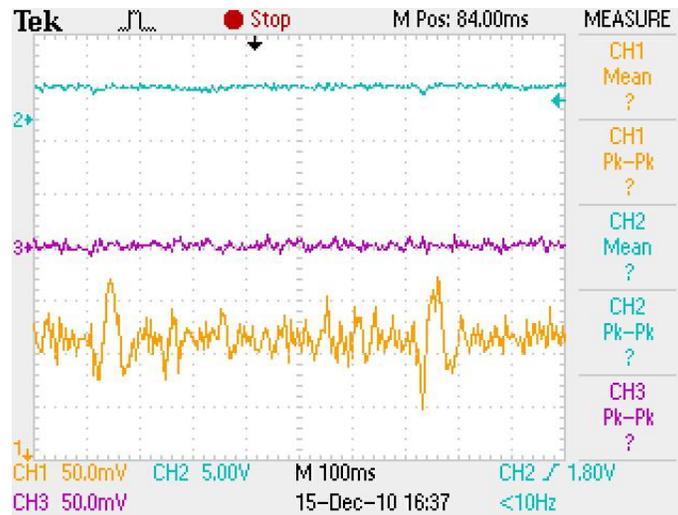


Figure 77 Output pulse on thumbs zoomed in (ch1)

AD8236

When the AD624 was replaced with the AD8236, there was little to no improvement when compared to the first circuit. The next obstacle is to get better results using the AD8236.

AD8236: AC Coupling

This section will discuss the method used to help make the AD8236 more stable in the ECG circuit.

Design

One issue that was observed when using the AD8236 concerned biasing. The signal was inconsistent: jumping from rail to rail when the user shifted positions or did not ground his body. One potential solution to this biasing problem is to AC couple the instrumentation amplifier. This would allow the designer to set a referenced bias voltage and will ideally cause the signal to constantly ride on this DC voltage. Page 18 of the AD8236 datasheet²⁵

²⁵ http://www.analog.com/static/imported-files/data_sheets/AD8236.pdf

demonstrates a method that utilizes an integrator to AC couple the AD8236. The circuit from the datasheet is seen in Figure 78.

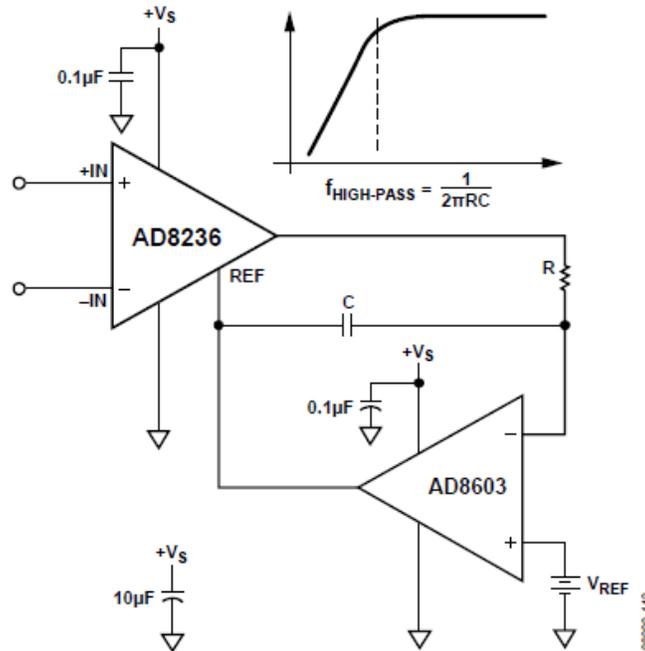


Figure 78 AC coupled AD8236 configuration from datasheet

For this application, V_{REF} is set in the center of the rails, at $\frac{V_{CC}}{2}$. This is done with a simple voltage divider configuration. The equation for the high-pass cutoff frequency $f_{HIGH-PASS}$ is given in Figure 78. Using a $1M\Omega$ resistor and a $0.022\mu F$ capacitor yields a frequency of $f_{HIGH-PASS} = \frac{1}{2 * \pi * 1M * 0.022} = 7.23 Hz$. This will not only reject all DC voltages and offsets, but will act as an extra pole in the ECG's filter. As an extra precaution, each input of the in amp is also AC coupled with reference to V_{REF} . The cutoff frequency for these inputs was set to the same as that of $f_{HIGH-PASS}$, which allowed for a simple component selection process. The final AC coupled in amp circuit is seen below in Figure 79.

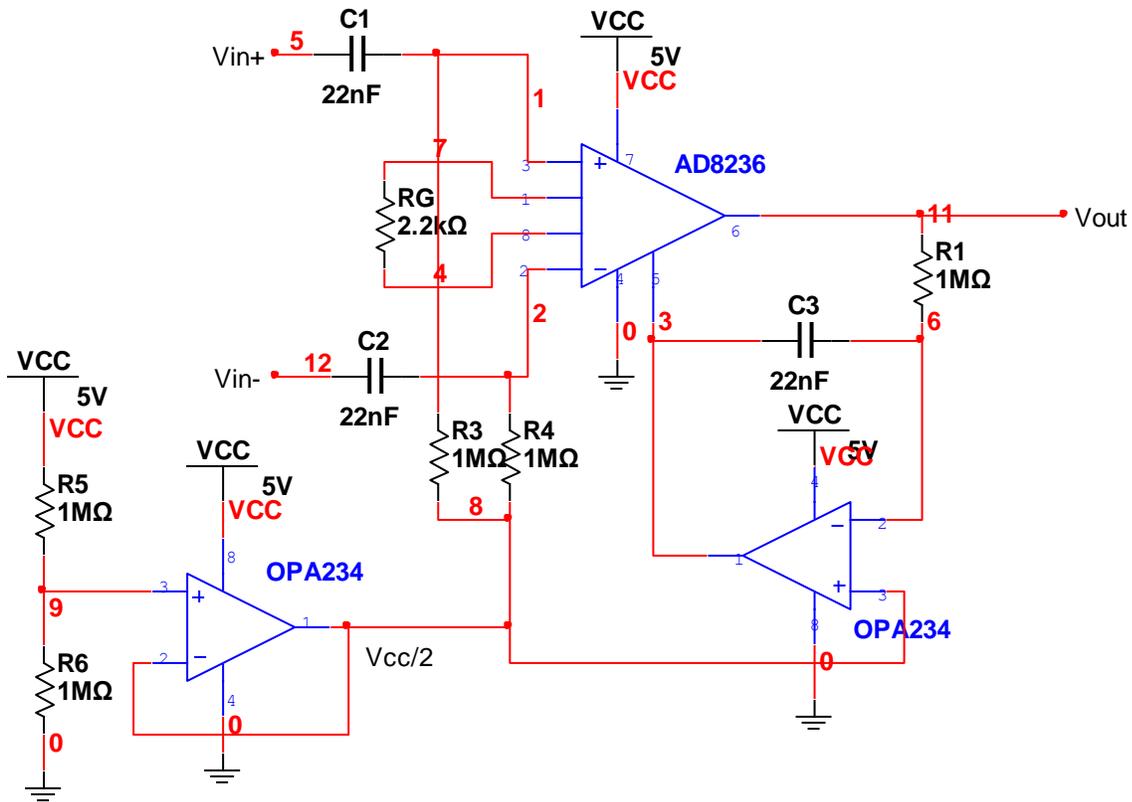


Figure 79 AC coupled AD8236 configuration used in the design

Implementation

The output Vout of the circuit shown in Figure 79 was then connected to the input of the ECG filter discussed in the previous section (Figure 67). This circuit, with the electrodes across the user's heart and his foot connected to ground, produced the unamplified signal seen in Figure 80.



Figure 80 Pulse output across heart using AC coupling

This is a clean signal, clearly showing each individual pulse with minimal noise interference.

Next, one electrode was placed on each of the user's thumbs. This produced the signal seen below in Figure 81.

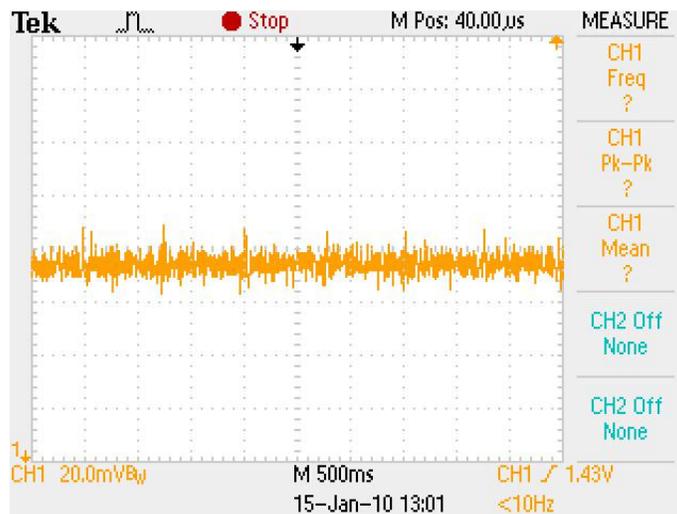


Figure 81 Pulse output on thumbs using AC coupling

Although not very clean, a pulse is detected and can be seen by the human eye. This is the first time a pulse has been seen using the AD8236.

When dealing with extremely small signals and sensitive filters, it is important to have proper and efficient grounding of the entire circuit. The next step in improving the signal is to solder the circuit onto a single PCB. This will hopefully solve any grounding discrepancies between the PCB and the breadboard.

Completely Soldered

There was not enough room or footprints on one PCB to fit every component of the ECG. Therefore, two boards were used in the design. A picture of the configuration is shown in Figure 82. The AC coupling circuit is the board on top, with its output being sent to the filter via the long green wire on the right side of the picture.

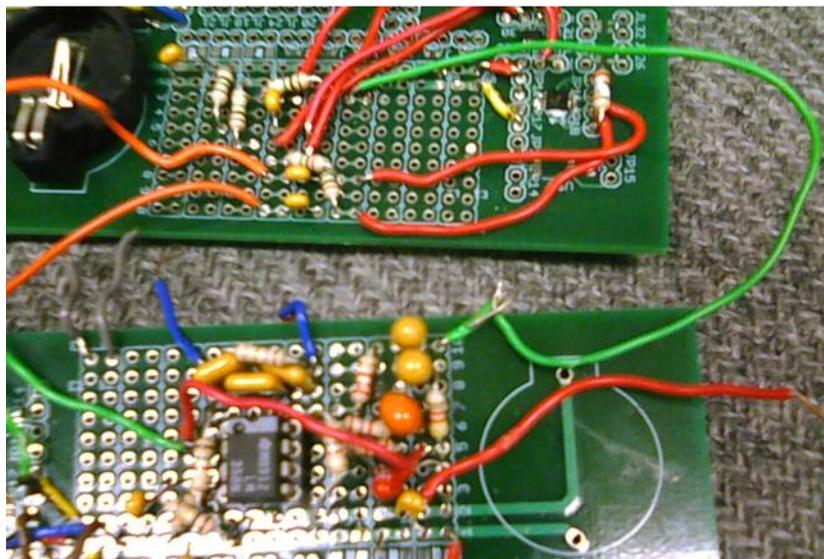


Figure 82 Second ECG circuit, with AC coupled AD8236

A frequency response of the entire circuit was produced by passing a 5Vpp sine wave with an offset of 2.5V into the input of the in amp, and varying the frequency from 1 to 1 kHz. The results of this test are seen in Figure 83.

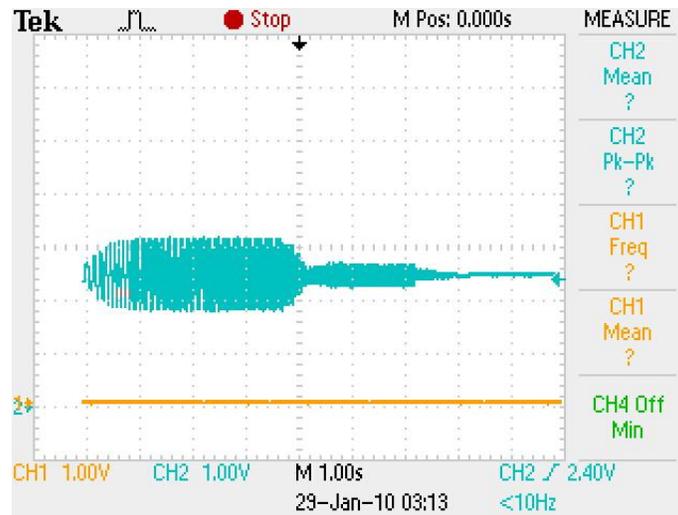


Figure 83 Frequency response of AC coupled circuit

A sudden drop in the output voltage of the circuit is seen at 60 Hz, and the voltage steadily declines as the frequency is increased. The frequency was held at 17 for ~1.5s in order to better display its characteristic.

In order to get a better representation of the pulse, the output voltage will be amplified. The typical peak-to-peak voltage of the output when the electrodes are connected to the thumbs is ~50mV. Therefore an amplifier with a gain of $\frac{5V}{0.050V} = 100 \frac{V}{V}$ is ideal. In the next experiment, the unamplified output signal was sent to a non inverting gain amplifier on a breadboard. The amplifier uses 1M Ω and 10k Ω resistors for a gain of $G = 1 + \frac{1M}{10k} = 101 \frac{V}{V}$. This circuit was tested using one electrode on each thumb, and without the user grounding his foot. The corresponding waveform can be seen below in Figure 84.

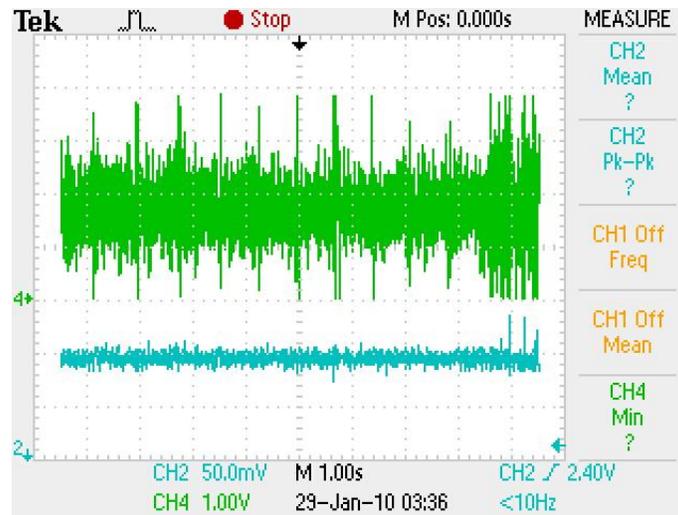


Figure 84 Amplified pulse output on thumbs (ch4)

This signal shows a pulse. However, it should be noted that when the user does not ground his foot, achieving an accurate pulse reading requires the subject to sit extremely still in order to avoid any muscle spasms or exterior signals.

One Input Grounded

Through experimentation, a new electrode configuration was found to be more accurate than simply sending the two electrode signals to the in amp. If one of the in amp inputs is grounded, and an electrode is tied to ground, a cleaner signal can be obtained. This configuration effectively grounds one thumb via the grounded electrode, and sends the heartbeat voltage through the other thumb via the ungrounded electrode. This configuration is shown in Figure 85.

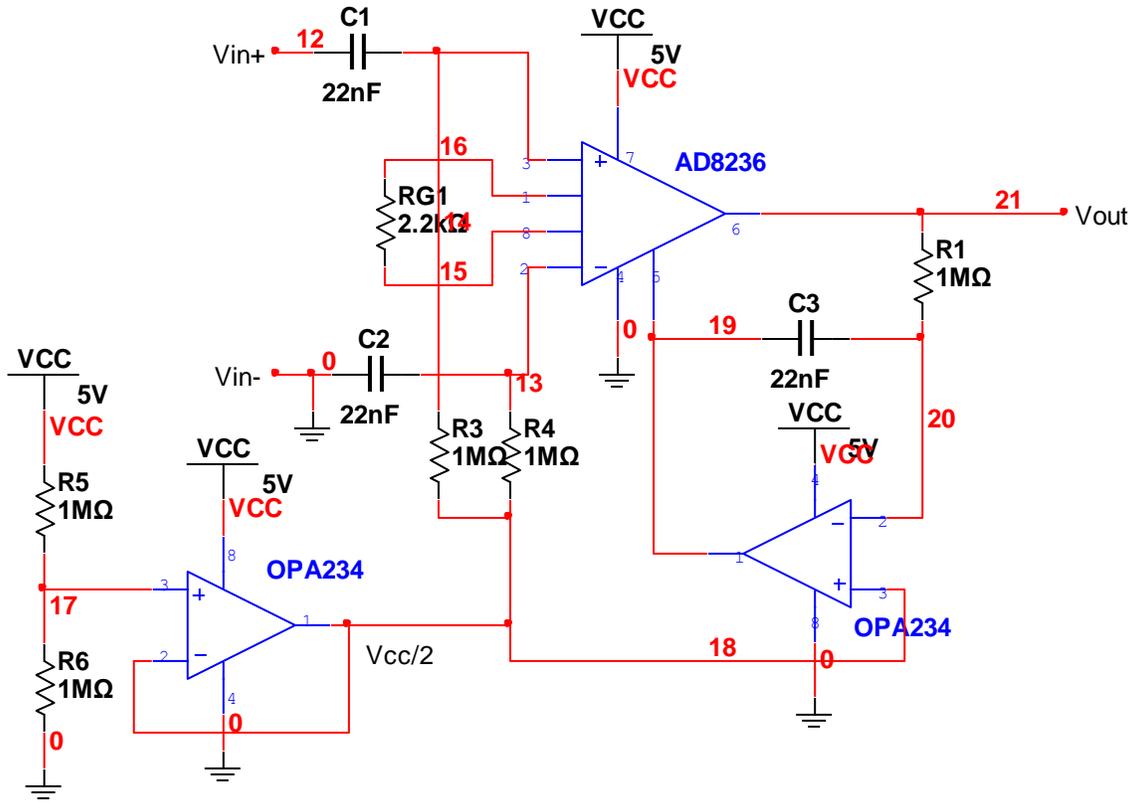


Figure 85 AC Coupled in amp with one electrode grounded

The results of this configuration are shown in Figure 86.

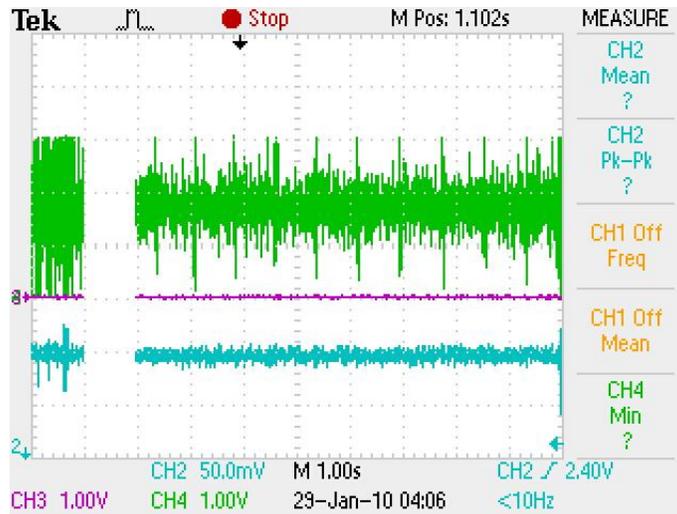


Figure 86 Amplified pulse output one electrode grounded (ch4)

This signal has less noise than the previous electrode configuration seen in Figure 84. It is also more efficient, showing a clear pulse more often than before. The electrode-grounding configuration seen in Figure 85 will now be used instead of the previous electrode configuration where neither input was grounded.

Although a pulse can be detected, there is still room for improvement. The current configuration has four high-pass poles and three low-pass poles near 17 Hz. The bandpass response can still be improved in order to block out more unwanted frequencies. The following section will explore the option of adding a second Sallen-Key second order Butterworth filter stage to the design.

3.5.2.4 Third Prototype

Although it may seem redundant to add more filters, this section will show that, by adding more poles to the filter, a more accurate pulse can be obtained.

Double Filter

The third prototype implements two more Sallen-Key second order Butterworth filters that are both identical to the previously designed ones. The current output signal coming out of the 60 Hz notch filter is very small ($\leq \sim 50\text{mVpp}$). Therefore, the voltage will need to be amplified before it is filtered again. We can use the non inverting gain amplifier with a gain of $101 \frac{V}{V}$ that was built in the previous section. After the amplification, the signal is sent into another Sallen-Key second order Butterworth bandpass filter. The resulting circuit is the final ECG filter design, and is seen below in Figure 87.

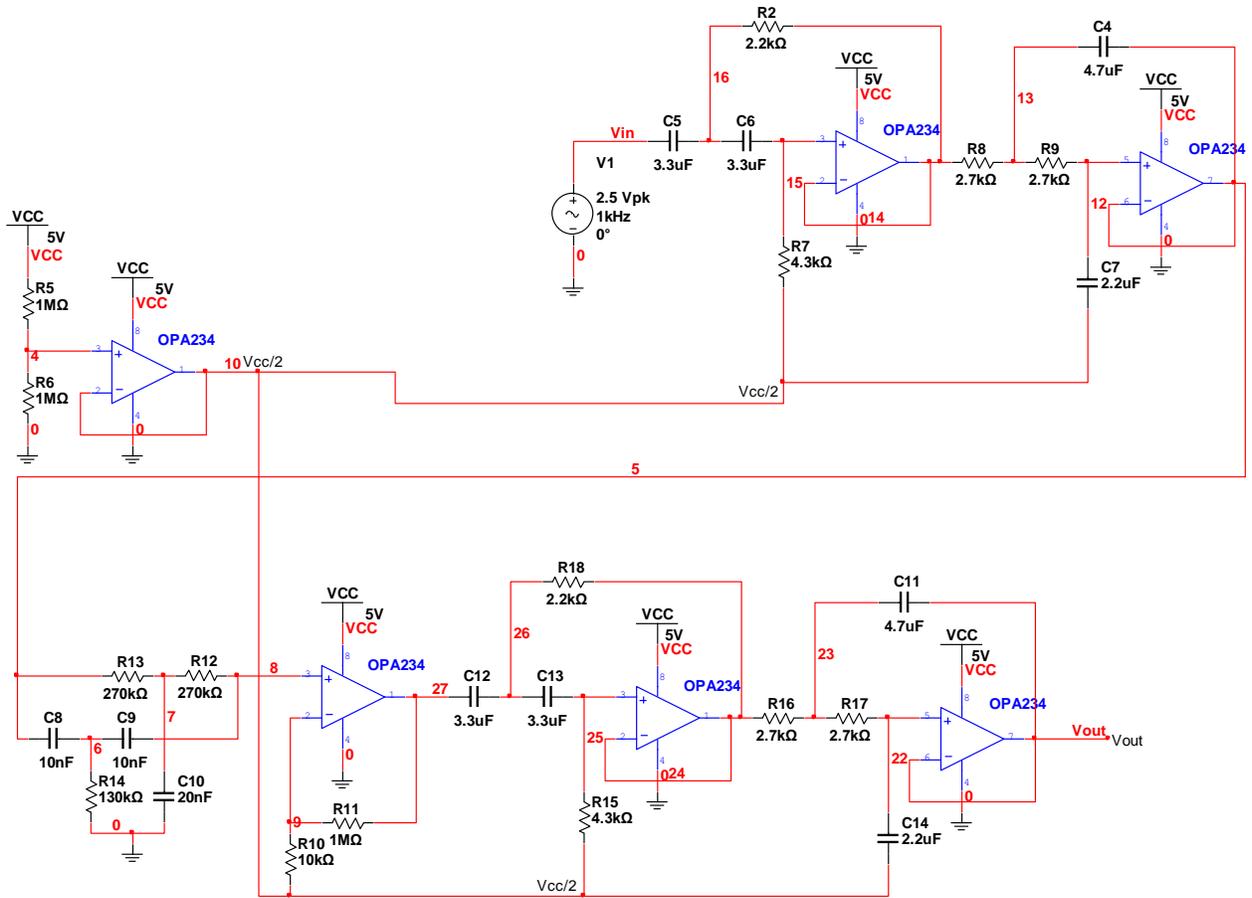


Figure 87 Complete ECG filter circuit

Simulation

The circuit in Figure 87 was simulated. The results of the simulation are seen in Figure

88.

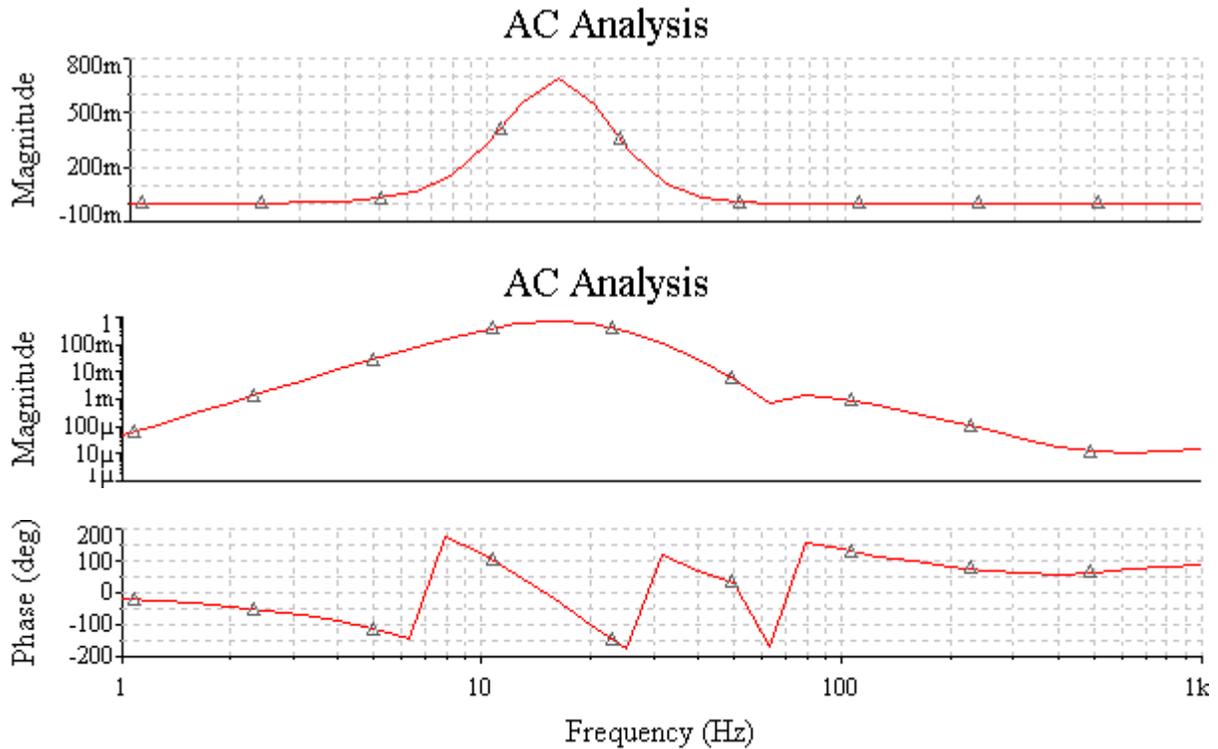


Figure 88 Frequency response of full filter

The phase of this circuit is unpredictable. However, the phase of the pulse is not important; it is the magnitude that will be seen by the user.

There is a definite improvement in the frequency cutoff. To portray this, a direct comparison is made with the previous two circuits, seen in Figure 89. The plot of the first circuit is the green trace, the second is blue, and the third is red.

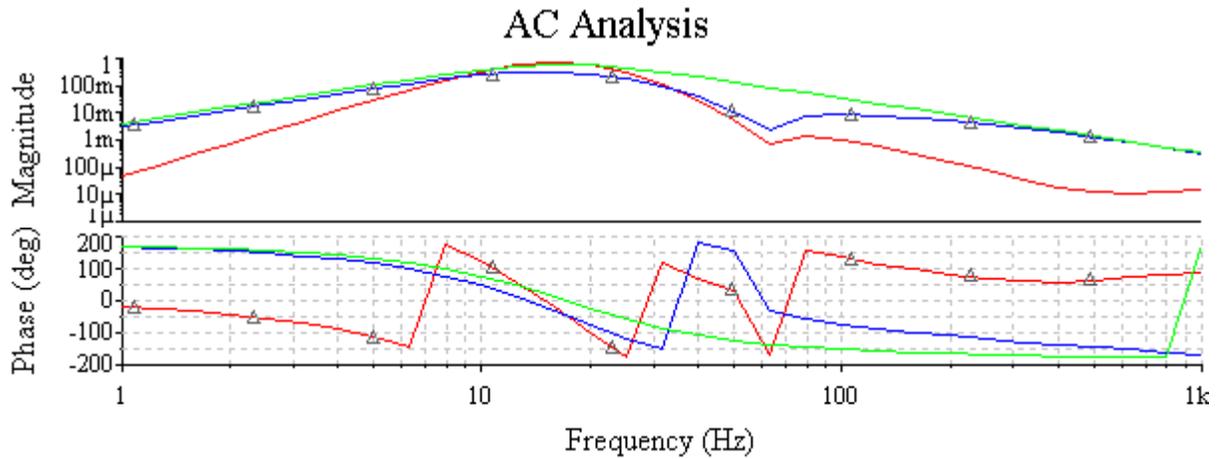


Figure 89 Bode Plot comparison of the first filter (green), second filter (blue), and final filter (red)

The figure above shows that the new filter design efficiently rejects more frequencies than before.

Final Design

The completed filter was added to the circuit. The new prototyping circuit is seen in Figure 90. The last filter section was built on a breadboard due to lack of components and board space. The long green wire in the center of the photo is the reference voltage V_{REF} used for the filter and the orange wire just below it is the output of the notch filter being sent to the input of the amplifier stage.

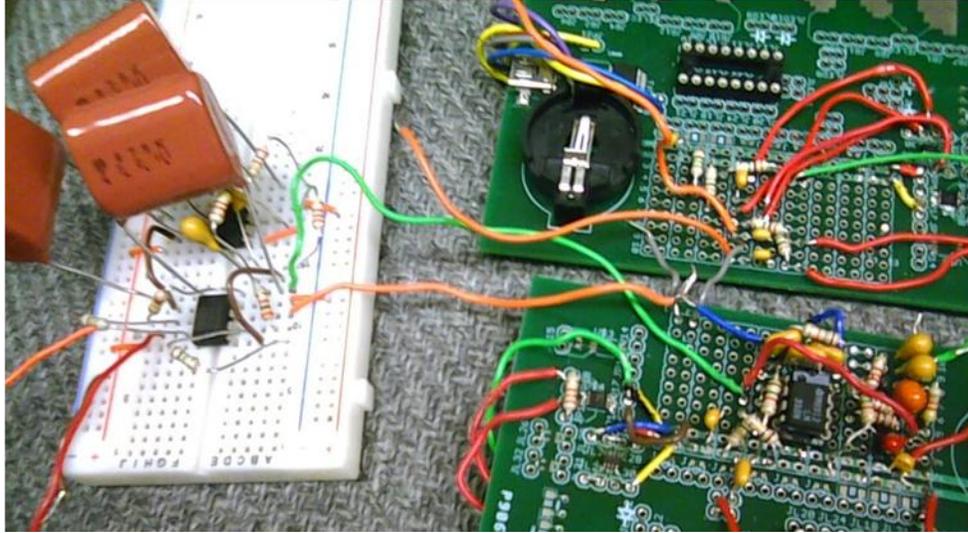


Figure 90 Completed ECG prototype

The last part of the design process was to test the final circuit. The details are explained in the next two subsections.

Experiments

For proof of concept, two experiments were run that show the benefit of the second filter topology. In the first experiment, the non inverting amplifier gain was increased to $G = 1 + \frac{1M}{3k} = 334 \frac{V}{V}$. This caused the noise to bounce almost to the rails, as seen in channel 2 of Figure 91. This signal was then sent through the second set of Sallen-Key filters, and produced a clean output pulse, as seen in channel 4.

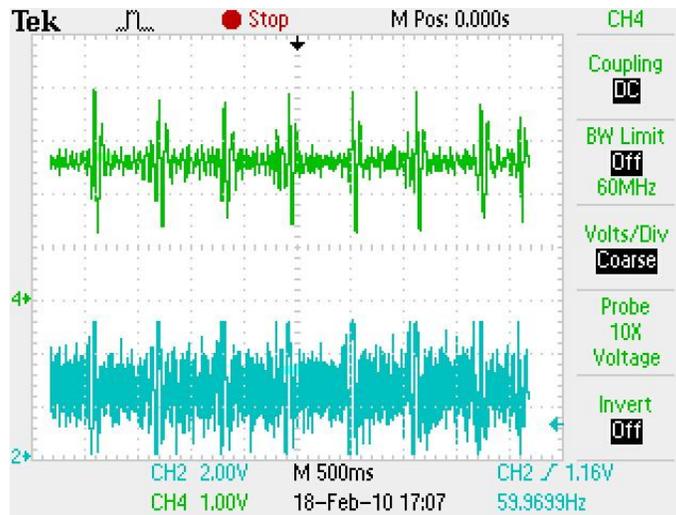


Figure 91 Pulse output across heart before second filter (ch2) and after second filter (ch4)

In the second experiment, the non inverting gain stage remained the same (to increase the noise), and the user only has to touch the tip of his thumb to the sensing electrode. The stage before the filter and after the filter is seen in Figure 92 on channels 2 and 4, respectively.

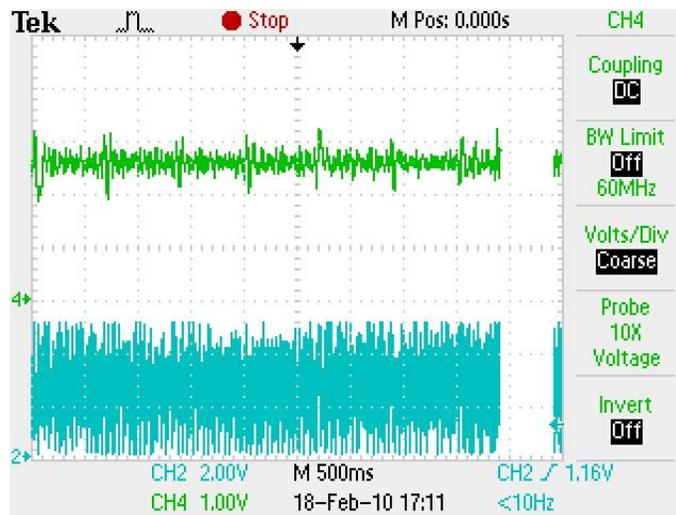


Figure 92 Pulse output on thumbs before second filter (ch2) and after second filter (ch4)

Final Output

Next, the gain of the non inverting op amp stage was reset back to $101 \frac{V}{V}$, and a signal was obtained at the output of the whole system using the two thumbs. This waveform is seen in Figure 93.

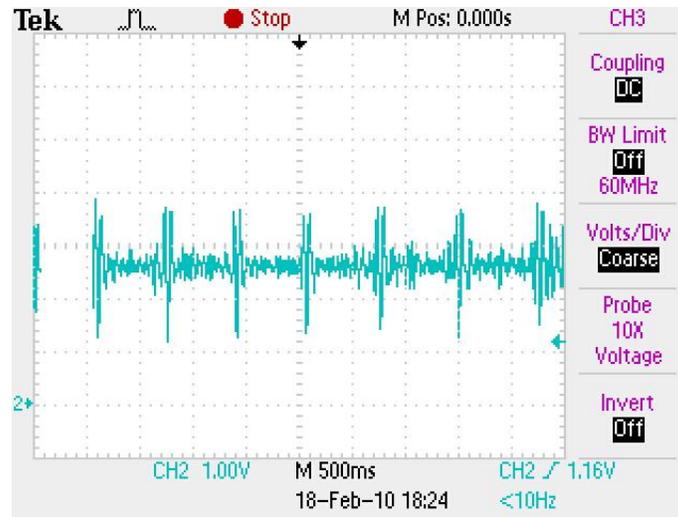


Figure 93 Pulse output on thumbs after full filtering

This is the cleanest pulse signal obtained thus far using the two-electrode thumb method. It works in any situation, as long as the user remains still while the pulse is being read.

3.5.3 Final Circuit Design

This section serves as an overview of the final circuit design for the electrocardiogram (ECG). In order to best describe the full workings of this circuit, it is broken up into seven sections. The circuit can be seen in Figure 94, along with the appropriate circuit segment labels. The power supply (V_{cc}) is set at 5V, because that is what the USB connection will provide.

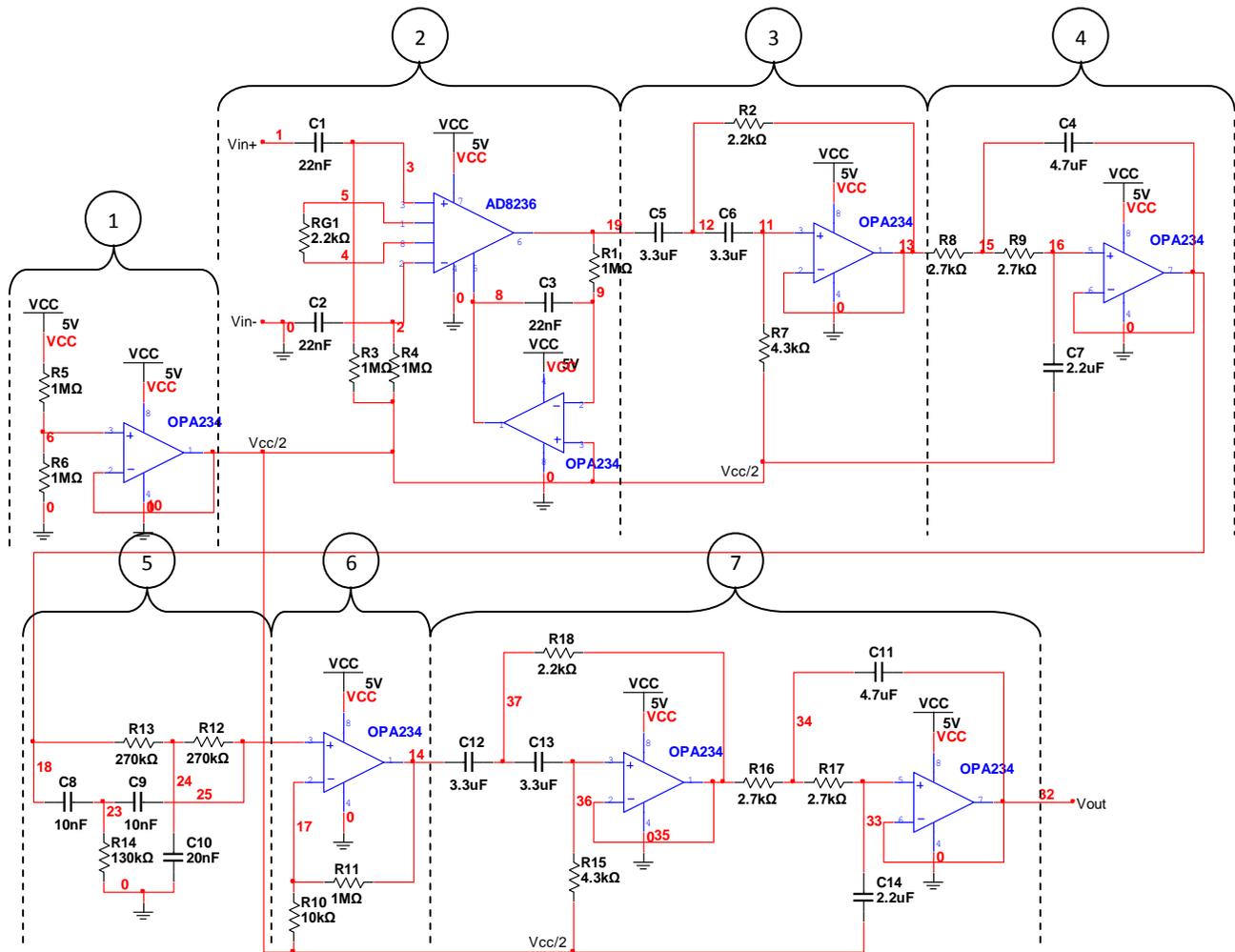


Figure 94 ECG - Full Circuit

Section 1 – DC Bias (V_{REF})

The first circuit segment is the simplest. It uses two equivalent 1MΩ resistors and an operational amplifier. The resistors act as a voltage divider that sets $V_{REF} = \frac{V_{CC}}{2}$. The op amp is set for unity gain and acts as a buffer. This allows other components in the circuit to use V_{REF} as a stable reference voltage, without any voltage or current swings.

Section 2 – Instrumentation Amplifier Input

The purpose of this section is to provide a clean and stable electrical signal from the body. Its design was focused around the smallest low-power instrumentation amplifier on the market today, the AD8235. This circuit uses the AD8236, which has the same internal circuit

configuration as the AD8235, but with a larger external package. It runs on a single supply and has a programmable gain.

The inputs V_{in+} and V_{in-} represent the two electrode inputs. The user places one thumb on each electrode. The electrode obtains the highest voltage signal from the contact skin as possible. Note that one of the electrodes, V_{in-} , is grounded. This serves as a reference point between the user and the circuit.

Each input signal is AC coupled with respect to the reference voltage V_{REF} by using an RC high-pass filter configuration set for $f_c = \frac{1}{2\pi * 22n * 1M} = 7.23 \text{ Hz}$. The output of the AD8236 (pin 6) is also AC coupled to the reference voltage. This is done via the resistor R1, the capacitor C3, and the op amp below them. These three components create an integrator, which couples the output pin to the reference pin (pin 5). The reference is set at $V_{REF} = \frac{V_{CC}}{2}$.

The final component in this section is the gain resistor RG1. This resistor is tied across pins 2 and 3 of the AD8236. Its value of 2.2k Ω provides the in amp with a gain of 196 $\frac{V}{V}$.

Section 3 – Sallen-Key Second Order High-pass Butterworth Filter

The output signal of the AD8236 now needs to be filtered in order to obtain an accurate pulse reading. As previously explained in the Filter Design section, a Quality Value of 5 and a center frequency of 17 Hz are best to obtain an accurate reading of the human pulse. This results in a bandwidth of $BW = \frac{f_c}{Q} = \frac{17}{5} = 3.4 \text{ Hz}$. Hence, to create a 3.4 Hz bandpass filter centered at 17 Hz, the high-pass filter cutoff frequency was set at $f_{3dB} = 17 - \frac{3.4}{2} = 15.3 \text{ Hz}$.

The Sallen-Key high-pass filter topology (Figure 44) was used to design the high-pass filter. The R and C ratios of $R_1 = 2 * R$, $R_2 = R$, $C_1 = C$, and $C_2 = C$ will allow for a Q of $\frac{1}{\sqrt{2}}$, which will give a flat unity gain frequency response, classifying this as a Butterworth filter. The capacitor and resistor values were chosen by using these ratios and the equation for the cutoff frequency of a Sallen-Key second order filter (Equation 11).

Section 4 – Sallen-Key Second Order Low-pass Butterworth Filter

Section 4 of the ECG circuit shown in Figure 94 is the second half of the bandpass filter. The cutoff frequency was set at $f_{3dB} = 17 + \frac{3.4}{2} = 18.7 \text{ Hz}$. The Sallen-Key low-pass filter (Figure 46) was used for this section of the design. The R and C ratios of $R_1 = R$, $R_2 = R$, $C_1 = C$, and $C_2 = 2 * C$ were used along with Equation 11 to help choose the component values.

Section 5 – 60 Hz Twin T Notch Filter

The actual output of the circuit after section 4 saw a large amount of 60 Hz noise. Section 5 is a notch filter designed to stop any 60 Hz signal from passing through. The Twin T topology seen in Figure 95 was used to design this filter.

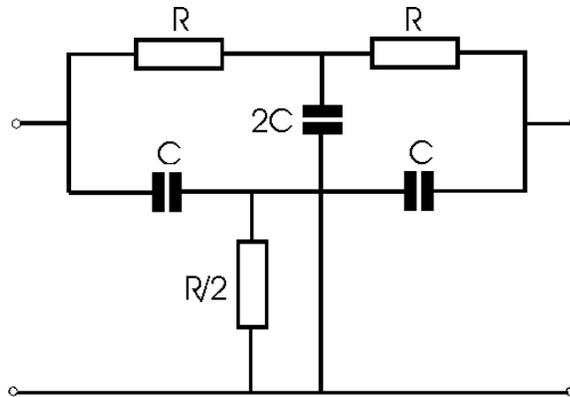


Figure 95 Twin T filter topology

Using the above figure as reference, the filter in this circuit is set for $R = 270k\Omega$ and $C = 10nF$. This yields a notch frequency of $f_n = \frac{1}{2\pi * 270k * 10n} = 59.0 \text{ Hz}$.

Section 6 – Non-inverting Gain

Due to the high concentration of poles centered around 17 Hz, the signal is significantly attenuated once it passes through section 5. Section 6 is a non-inverting gain amplifier used to counteract this attenuation.

The typical amplitude of the signal after section 5 is $\sim 50\text{mVpp}$. Since the supply voltage is 5V, this allows for a gain of $G = \frac{5V}{0.050V} = 100 \frac{V}{V}$. Choosing $R_{11} = 1M\Omega$ and $R_{10} = 10k\Omega$ yields a gain of $G = 1 + \frac{1M}{10k} = 101 \frac{V}{V}$. This gain allows for the signal to approach the supply rails, henceforth making it much easier to see for the user.

Section 7 – Second Sallen-Key Filter Stage

In order to achieve a more visible pulse using two electrodes touching the thumbs, a second Sallen-Key filter stage was added. This filter is an exact duplicate of sections 3 and 4. It

adds two more high-pass poles and two more low-pass poles to the filter. A simulated Bode Plot of the entire filter is seen below in Figure 96.

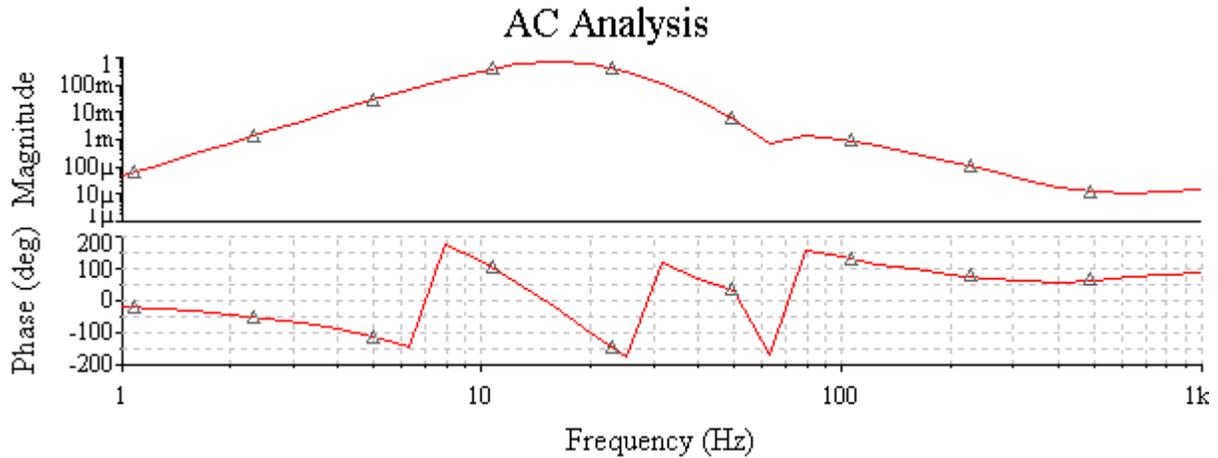


Figure 96 Bode Plot of full filter

Figure 97 shows an actual pulse taken using this circuit.

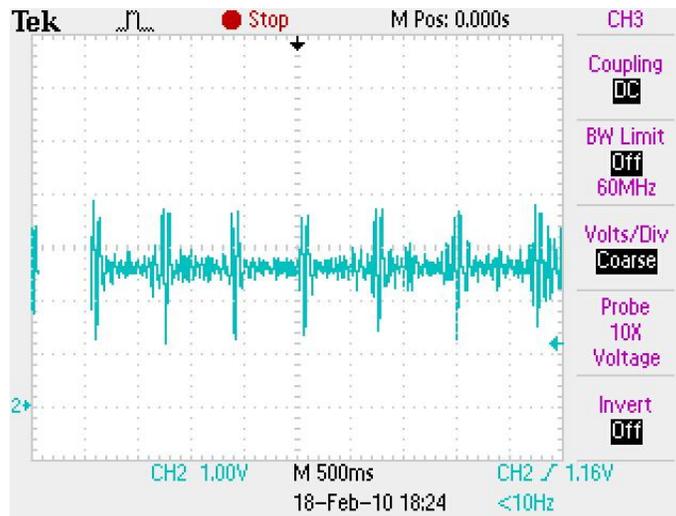


Figure 97 Pulse output of ECG

3.5.4 Component Selection

The selection of components for the final product of the ECG was quite straightforward. Every component selected was surface mount. Every resistor in the circuit will have a tolerance of $\pm 5\%$. This is a very common type of resistor, and the $\pm 5\%$ resistors were used in the

prototyping of the design. The capacitors will have a tolerance of $\pm 10\%$: the same type used during the design process. All of the resistors and capacitors will be size 1206.

The AD8236 selection was nonexistent—it only comes in one package size.

Lastly, the op amp selected was the OPA4348. This is a low power, single supply, rail-to-rail output, general purpose amplifier made by Texas Instruments. It is one of the cheapest op amps of its kind. The seven op amps in the circuit can be implemented using just two quad-package op amps—the OPA4348. It comes in two sizes: SOIC-14 and TSSOP-14. The SOIC package is slightly larger than the TSSOP, but it is slightly cheaper. Since a single package will contain four op amps, a larger size will be more ideal for the layout of the PCB. A smaller package would make for a more complex layout.

A list of the components for the circuit is seen below in Table 4.

Table 4 ECG circuit components

Name	Description	Package	Amt per PCB
Resistors	All	1206	19
Capacitors	All	1206	14
AD8236	In amp	MSOP-8	1
OPA4348	Op amp	SOIC-14	2

3.6 PC Interface

A standard requirement for the input sensor design is to have the measured data available for real time viewing and analysis. As such the decision was made to include a PC interface in the enhanced input sensor circuit. Three out of the four initial data inputs would be sampled and transmitted serially to the PC in this enhanced circuit; these include: temperature obtained from the Thermistor circuit discussed in section 3.3, and the heart rate obtained from the Pulse Oximeter and ECG circuit discussed in section 3.4 and 3.5 respectively.

The PC Interface required a microcontroller to accurately sample and transmit the data at an appropriate Nyquist Frequency that would be sufficient for all three circuits. The PC Interface would also include a UART serial converter to convert the sampled data obtained from the microcontroller to a USB readable format that can ultimately be displayed on a PC. The final component of the PC Interface is data acquisition software that accepts serial data input and permits the user to manipulate and analyze the data. A system level diagram of the PC Interface is included below.

[INSERT BLOCK DIAGRAM HERE]

3.6.1 Selection of Components

This section will discuss the process of selection for the key components of the PC Interface as well as the method of data sampling and data transmission and the final analysis of the data using software after it has been inputted to the PC.

3.6.1.1 Microcontroller

Two features that were essential for the chosen microcontroller were an Analog to Digital Converter (ADC) and a Universal Synchronous/Asynchronous Receive Transmit (UART) mode. The ADC would be used to convert the analog signal obtained from each circuit and convert it to a digital number that can then be transmitted serially and ultimately converted back to its true analog equivalent. The UART mode of the MSP430 would be used to serially transmit data externally to a UART serial converter which can then send the data to the PC via a USB connection.

After comparing all the possible microcontrollers that possessed these two features it was necessary to choose a microcontroller that was able to be programmed in a language that was fairly familiar to the team. An even greater advantage would be to choose a microcontroller with which the team has worked with in prior projects. Finally, based on these combined requirements the decision was made to use the TI manufactured MSP430F449 microcontroller. The implementation of the ADC AND UART mode of the MSP430 will be discussed in detail in the following two sections.

3.6.1.2 *UART/USB*

3.6.1.3 *LabView (?)*

3.6.2 Progression of Design: Measurement and Results

3.6.3 Final Design

4 Final Board Design

4.1 Simple Board

4.1.1 Circuits Chosen for Simple Board

4.1.2 MOSFET integration switch

4.1.3 Final Simple Board

4.2 Complex Board

4.2.1 Circuits Chosen for Complex Board

4.2.2 Final Complex Board

5. Conclusion

Appendix A – Derivation of Cut-off Frequency for Sallen-Key Filter

Figure 98 below shows the Sallen-Key filter topology used in the ECG circuit.

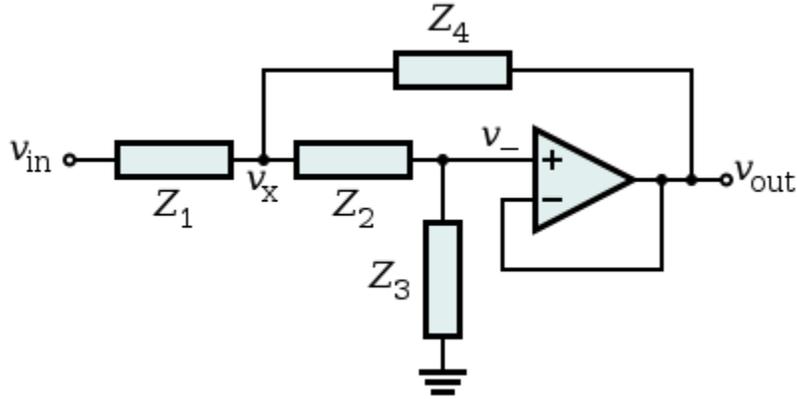


Figure 98 Generalized Sallen-Key filter topology

Using Kirchoff's Current Law (KCL) at node V_- :

$$0 = \frac{V_-}{Z_3} + \frac{V_- - V_x}{Z_2}, \text{ and } V_- = V_{out} \text{ (unity gain)}$$

$$0 = Z_2 V_{out} + Z_3 (V_{out} - V_x)$$

$$Z_3 V_x = V_{out} (Z_2 + Z_3)$$

$$V_x = V_{out} \left(1 + \frac{Z_2}{Z_3} \right)$$

Equation 16 (above)

KCL at node V_x :

$$0 = \frac{V_x - V_{in}}{Z_1} + \frac{V_x - V_-}{Z_2} + \frac{V_x - V_{out}}{Z_4}, \text{ and } V_- = V_{out} \text{ (unity gain)}$$

$$0 = Z_2 Z_4 (V_x - V_{in}) + Z_1 Z_4 (V_x - V_{out}) + Z_1 Z_2 (V_x - V_{out})$$

$$0 = V_x Z_2 Z_4 - V_{in} Z_2 Z_4 + V_x Z_1 Z_4 - V_{out} Z_1 Z_4 + V_x Z_1 Z_2 - V_{out} Z_1 Z_2, \text{ and}$$

substituting in Equation 16,

$$0 = V_{out} \left(1 + \frac{Z_2}{Z_3}\right) (Z_2Z_4) - V_{in}Z_2Z_4 + V_{out} \left(1 + \frac{Z_2}{Z_3}\right) (Z_1Z_4) - V_{out}Z_1Z_4 \\ + V_{out} \left(1 + \frac{Z_2}{Z_3}\right) (Z_1Z_2) - V_{out}Z_1Z_2$$

$$V_{out} \left(\left(Z_2Z_4 + \frac{Z_2^2Z_4}{Z_3} \right) + \left(Z_1Z_4 + \frac{Z_1Z_2Z_4}{Z_3} \right) + \left(Z_1Z_2 + \frac{Z_1Z_2^2}{Z_3} \right) - Z_1Z_4 - Z_1Z_2 \right) = V_{in}Z_2Z_4$$

$$\frac{V_{out}}{V_{in}} = \frac{Z_2Z_4}{\left(Z_2Z_4 + \frac{Z_2^2Z_4}{Z_3} \right) + \left(Z_1Z_4 + \frac{Z_1Z_2Z_4}{Z_3} \right) + \left(Z_1Z_2 + \frac{Z_1Z_2^2}{Z_3} \right) - Z_1Z_4 - Z_1Z_2}$$

$$\frac{V_{out}}{V_{in}} = \frac{1}{\left(1 + \frac{Z_2}{Z_3}\right) + \left(\frac{Z_1}{Z_2} + \frac{Z_1}{Z_3}\right) + \left(\frac{Z_1}{Z_4} + \frac{Z_1Z_2}{Z_3Z_4}\right) - \frac{Z_1}{Z_2} - \frac{Z_1}{Z_4}}$$

$$\frac{V_{out}}{V_{in}} = \frac{1}{\frac{Z_1Z_2}{Z_3Z_4} + \frac{Z_2}{Z_3} + \frac{Z_1}{Z_3} + 1}$$

Equation 17 Transfer function for Sallen-Key topology (above)

Substituting $Z_1 = \frac{1}{sC_1}$, $Z_2 = \frac{1}{sC_2}$, $Z_3 = R_1$, and $Z_4 = R_2$ into Equation 17 for the high-

pass configuration:

$$\frac{V_{out}}{V_{in}} = \frac{1}{\frac{1}{s^2R_1R_2C_1C_2} + \frac{1}{sR_1C_2} + \frac{1}{sR_1C_1} + 1}$$

$$\frac{V_{out}}{V_{in}} = \frac{1}{\frac{1}{s^2R_1R_2C_1C_2} + \left(\frac{1}{s}\right) \left(\frac{1}{R_1C_2} + \frac{1}{R_1C_1}\right) + 1}$$

$$\frac{V_{out}}{V_{in}} = \frac{s^2R_1R_2C_1C_2}{1 + s(R_2C_1 + R_2C_2) + s^2R_1R_2C_1C_2}$$

Equation 18 Transfer function for Sallen-Key high-pass filter

Letting $s = j2\pi f$ yields the high-pass cutoff frequency (Equation 11) and the Q Factor (Equation 12). Both equations are shown below.

$$f_c = \frac{1}{2\pi\sqrt{R_1R_2C_1C_2}}$$

$$Q = \frac{\sqrt{R_1R_2C_1C_2}}{R_2C_2 + R_2C_1}$$

Substituting $Z_1 = R_1$, $Z_2 = R_2$, $Z_3 = \frac{1}{sC_1}$, and $Z_4 = \frac{1}{sC_2}$ into Equation 17 for the low-pass configuration:

$$\frac{V_{out}}{V_{in}} = \frac{1}{s^2R_1R_2C_1C_2 + sR_2C_1 + sR_1C_1 + 1}$$

$$\frac{V_{out}}{V_{in}} = \frac{1}{s^2R_1R_2C_1C_2 + s(R_1C_1 + R_2C_1) + 1}$$

Equation 19 Transfer function for Sallen-Key low-pass filter

Letting $s = j2\pi f$ yields the high-pass cutoff frequency (Equation 11) and the Q Factor (Equation 13). Both equations are shown below.

$$f_c = \frac{1}{2\pi\sqrt{R_1R_2C_1C_2}}$$

$$Q = \frac{\sqrt{R_1R_2C_1C_2}}{R_1C_1 + R_2C_1}$$